UNIVERSITAT POLITÈCNICA DE CATALUNYA
E.T.S. D'ENGINYERS DE CAMINS, CANALS I PORTS
DEPARTAMENT DE MATEMÀTICA APLICADA III

ANALYSIS OF FRACTIONAL STEP, FINITE ELEMENT METHODS FOR THE INCOMPRESSIBLE NAVIER–STOKES EQUATIONS

by

Jorge Blasco Lorente

Advisors: Antonio Huerta Cerezuela, Ramon Codina Rovira.

Program: Applied Mathematics.

Barcelona, December 1996.

Chapter 5

A predictor–multicorrector algorithm

In this Chapter we study a form of a predictor–multicorrector algorithm customized to the unsteady, incompressible Navier–Stokes equations. This algorithm, developed originally for general evolution equations in a discrete setting, was applied succesfully to several unsteady incompressible flow problems in the eighties, such as fluid–structure interaction problems. Here, and in the light of the viscositty splitting methods developed in the previous Chapter, we redevelop the algorithm in a semidiscrete formulation, thus providing an interpretation of it within the context of fractional step methods. This gives a theoretical explanation for some properties of the algorithm such the need for the spatial interpolation used to satisfy the discrete LBB condition, the order of accuracy of the discrete solutions with respect to the time step or the reason behind the imposition of boundary conditions in each phase of the algorithm. We will see, in particular, that our viscosity splitting method can in some cases be understood as a predictor–corrector form of this algorithm. Most of these ideas can be found in [26].

The predictor–multicorrector algorithm is usually implemented together with a bilinear velocity, constant pressure (Q_1P_0) finite element interpolation; we implemented also the biquadratic velocity, linear pressure (Q_2P_1) element, which satisfies the LBB condition, to compare the properties of the two discretizations.

The outline of the Chapter is the following: in Section 5.1 we present our semidiscrete formulation of the scheme, proving that it corresponds to the predictor–multicorrector algorithm and showing in what sense it can be understood as a fractional step method. In 5.2 we introduce the two finite element interpolations considered, the resulting fully discrete equations and some considerations relative to the actual implementation of the scheme. Finally, in 5.3 we present some numerical results obtained with the algorithm on several test problems.

5.1 Semidiscrete form of the algorithm

Let us consider the predictor–multicorrector algorithm developed by T.J.R. Hughes and coworkers, which was applied to the incompressible Navier–Stokes equations in [20]; it can also be found in [75] in a similar context. We give here an alternative derivation of the algorithm, within the context of fractional step methods.

Given a time step $\delta t > 0$ and a parameter γ such that $0 < \gamma \leq 1$, and assuming that the velocity $\mathbf{u}^n$ and pressure p^n are known at time $t_n = n\,\delta t$, an implicit method of the form:

$$\begin{aligned} \frac{\mathbf{u}^{n+1} - \mathbf{u}^n}{\delta t} - \gamma\, \mathbf{a}^{n+1} - (1-\gamma)\mathbf{a}^n &= 0 \\ \nabla \cdot (\mathbf{u}^{n+1}) &= 0 \\ \mathbf{u}^{n+1}|_\Gamma &= 0 \end{aligned} \tag{5.1}$$

is considered for the solution of 1.7–1.5 with homogeneous Dirichlet boundary conditions 1.10, where we define:

$$\mathbf{a}^m \;=\; \mathbf{f}(t_m) \;-\; \nabla p^m \;-\; (\mathbf{u}^m \cdot \nabla)\mathbf{u}^m \;+\; \nu \Delta \mathbf{u}^m \tag{5.2}$$

An iterative scheme is introduced for the solution of the nonlinear, coupled problem 5.1. It starts with some predictions $\mathbf{u}_0^{n+1}$ and p_0^{n+1} for $\mathbf{u}^{n+1}$ and p^{n+1}, respectively, which will be specified next. Then, each iteration is split into two steps. The first one accounts for viscous and convective effects, but not for the incompressibility condition; this is dealt with in the second step, in a similar way to the fractional step methods of Chapter 4. Pressure correction is used, and the convective term is approximated explicitly for simplicity. Given the i–th iteration approximations $\mathbf{u}_i^{n+1}$ and p_i^{n+1} to $\mathbf{u}^{n+1}$ and p^{n+1}, the first step of the $(i+1)$–th iteration then consists of finding an *intermediate iteration* velocity $\mathbf{u}_{i+1/2}^{n+1}$ such that:

$$\begin{aligned} \frac{\mathbf{u}_{i+1/2}^{n+1} - \mathbf{u}^n}{\delta t} \;-\; \gamma \nu \Delta \mathbf{u}_{i+1/2}^{n+1} &= \gamma \mathbf{f}(t_{n+1}) \;+\; (1-\gamma)\mathbf{a}^n \\ &\quad -\; \gamma(\mathbf{u}_i^{n+1} \cdot \nabla)\mathbf{u}_i^{n+1} \;-\; \gamma \nabla p_i^{n+1} \\ \mathbf{u}_{i+1/2}^{n+1}|_\Gamma &= 0 \end{aligned} \tag{5.3}$$

The notation $\mathbf{u}_{i+1/2}^{n+1}$ has been chosen deliverately to emphasise that the solution of 5.3 is an intermediate iteration aproximation of the velocity at time t_{n+1}. In the second step of each iteration, a pressure increment is used to enforce incompressibility, in a similar way to the method of Section 4.5. Thus, one looks for an *end–of–iteration* velocity $\mathbf{u}_{i+1}^{n+1}$ and pressure p_{i+1}^{n+1} such that:

$$\begin{aligned}\frac{\mathbf{u}_{i+1}^{n+1}-\mathbf{u}_{i+1/2}^{n+1}}{\delta t} - \gamma\nu\Delta(\mathbf{u}_{i+1}^{n+1}-\mathbf{u}_{i+1/2}^{n+1}) + \gamma\nabla(p_{i+1}^{n+1}-p_i^{n+1}) &= 0\\ \nabla\cdot\mathbf{u}_{i+1}^{n+1} &= 0\\ \mathbf{u}_{i+1}^{n+1}|_\Gamma &= 0\end{aligned}\qquad(5.4)$$

The multicorrector scheme 5.3–5.4 is performed, in principle, to convergence in i, that is, until $\mathbf{u}_{i+1}^{n+1}=\mathbf{u}_i^{n+1}$ and $p_{i+1}^{n+1}=p_i^{n+1}$, at which time one sets $\mathbf{u}^{n+1}=\mathbf{u}_{i+1}^{n+1}$ and $p^{n+1}=p_{i+1}^{n+1}$ and goes back to the predictor phase.

We can show that this method is another version, independent of any particular spatial discretization, of the predictor–multicorrector algorithm of [20], which was given in a discrete setting after a Q_1P_0 finite element interpolation of the Navier–Stokes equations, which results in the following constrained system of ODEs:

$$\begin{aligned}M\dot{U} + KU + A(U)U + G_0P &= F\\ G_0^tU &= 0\end{aligned}$$

In terms of accelerations ($\mathcal{A}$) and time derivatives of elemental pressures ($\dot{P}$), the algorithm then reads:

Predictor phase:

$$\begin{aligned}U_0^{n+1} &= U^n + (1-\gamma)\,\delta t\,\mathcal{A}^n\\ \mathcal{A}_0^{n+1} &= 0\\ P_0^{n+1} &= P^n + (1-\gamma)\,\delta t\,\dot{P}^n\\ \dot{P}_0^{n+1} &= 0\end{aligned}$$

Solution phase:

$$B\ \delta\mathcal{A}_1 = R_1 \qquad (5.5)$$

$$\gamma^2\ (\delta t)^2\ (G_0^tB^{-1}G_0)\ (\delta\dot{P}) = G_0^t\ (U_i^{n+1}+\gamma\delta t(\delta\mathcal{A}_1)) \qquad (5.6)$$

$$B\ \delta\mathcal{A}_2 = -\gamma\ \delta t\ G_0\,(\delta\dot{P}) \qquad (5.7)$$

where all the matrices have been defined before and the residual vector R_1 is given by:

$$R_1 = F^{n+1} - M\mathcal{A}_i^{n+1} - KU_i^{n+1} - A(U_i^{n+1})U_i^{n+1} - G_0P_i^{n+1}$$

Corrector phase:

$$
\begin{aligned}
\mathcal{A}_{i+1}^{n+1} &= \mathcal{A}_i^{n+1} + \delta\mathcal{A}_1 + \delta\mathcal{A}_2 \\
U_{i+1}^{n+1} &= U^n + (1-\gamma)\,\delta t\,\mathcal{A}^n + \gamma\,\delta t\,\mathcal{A}_{i+1}^{n+1} \\
\dot{P}_{i+1}^{n+1} &= \dot{P}_i^{n+1} + \delta\dot{P} \\
P_{i+1}^{n+1} &= P^n + (1-\gamma)\,\delta t\,\dot{P}^n + \gamma\,\delta t\,\dot{P}_{i+1}^{n+1}
\end{aligned}
$$

The value of i is then incremented in 1 and the scheme goes back to the solution phase again. We now have:

Lemma 5.1: *the scheme* 5.3–5.4 *is equivalent to the predictor–multicorrector algorithm of* [20].

PROOF: assume the velocity $\mathbf{u}^n$, acceleration $\mathbf{a}^n$, pressure p^n and pressure temporal variation $\dot{p}^n$ are known at time $t_n = n\delta t$, satisfying 5.2 and the incompressibility condition 1.5. The iterative predictor–multicorrector procedure starts with the following predictions:

$$
\begin{aligned}
\mathbf{u}_0^{n+1} &= \mathbf{u}^n + (1-\gamma)\,\delta t\,\mathbf{a}^n && (5.8)\\
\mathbf{a}_0^{n+1} &= 0 && (5.9)\\
p_0^{n+1} &= p^n + (1-\gamma)\,\delta t\,\dot{p}^n && (5.10)\\
\dot{p}_0^{n+1} &= 0 && (5.11)
\end{aligned}
$$

Assume, further that after each correction phase the approximation of velocity and pressure may be written as:

$$
\begin{aligned}
\mathbf{u}_i^{n+1} &= \mathbf{u}^n + (1-\gamma)\,\delta t\,\mathbf{a}^n + \gamma\,\delta t\,\mathbf{a}_i^{n+1} && (5.12)\\
p_i^{n+1} &= p^n + (1-\gamma)\,\delta t\,\dot{p}^n + \gamma\,\delta t\dot{p}_i^{n+1} && (5.13)
\end{aligned}
$$

where $\mathbf{a}_i^{n+1}$ and $\dot{p}_i^{n+1}$ are the corrected values at the end of the i–th iteration. Note that equations 5.12–5.13 are also valid for the initial prediction ($i = 0$).

The objective of each iteration is to compute new approximations $\mathbf{u}_{i+1}^{n+1}$ and p_{i+1}^{n+1} by computing corrected values of $\mathbf{a}_{i+1}^{n+1}$ and $\dot{p}_{i+1}^{n+1}$. Since each iteration is split into two steps, an intermediate velocity $\mathbf{u}_{i+1/2}^{n+1}$ and acceleration $\mathbf{a}_{i+1/2}^{n+1}$ are first calculated. If the intermediate velocity is expressed as:

$$
\mathbf{u}_{i+1/2}^{n+1} = \mathbf{u}^n + (1-\gamma)\,\delta t\,\mathbf{a}^n + \gamma\,\delta t\,\mathbf{a}_{i+1/2}^{n+1} \qquad (5.14)
$$

and the intermediate acceleration is defined as:

$$
\mathbf{a}_{i+1/2}^{n+1} = \mathbf{a}_i^{n+1} + \delta\mathbf{a}_1
$$

then the following relation is deduced from 5.12:

$$\mathbf{u}_{i+1/2}^{n+1} = \mathbf{u}_i^{n+1} + \gamma\,\delta t\,\delta\mathbf{a}_1$$

The intermediate velocity and acceleration are computed from the first split step, namely equations 5.3, which can thus be rewritten as:

$$\begin{aligned} \delta\mathbf{a}_1 - \gamma\nu\delta t(\Delta\delta\mathbf{a}_1) &= \mathbf{f}^{n+1} - \mathbf{a}_i^{n+1} - \nabla p_i^{n+1} + \nu\Delta\mathbf{u}_i^{n+1} - (\mathbf{u}_i^{n+1}\cdot\nabla)\mathbf{u}_i^{n+1} \\ \delta\mathbf{a}_1|_\Gamma &= 0 \end{aligned} \tag{5.15}$$

The end–of–step velocity $\mathbf{u}_{i+1}^{n+1}$ is expressed, using 5.12, as:

$$\mathbf{u}_{i+1}^{n+1} = \mathbf{u}^n + (1-\gamma)\,\delta t\,\mathbf{a}^n + \gamma\,\delta t\,\mathbf{a}_{i+1}^{n+1} \tag{5.16}$$

and can be further simplified in terms of the intermediate velocity, using equation 5.14, and the end–of–step acceleration, which is defined as:

$$\mathbf{a}_{i+1}^{n+1} = \mathbf{a}_{i+1/2}^{n+1} + \delta\mathbf{a}_2$$

Thus:

$$\mathbf{u}_{i+1}^{n+1} = \mathbf{u}_{i+1/2}^{n+1} + \gamma\,\delta t\,\delta\mathbf{a}_2 \tag{5.17}$$

Likewise, from 5.13, the end–of–step pressure p_{i+1}^{n+1} is expressed as:

$$p_{i+1}^{n+1} = p^n + (1-\gamma)\,\delta t\,\dot{p}^n + \gamma\,\delta t\,\dot{p}_{i+1}^{n+1} \tag{5.18}$$

where the new pressure variation is determined by:

$$\dot{p}_{i+1}^{n+1} = \dot{p}_i^{n+1} + \delta\dot{p}$$

and consequently one gets:

$$p_{i+1}^{n+1} = p_i^{n+1} + \gamma\,\delta t\,\delta\dot{p} \tag{5.19}$$

With the previous expressions of the end–of–step velocity and pressure, equations 5.17 and 5.19 respectively, the second split step defined by the equation system 5.4 can be written as:

$$\begin{aligned} \delta\mathbf{a}_2 - \gamma\nu\delta t(\Delta\delta\mathbf{a}_2) + \gamma\delta t\nabla(\delta\dot{p}) &= 0 \\ \nabla\cdot(\delta\mathbf{a}_2) &= \frac{-1}{\gamma\delta t}\nabla\cdot(\mathbf{u}_i^{n+1} + \gamma\delta t\,\delta\mathbf{a}_1) \\ \delta\mathbf{a}_2|_\Gamma &= 0 \end{aligned} \tag{5.20}$$

Given the time–discretization scheme defined by 5.12–5.13, equations 5.15 and 5.20 are another version of the two split–step equations 5.3 and 5.4 defined previously. After they have been solved, the corresponding corrections are performed, namely equations 5.16 and 5.18. The weak for of the split equations 5.3–5.4 is the following:

First step: find $\mathbf{u}_{i+1/2}^{n+1} \in \mathbf{H}_0^1(\Omega)$ such that:

$$\begin{aligned}\frac{1}{\delta t}(\mathbf{u}_{i+1/2}^{n+1} - \mathbf{u}^n, \mathbf{v}) \;+\; \gamma\nu((\mathbf{u}_{i+1/2}^{n+1}, \mathbf{v})) \;&=\; \gamma(\mathbf{f}(t_{n+1}), \mathbf{v}) \;+\; (1-\gamma)(\mathbf{a}^n, \mathbf{v}) \\ &-\; \gamma c(\mathbf{u}_i^{n+1}, \mathbf{u}_i^{n+1}, \mathbf{v}) \;-\; \gamma b(\mathbf{v}, p_i^{n+1}), \forall \mathbf{v} \in \mathbf{H}_0^1(\Omega) \quad (5.21)\end{aligned}$$

Second step: find $\mathbf{u}_{i+1}^{n+1} \in \mathbf{H}_0^1(\Omega)$ and $s_{i+1}^{n+1} = \gamma\, \delta t\, p_{i+1}^{n+1} \in L_0^2(\Omega)$ such that:

$$\begin{aligned}a_\gamma(\mathbf{u}_{i+1}^{n+1}, \mathbf{v}) \;+\; b(\mathbf{v}, s^{n+1}) \;&=\; a_\gamma(\mathbf{u}_{i+1/2}^{n+1}, \mathbf{v}), \qquad \forall \mathbf{v} \in \mathbf{H}_0^1(\Omega) \\ b(\mathbf{u}_{i+1}^{n+1}, q) \;&=\; 0, \qquad\qquad\qquad\qquad \forall q \in L_0^2(\Omega) \quad (5.22)\end{aligned}$$

where the bilinear form a_γ was defined in 4.14. Existence and uniqueness of solutions to these problems are established the same way as for the fractional step methods of Chapter 4. In terms of accelerations and pressure time derivatives, the corresponding weak forms of equations 5.15 and 5.20 are:

First step: find $\delta\mathbf{a}_1 \in \mathbf{H}_0^1(\Omega)$ such that:

$$\begin{aligned}a_\gamma(\delta\mathbf{a}_1, \mathbf{v}) \;&=\; (\mathbf{f}^{n+1}, \mathbf{v}) \;-\; (\mathbf{a}_i^{n+1}, \mathbf{v}) \;-\; b(\mathbf{v}, p_i^{n+1}) \\ &-\; \nu((\mathbf{u}_i^{n+1}, \mathbf{v})) \;-\; c(\mathbf{u}_i^{n+1}, \mathbf{u}_i^{n+1}, \mathbf{v}), \quad \forall \mathbf{v} \in \mathbf{H}_0^1(\Omega) \quad (5.23)\end{aligned}$$

Second step: find $\delta\mathbf{a}_2 \in \mathbf{H}_0^1(\Omega)$ and $\delta\dot{p} \in L_0^2(\Omega)$ such that:

$$\begin{aligned}a_\gamma(\delta\mathbf{a}_2, \mathbf{v}) \;+\; \gamma\,\delta t\, b(\mathbf{v}, \delta\dot{p}) \;&=\; 0, \qquad\qquad \forall \mathbf{v} \in \mathbf{H}_0^1(\Omega) \\ b(\delta\mathbf{a}_2, q) \;&=\; \frac{1}{\gamma\,\delta t} b(\mathbf{u}_i^{n+1} + \gamma\delta t\, \delta\mathbf{a}_1, q), \; \forall q \in L_0^2(\Omega) (5.24)\end{aligned}$$

A finite element discretization of this scheme is the same algorithm as the one considered in [20]. □

There is a clear formal relationship between the structure of the split equations 5.3–5.4 and the viscosity–splitting pressure–correction method of Section 4.3. In fact, the latter method with parameters $\theta = \phi = 1$ is equivalent to a single correction of the former with $\gamma = 1$, since in that case $\mathbf{u}_0^{n+1} = \mathbf{u}^n$ and $p_0^{n+1} = p^n$ (see 5.8 and 5.10); the only difference, though, is the treatment of the nonlinear term, which is then explicit in the predictor–multicorrector algorithm. One then has that $\mathbf{u}_{1/2}^{n+1} = \mathbf{u}^{n+1/2}$, $\mathbf{u}_1^{n+1} = \mathbf{u}^{n+1}$ and $p_1^{n+1} = p^{n+1}$. The paralelism between these two methods implies that discrete interpolations of the predictor–multicorrector algorithm are subject to the satisfaction of the LBB condition, so that in confined flow problems the Q_1P_0 element will develop checkboard pressure modes; that, at least for $\gamma = 1$, one correction is enough to achieve first order accuracy in the time step, and that when a steady state is reached with this algorithm, it will be independent of the time step.

5.2 Finite element discretization

We now introduce a finite element space discretization into the multicorrector scheme 5.23–5.24. If $V_h \subset \mathbf{H}_0^1(\Omega)$ and $Q_h \subset L_0^2(\Omega)$ denote finite dimensional subspaces defined through a finite element discretization of Ω, the discrete version of 5.23 consists of finding $\delta \mathbf{a}_{1,h} \in V_h$ such that:

$$\begin{aligned} a_\gamma(\delta \mathbf{a}_{1,h}, \mathbf{v}_h) &= (\mathbf{f}^{n+1}, \mathbf{v}_h) - (\mathbf{a}_{i,h}^{n+1}, \mathbf{v}_h) - b(\mathbf{v}_h, p_{i,h}^{n+1}) \\ &- \nu((\mathbf{u}_{i,h}^{n+1}, \mathbf{v}_h)) - c(\mathbf{u}_{i,h}^{n+1}, \mathbf{u}_{i,h}^{n+1}, \mathbf{v}_h), \ \forall \mathbf{v}_h \in V_h \end{aligned} \quad (5.25)$$

whereas in the discrete version of 5.24 we look for $\delta \mathbf{a}_{2,h} \in V_h$ and $\delta \dot{p}_h \in Q_h$ such that:

$$\begin{aligned} a_\gamma(\delta \mathbf{a}_{2,h}, \mathbf{v}_h) + \gamma\, \delta t\, b(\mathbf{v}_h, \delta \dot{p}_h) &= 0, \qquad \forall \mathbf{v}_h \in V_h \quad (5.26) \\ b(\delta \mathbf{a}_{2,h}, q_h) &= \frac{1}{\gamma\, \delta t} b(\mathbf{u}_{i,h}^{n+1} + \gamma \delta t\, \delta \mathbf{a}_{1,h}, q_h), \forall q_h \in Q_h \end{aligned}$$

Calling again $\mathcal{A}$ and $\dot{P}$ the vectors of nodal accelerations and pressure time derivatives representing the functions $\mathbf{a}_h$ and $\dot{p}_h$, respectively, the weak form of equations 5.25–5.26 can be written in matrix form, with the notation introduced up to now, as:

$$B\, \delta \mathcal{A}_1 = R_1 \quad (5.27)$$

$$B\, \delta \mathcal{A}_2 + \gamma\, \delta t\, G_0\, (\delta \dot{P}) = 0 \quad (5.28)$$

$$G_0^t\, \mathcal{A}_2 = -\frac{1}{\gamma\, \delta t} G_0^t\, (U_i^{n+1} + \gamma\, \delta t\, \delta \mathcal{A}_1) \quad (5.29)$$

By isolating $\delta \mathcal{A}_2$ from 5.28 and substituting it into 5.29, one gets equation 5.6, that is, the pressure update equation of the solution phase of the predictor multicorrector algorithm. This equation, however, is not affordable in practice, since it involves the inversion of a full matrix B to form the system matrix $G_0^t B^{-1} G_0$, which is prohibitive in general. Some approximations are introduced in [20] in this scheme, which make it computationally feasible. The matrix B is approximated by M in all its appearances (the difference between the two, $\delta t\, \nu\, L$, is dropped). This approximation is first order accurate in the time step, so that the errors it introduces are of the same order of magnitude as those of the method itself. Moreover, the matrix M is then lumped, which allows the pressure system 5.6 to be a possible way to compute the pressure variation in each iteration. Thus, the final scheme reads:

$$\begin{aligned} M^L\ \delta A_1 &= R_1 \\ \gamma^2\ (\delta t)^2\ (G_0^t (M^L)^{-1} G_0)\ (\delta \dot{P}) &= G_0^t\ (U_i^{n+1} + \gamma \delta t (\delta A_1)) \\ M^L\, \delta A_2 &= -\gamma\, \delta t\, G_0\, (\delta \dot{P}) \end{aligned}$$

Inversion of the diagonal matrix M^L is now trivial. This is the algorithm actually implemented in practice. It has to be said that the introduction of these simplifications (which are due to T.J.R. Hughes and coworkers) has a double theoretical implication: on the one hand, the approximation of B by M in 5.5 leads to an explicit treatment of diffusion in each iteration (although not in each time step, if the algorithm is iterated at least twice per step); on the other hand, the approximation of B by M in 5.6 and 5.7 implies that the algorithm actually used admits an interpretation within the context of fractional step methods relative to the standard projection method, that is, without a viscous term in the incompressibility phase. A single iteration of this simplified predictor–multicorrector algorithm is actually equivalent to the standard projection method. If it is understood this way, a question arises about which boundary conditions are to be imposed in the incompressibility phase, whether the full Dirichlet condition or only the normal component of it.

If two or more iterations of this scheme are performed, all terms in the Navier–Stokes equations are treated implicitly. Thus, no δt limitations are expected for the stability of the algorithm over a wide range of Reynolds numbers. However, the iterative nature of the scheme and the simplifications introduced in it (such as the explicit treatment of the convective term) impose restrictions on δt for the stability of the iterative process, specially for quadratic elements, as will be seen in the next Section.

5.3 Numerical results

We now present some results obtained with the predictor–multicorrector algorithm just considered, both with a Q_1P_0 and a Q_2P_1 finite element interpolation, on five test problems. First, van Kan's problem is used again to study numerically the order of accuracy in the time step of this algorithm with different values of the parameter γ and different numbers of iterations per time step; then, we consider again the Kovasznay flow problem, this time to prove numerically the independence of the steady state reached with a pressure correction algorithm from the time step used, and to study the dependence of the error with respect to the analytical solution on the mesh size for each of the two elements; we then solve the standard cavity flow problem with both interpolations, and the so called 'no flow test', and finally, we consider a plane jet simulation as another example of a purely unsteady problem.

5.3.1 Numerical accuracy study

We considered again the test problem introduced by van Kan in [62], this time to study numerically the order of accuracy with respect to the time step of the predictor–multicorrector algorithm with different values of the parameter γ and different number of iterations in each time step. The same mesh, boundary conditions and Reynolds number as in Subsection 4.5.1 were

δt	$\kappa_1(\delta t)$	$\kappa_2(\delta t)$	$\kappa_p(\delta t)$
1/16	2.04	2.02	2.03
1/32	2.02	2.01	2.02
1/64	2.01	2.01	2.01
1/128	1.99	1.99	2.00

Table 5.1: Q_1P_0 element, $\gamma = 1$, 1 iteration per step.

considered, and also the same definitions of the quotients $\kappa_i(\delta t)$ $(i = 1, 2)$ and $\kappa_p(\delta t)$.

In Tables 5.1 to 5.10, we present the results obtained with $\gamma = 1$ both for 1 and 2 iterations of the multicorrector scheme per time step and iterating it to convergence in each time step, and for $\gamma = 1/2$ with 2 iterations and iterating to convergence, both for the Q_1P_0 and the Q_2P_1 elements (the latter was unstable for large values of the time step).

The backward Euler scheme $\gamma = 1$ is clearly first order accurate, both for the Q_1P_0 and the Q_2P_1 elements and both for 1 and 2 iterations per step and iterating to convergence in each time step. In this last case, it took an average of 10 iterations per time–step to reduce the initial residuals by 7 orders of magnitude. For this value of γ, anyway, it is unnecessary to converge in each time step in order to obtain first order accuracy, since either 1 or 2 iterations are sufficient for that purpose. In all these cases, the pressure solution was also first order accurate.

For the Crank–Nicholson case $\gamma = 1/2$, however, iterating to convergence is compulsory to achieve second order accuracy in the velocity solution. If a fixed number of 2 iterations per time step is chosen, second order accuracy is lost, but the quotients obtained are still larger than 2 (indicating a higher order than 1).

5.3.2 Kovasznay flow

We then solved the Kovasznay flow problem considered in Section 3.5, this time with the predictor–multicorrector algorithm of the previous Section, with $\gamma = 1$ and 1 iteration per step, until a steady state was reached. Our main interest here was proving numerically that the steady state obtained with this pressure–correction method is independent of the time step used, in agreement with the theoretical results of Section 4.6, as well as performing a numerical study of the order of accuracy of the solution with respect to the mesh size, for each of the two finite elements employed.

δt	$\kappa_1(\delta t)$	$\kappa_2(\delta t)$	$\kappa_p(\delta t)$
1/16	2.55	3.73	2.11
1/32	1.99	2.23	2.03
1/64	1.98	2.06	2.01
1/128	1.98	1.99	2.00

Table 5.2: Q_1P_0 element, $\gamma = 1$, 2 iterations per step.

δt	$\kappa_1(\delta t)$	$\kappa_2(\delta t)$	$\kappa_p(\delta t)$
1/16	2.00	1.99	2.02
1/32	1.97	2.02	2.00
1/64	1.97	1.95	2.00
1/128	2.01	1.83	2.01

Table 5.3: Q_1P_0 element, $\gamma = 1$, iterating to convergence.

δt	$\kappa_1(\delta t)$	$\kappa_2(\delta t)$
1/7	4.41	5.90
1/8	2.47	4.08
1/10	1.69	2.91
1/12	1.66	2.51
1/14	1.70	2.33

Table 5.4: Q_1P_0 element, $\gamma = 1/2$, 2 iterations per step.

δt	$\kappa_1(\delta t)$	$\kappa_2(\delta t)$
1/7	4.06	4.08
1/8	4.04	4.04
1/10	4.03	4.01
1/12	3.75	3.99
1/14	4.00	3.79

Table 5.5: Q_1P_0 element, $\gamma = 1/2$, iterating to convergence.

δt	$\kappa_1(\delta t)$	$\kappa_2(\delta t)$	$\kappa_p(\delta t)$
1/16	2.24	2.27	2.04
1/32	2.01	1.99	2.02
1/64	2.00	1.99	2.01
1/128	1.97	1.99	2.01

Table 5.6: Q_2P_1 element, $\gamma = 1$, 1 iteration per step.

δt	$\kappa_1(\delta t)$	$\kappa_2(\delta t)$	$\kappa_p(\delta t)$
1/32	3.87	5.62	2.57
1/64	2.20	2.60	2.09
1/128	2.05	2.15	2.03
1/256	2.01	2.05	2.02

Table 5.7: Q_2P_1 element, $\gamma = 1$, 2 iterations per step.

δt	$\kappa_1(\delta t)$	$\kappa_2(\delta t)$	$\kappa_p(\delta t)$
1/32	1.98	1.98	2.01
1/64	1.99	2.00	2.01
1/128	2.00	1.95	1.99

Table 5.8: Q_2P_1 element, $\gamma = 1$, iterating to convergence.

δt	$\kappa_1(\delta t)$	$\kappa_2(\delta t)$
1/16	5.80	6.07
1/20	3.38	4.05
1/24	2.57	3.30

Table 5.9: Q_2P_1 element, $\gamma = 1/2$, 2 iterations per step.

δt	$\kappa_1(\delta t)$	$\kappa_2(\delta t)$
1/16	3.83	4.15
1/20	3.96	4.04
1/24	3.86	3.92

Table 5.10: Q_2P_1 element, $\gamma = 1/2$, iterating to convergence.

We took again $\Omega = [-\frac{1}{2}, 1] \times [-\frac{1}{2}, \frac{1}{2}]$ and a uniform mesh consisting of 31×21 nodes, which is used to define the elements for both the Q_1P_0 and Q_2P_1 cases. The Reynold's number was 10 this time. Since the flow is confined, i.e., the velocity is prescribed on all the boundary (and equal to the analytical solution 3.32), a linear restriction should be imposed on the pressure to remove the hydrostatic (constant) pressure mode. In our code we set the value of the pressure in the last element in the element numbering strategy equal to zero (this corresponds to the degree of freedom number $(3 \times n_e - 2)$ for the Q_2P_1 element, where n_e is the number of elements).

In order to compare the steady state obtained with two different time steps δt_i and δt_j, starting from the fluid at rest in the interior of Ω and the analytical solution on the boundary, we define the difference between these two solutions as the Euclidean norm of the difference of the nodal velocity vectors, namely:

$$\text{Diff}(\delta t_i, \delta t_j) \doteq |U(\delta t_i) - U(\delta t_j)|_2$$

where $|.|_2$ is again the Euclidean norm of a vector and $U(\delta t)$ is the nodal velocity vector obtained at steady state with time step δt. In this problem we can also compare the numerical solutions with the analytical solution 3.32; for that purpose we considered the relative maximum difference between the exact and computed nodal velocity vector:

$$\text{Err}(\delta t) \doteq \frac{\max_{i=1,\dots n_p}\left\{|U_{x,i}(\delta t) - U^{\text{ex}}_{x,i}|, |U_{y,i}(\delta t) - U^{\text{ex}}_{y,i}|\right\}}{\max_{i=1,\dots n_p}\left\{|U^{\text{ex}}_{x,i}|, |U^{\text{ex}}_{y,i}|\right\}} \tag{5.30}$$

where the subindex i refers to node a_i ($i = 1, \dots, n_p$, n_p being the number of nodal points), the subindeces x and y refer to the two components of velocity and U^{ex} is the vector of exact nodal velocities.

For the Q_1P_0 element and the present mesh, we tried with time steps $\delta t_1 = 0.01$, $\delta t_2 = 0.005$ and $\delta t_3 = 0.001$. In each case, a steady state was reached when $|U^n(\delta t) - U^{n+1}(\delta t)|_2$ was less than 10^{-12}. The three differences $\text{Diff}(\delta t_i, \delta t_j)$ computed were smaller than 10^{-10}, thus confirming independence of the steady state with respect to the time step.

For the Q_2P_1 element we took $\delta t_1 = 0.0025$, $\delta t_2 = 0.001$ and $\delta t_3 = 0.0005$, and a steady state was reached again at a tolerance of 10^{-12}. The differences were also smaller than 10^{-10} this time.

The velocity solutions obtained can be seen in Figures 5.1 and 5.2, where we show the streamlines for the two elements. As for the pressures, the Q_1P_0 developed an obvious *checkboard* mode, as could be anticipated by the structure of the second step of the method 5.22. The elemental pressures for this element can be seen in Figure 5.3; we also show, in Figure 5.4, the nodal pressure contours obtained with the Q_2P_1 element after a least–squares nodal interpolation process.

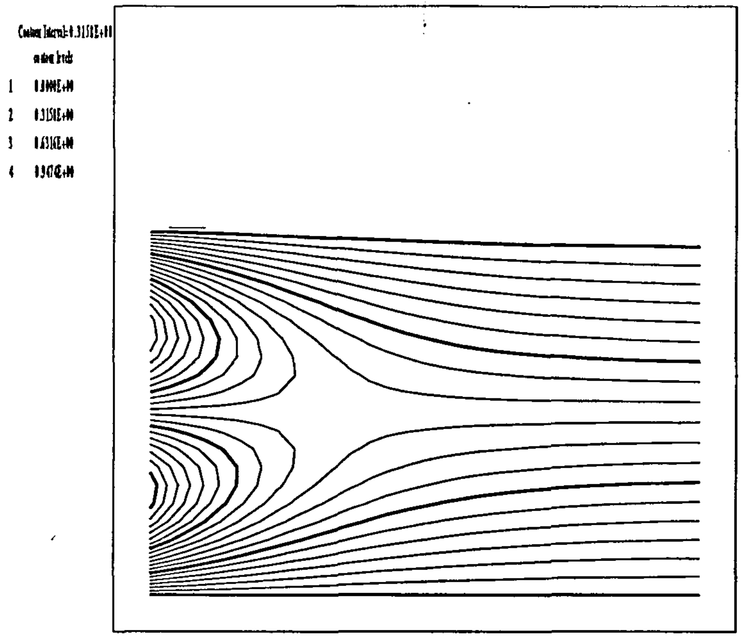

Figure 5.1: Kovasznay flow, $Q_1 P_0$ element, streamlines.

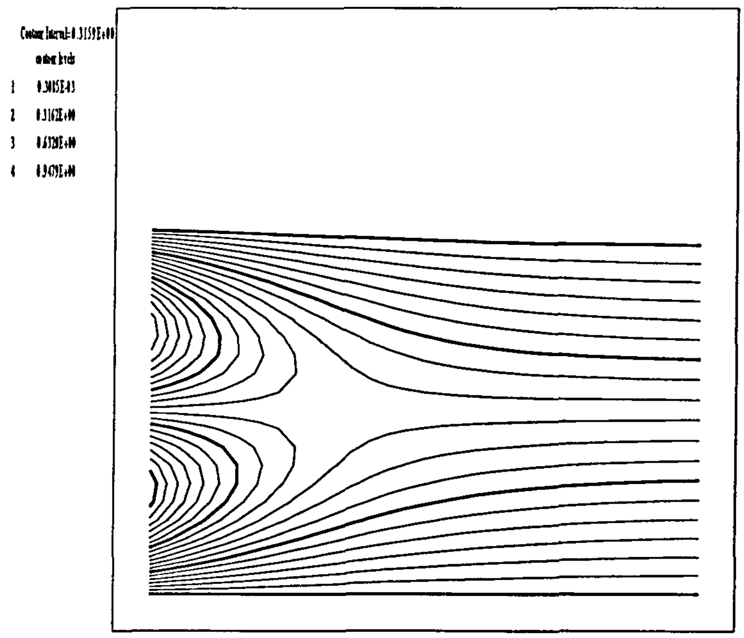

Figure 5.2: Kovasznay flow, $Q_2 P_1$ element, streamlines.

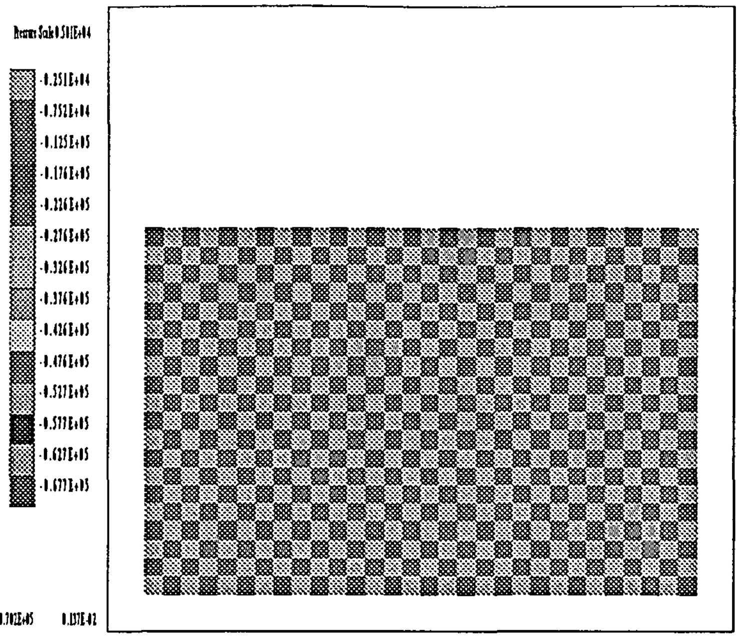

Figure 5.3: Kovasznay flow, Q_1P_0 element, element pressure values.

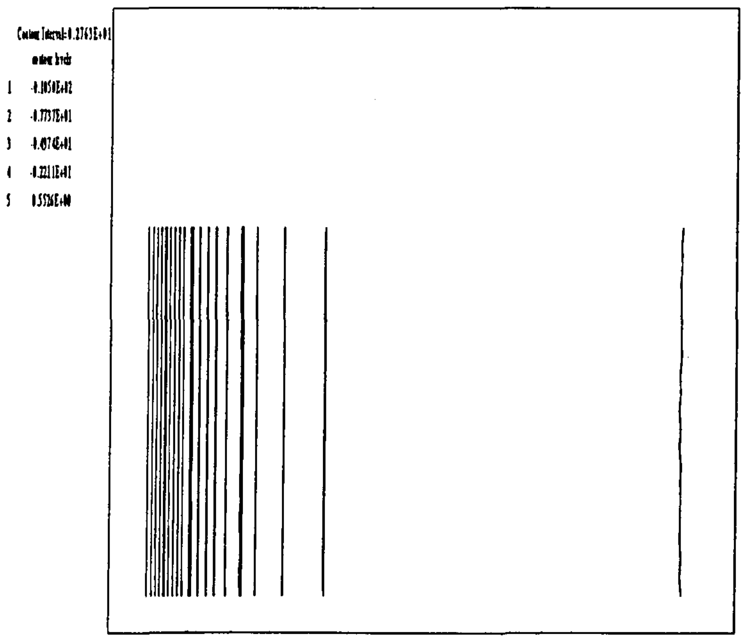

Figure 5.4: Kovasznay flow, Q_2P_1 element, nodal pressure contours.

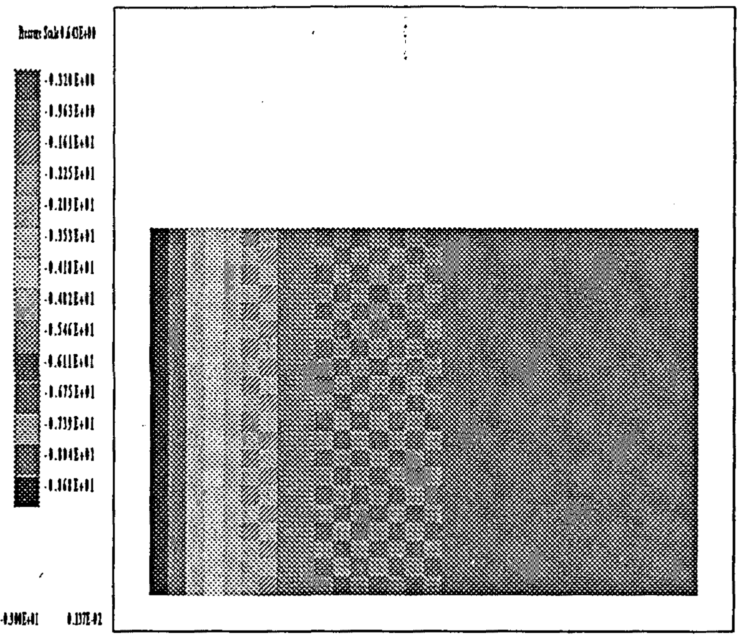

Figure 5.5: Kovasznay flow, Q_1P_0 element with checkboard mode filtered, element pressure values.

Since in this problem we know the exact pressure solution, we can determine the actual value of the spurious pressure mode present in the Q_1P_0 element solution. We can then filter this mode by subtracting it from the elements that it affects, given that on a uniform mesh the value of the *checkboard* mode is the same on all the 'red' cells of the mesh, assuming that the last element is 'black' (the value of the spurious mode on 'black' cells is thus 0). We did so, and recovered the exact analytical solution, which we show in Figures 5.5, in the form of elemental pressures, and 5.6, as nodal pressure contours.

Finally, we solved this problem on three different uniform meshes with each of the two elements, and computed the errors Errr (as defined in 5.30) with respect to the exact solution; we plot them in Figure 5.7 as a function of the mesh size. It can be seen that the steady states reached with this method provide optimal order accuracy in the mesh size for the velocity solution in the norm of $\mathbf{L}^2(\Omega)$ for these two elements, that is, quadratic for the Q_1P_0 and cubic for the Q_2P_1. These steady states are the solutions of a standard Galerkin mixed approximation of the steady, incompressible Navier–Stokes equations.

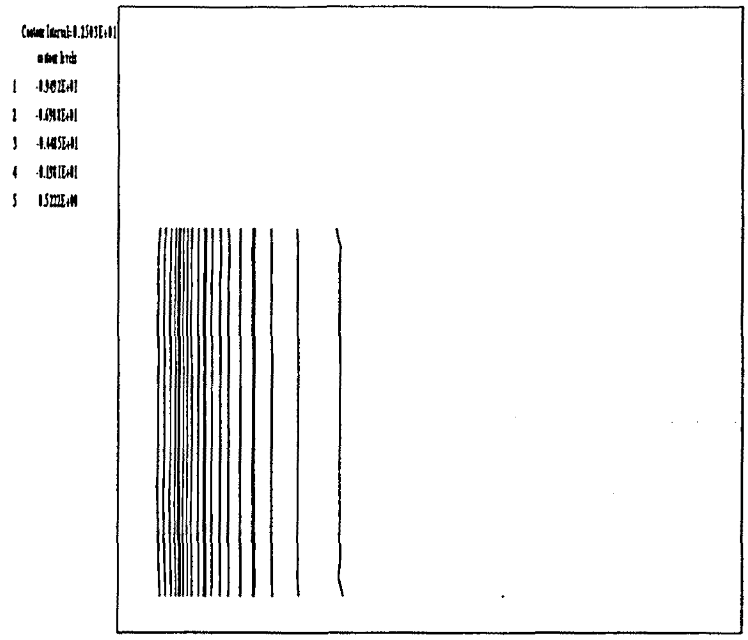

Figure 5.6: Kovasznay flow, Q_1P_0 element with checkboard mode filtered, nodal pressure contours.

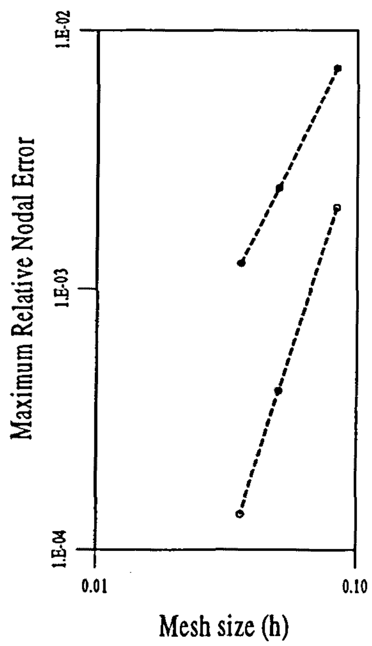

Figure 5.7: Kovasznay flow, maximum nodal error: • Q_1P_0 element, ∘ Q_2P_1 element.

5.3.3 Cavity flow problem

The third case we considered was again the lid-driven cavity flow problem, this time solved with the predictor-multicorrector algorithm starting from the fluid at rest (but for the velocity boundary condition) until a steady state was reached. We took the leaky lid case (that is, with unit horizontal velocity on the two top corners of the cavity) and a Reynolds number of 1000. A regular, nonuniform mesh, which is finer near the boundaries, was used; it is made up with 31×31 nodes. Two iterations of the multicorrector scheme were performed per time step, and the value of γ was set equal to 1 so as to get a converged solution fastest.

Figure 5.8 shows the steady streamlines obtained with both the Q_1P_0 and the Q_2P_1 elements. Secondary bottom left and right vortices can be observed, but no top left vortex was found. Again, this is in good agreement with benchmark solutions for this problem, ([42] or [88]) and other published numerical solutions ([30], [65], [96] or [99])

The element pressures computed with the Q_1P_0 element are shown in Figure 5.9. A checkerboarding phenomenon becomes apparent, which invalidates the pressure approximation without affecting the velocities. On the other hand, the Q_2P_1 element gave satisfactory pressure results; the pressure contours obtained can be seen in Figure 5.10, and compare well with those of the above mentioned references.

Finally, Figures 5.11 and 5.12 show the velocity profiles through the cavity centerlines $x = 0.5$ (horizontal velocity) and $y = 0.5$ (vertical velocity), respectively. As can be seen, these results compare well with the reference data of U. Ghia *et al.* ([42]), specially for biquadratic elements.

5.3.4 Noflow problem

The fourth example we present is the noflow test, introduced by P. Gresho *et al.* in [47] and studied in [39] and [40]. The geometry and mesh for this problem can be seen in Figure 5.13. Homogeneous Dirichlet boundary conditions are imposed on all the boundary, and an external gravitational force $\mathbf{f} = (0, -1)$ is applied. The exact analytical solution of this problem is $\mathbf{u} = \mathbf{0}$ and $p = -y + p_0$.

This simple case highlights another misbehaviour of the Q_1P_0 element (and some other related constant pressure elements). Although it is a confined flow problem, this time it is not the presence of checkboard pressure modes, since the distorted character of the mesh filters them out, or the lack of satisfaction of the LBB condition. The pressure space does not contain the analytical solution, and a wrong pressure field induces the appearance of a vortex of $O(h)$.

In this problem, we started from the fluid at rest and zero pressure until a steady state was reached, with a time step of 0.01, two iterations per step and a value of γ equal to 1. The same results as in [39] and [40] were obtained for the Q_1P_0 element after 300 steps, which can be seen in Figures 5.14 and

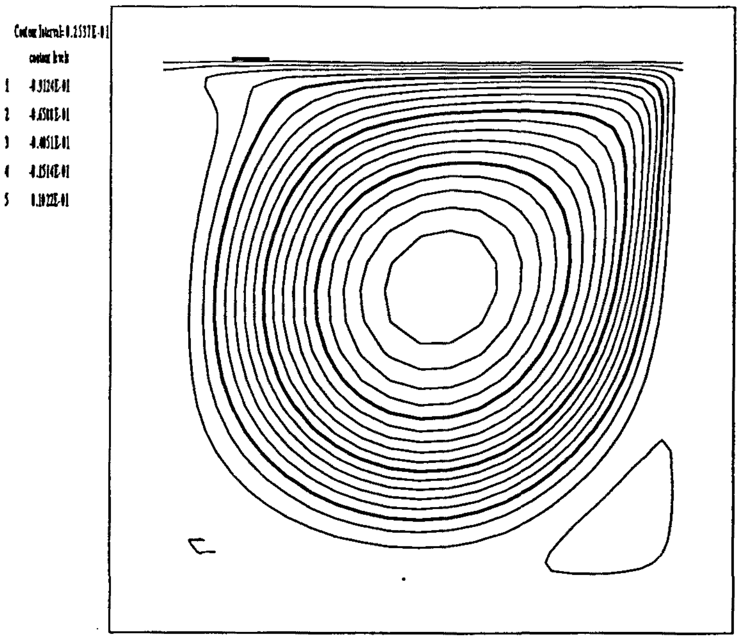

a)

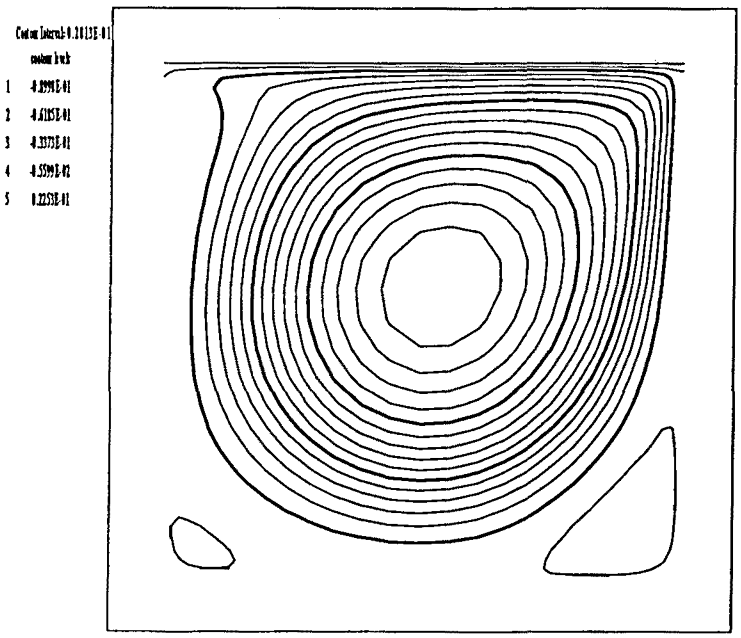

b)

Figure 5.8: Cavity flow, streamlines: a) Q_1P_0 element; b) Q_2P_1 element.

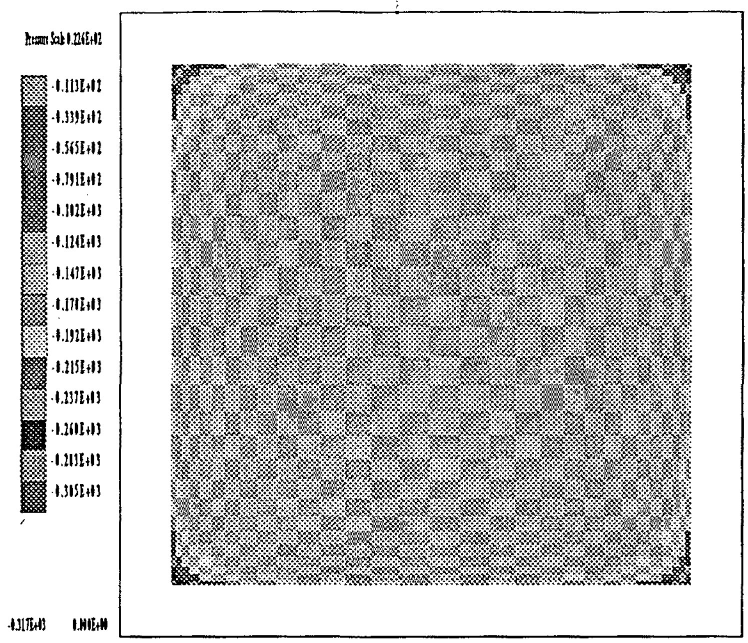

Figure 5.9: Cavity flow, Q_1P_0 element, element pressure values.

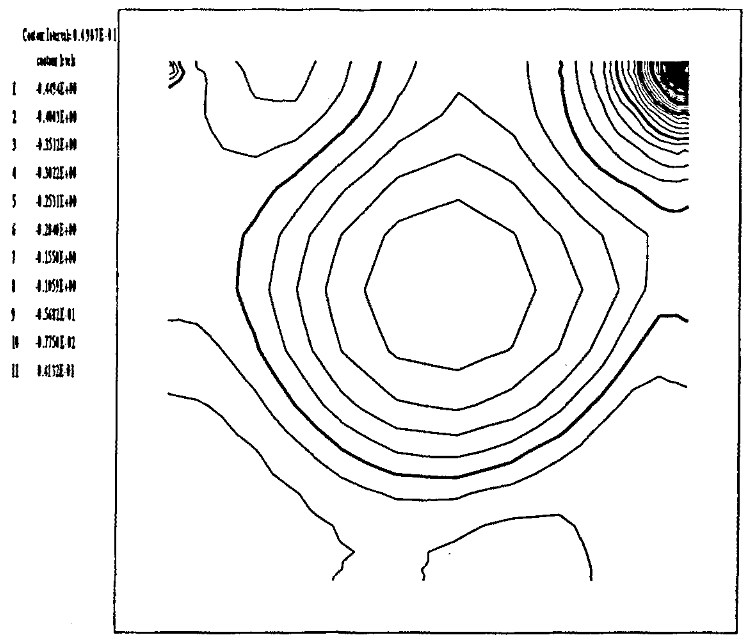

Figure 5.10: Cavity flow, Q_2P_1 element, nodal pressure contours.

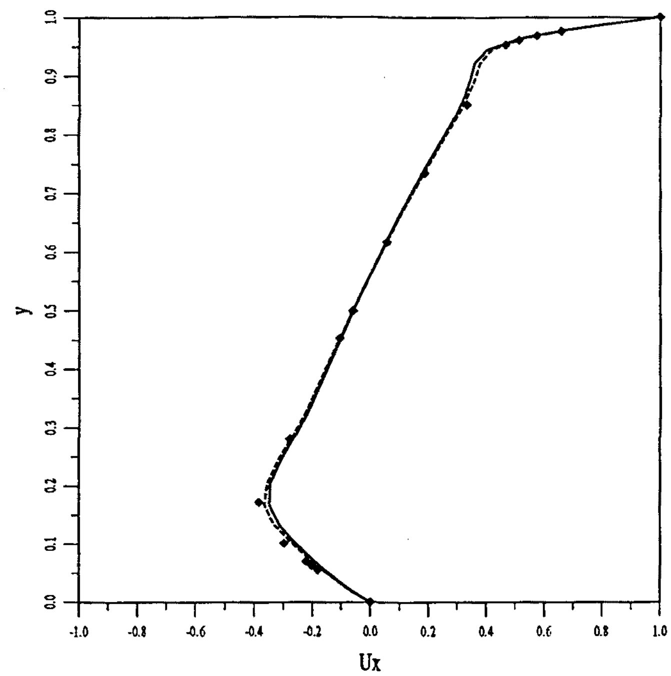

Figure 5.11: Cavity flow, horizontal velocity profile through cavity centerline $x = 0.5$: — $Q1P0$ element; - - - $Q2P1$ element; ◇ Reference [43].

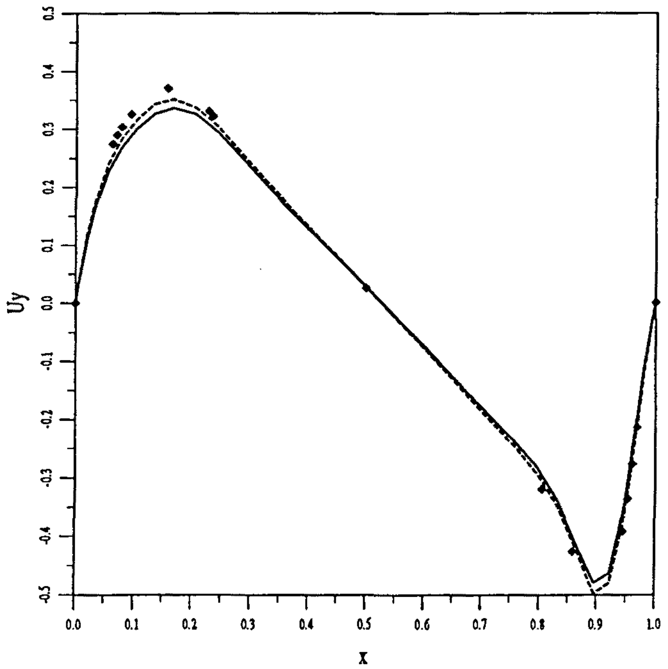

Figure 5.12: Cavity flow, vertical velocity profile through cavity centerline $y = 0.5$: — $Q1P0$ element; - - - $Q2P1$ element; ◇ Reference [43].

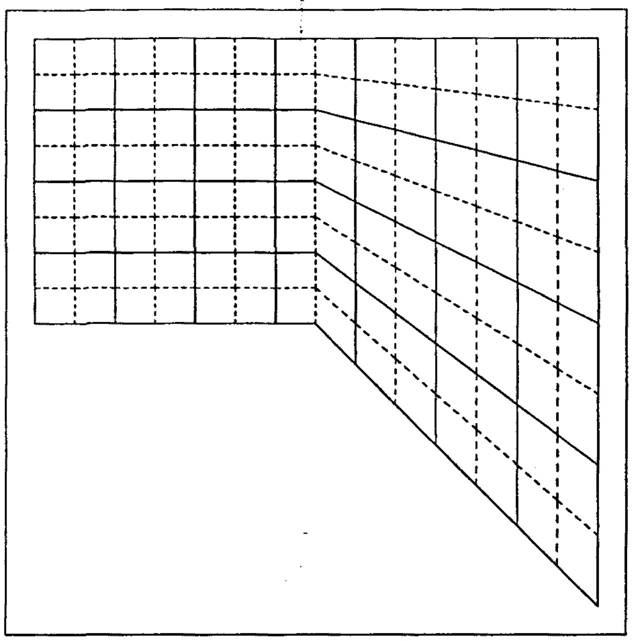

Figure 5.13: Noflow problem, mesh.

5.16 in the form of nodal velocity vectors and pressure contours, respectively. The Q_2P_1 element, on the contrary, yielded the exact analytical solution in 2 steps (see Figures 5.15 and 5.17).

5.3.5 Plane jet simulation

The fifth example considered is a purely unsteady case, consisting of a plane jet simulation. The same conditions and mesh as in [73] were taken, which are: a uniform 32×32 mesh of the 4 noded elements in the square $[0, 1] \times [-0.5, 0.5]$; a viscosity of $\nu = 5 \times 10^{-4}$; unit horizontal velocity at the central node of the left wall, with natural boundary conditions on the other walls and the fluid at rest at $t = 0$. A time step of $\delta t = 0.01$ was taken. Once again, 2 iterations per time step of the algorithm were performed, and γ was set equal to 1. The streamlines at different times are shown in Figures 5.18 and 5.19 for the Q_1P_0 and Q_2P_1 elements, respectively; the pressure contours for the same times can be found in Figures 5.20 and 5.21. They are all in good agreement with the results of [73]. The presence of outlet boundary conditions on part of the boundary prevents the appearance of spurious checkboard modes for the Q_1P_0 element. This example shows the capability of the algorithm to reproduce purely unsteady situations.

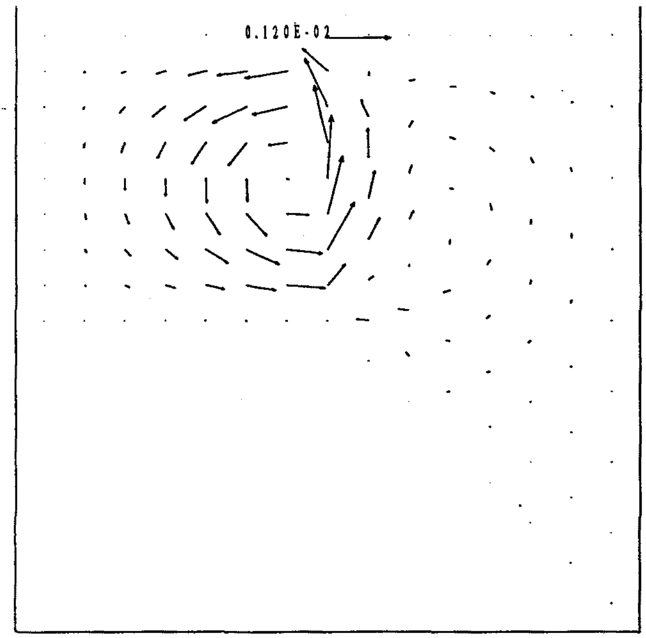

Figure 5.14: Noflow problem, Q_1P_0 element, velocity vectors.

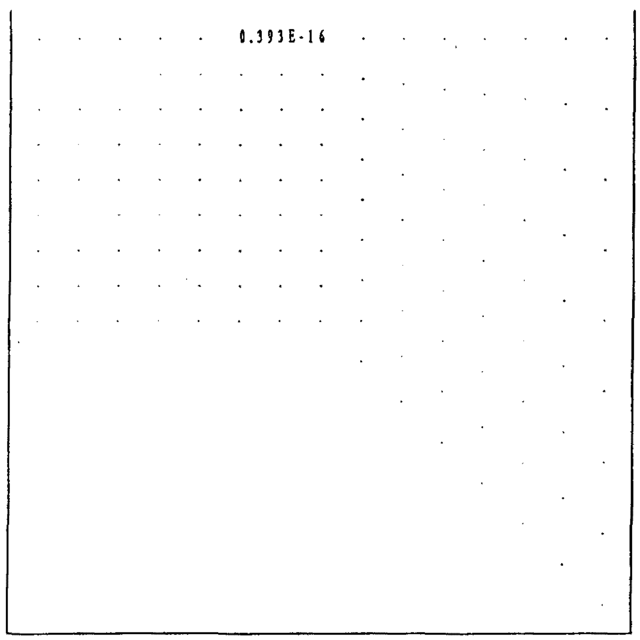

Figure 5.15: Noflow problem, Q_2P_1 element, velocity vectors.

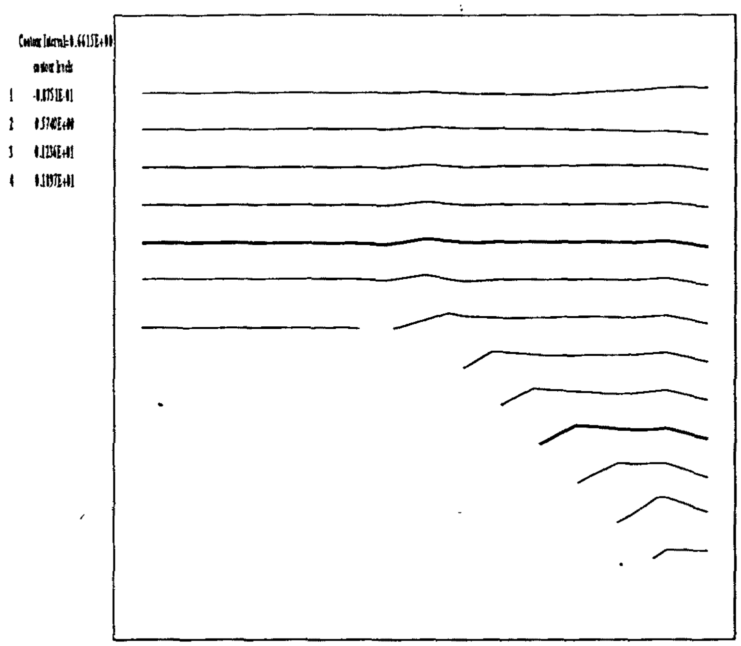

Figure 5.16: Noflow problem, Q_1P_0 element, pressure contours.

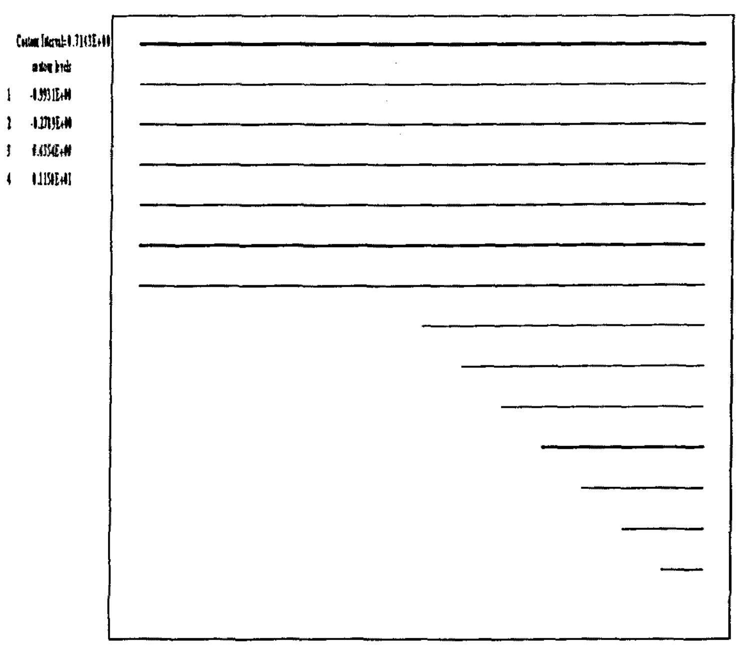

Figure 5.17: Noflow problem, Q_2P_1 element, pressure contours.

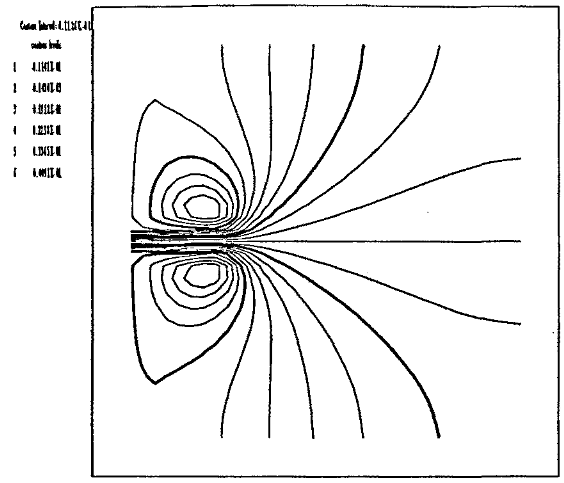

a)

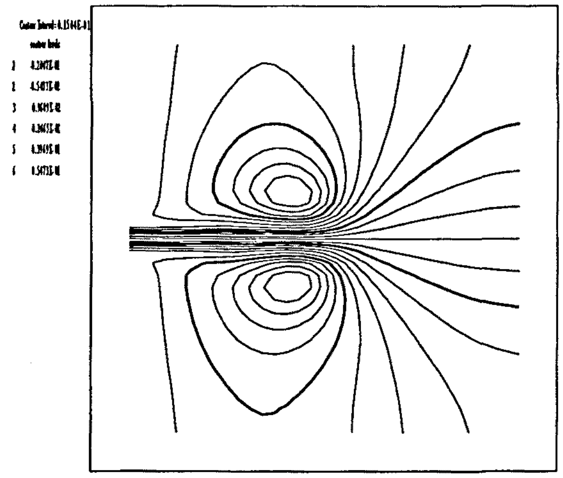

b)

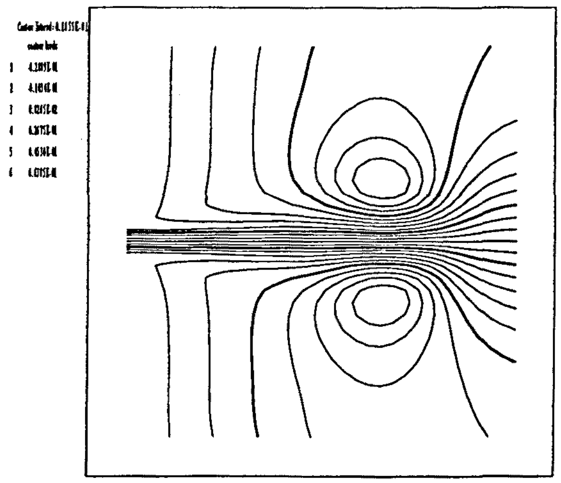

c)

Figure 5.18: Jet flow, $Q_1 P_0$ element, streamlines: a) $t = 1.2$; b) $t = 2.5$; c) $t = 4.0$.

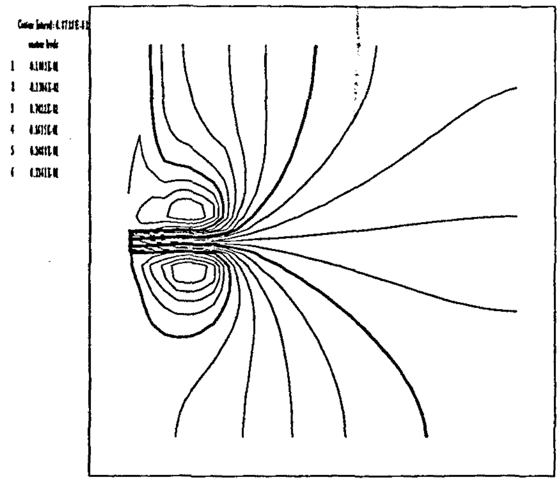

a)

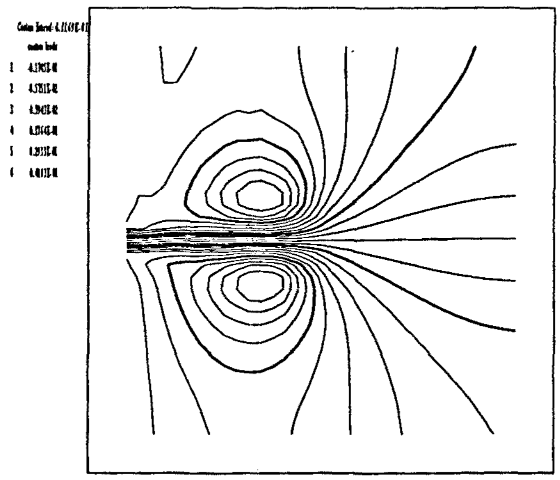

b)

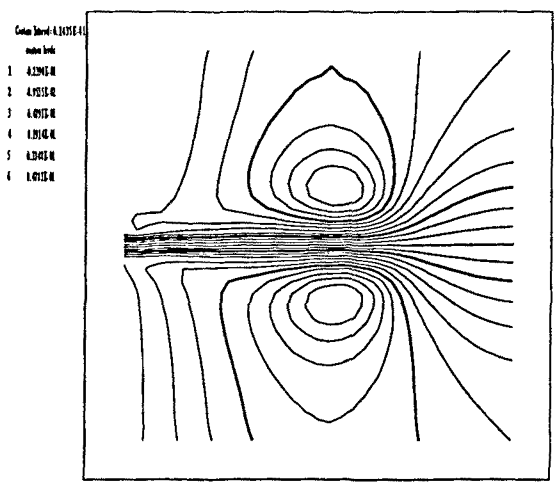

c)

Figure 5.19: Jet flow, Q_2P_1 element, streamlines: a) $t = 1.2$; b) $t = 2.5$; c) $t = 4.0$.

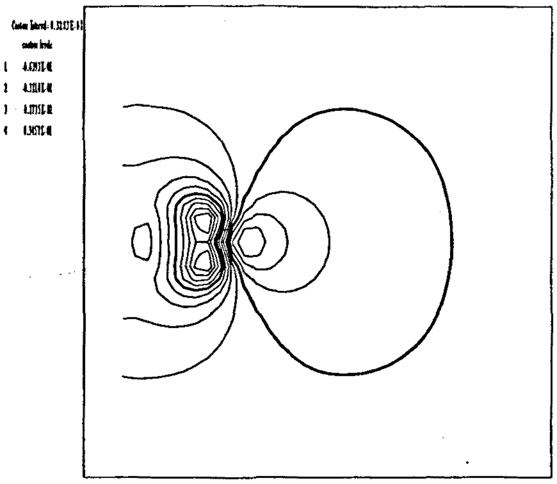

a)

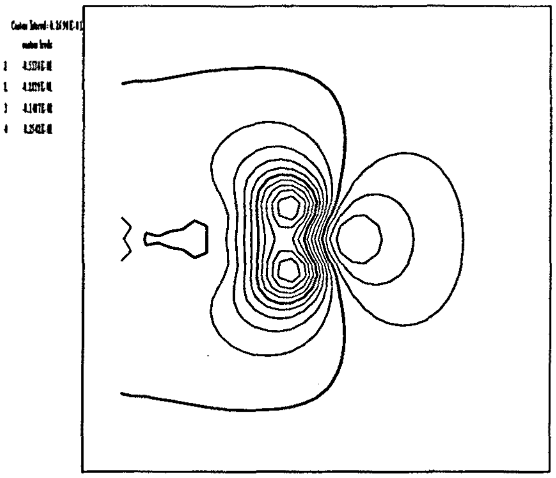

b)

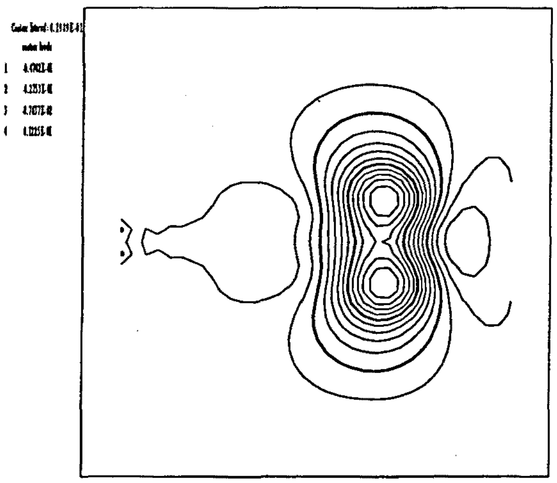

c)

Figure 5.20: Jet flow, Q_1P_0 element, nodal pressure contours: a) $t = 1.2$; b) $t = 2.5$; c) $t = 4.0$.

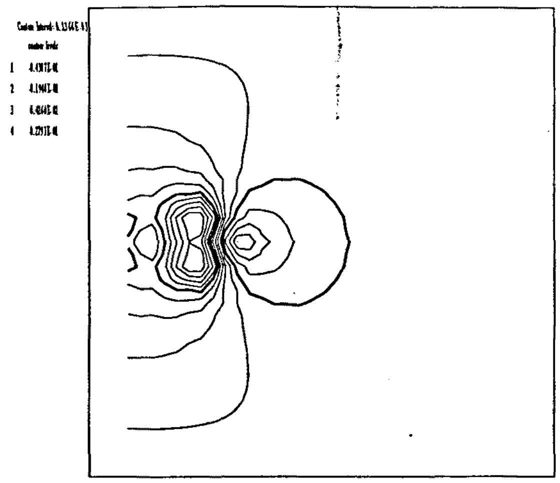

a)

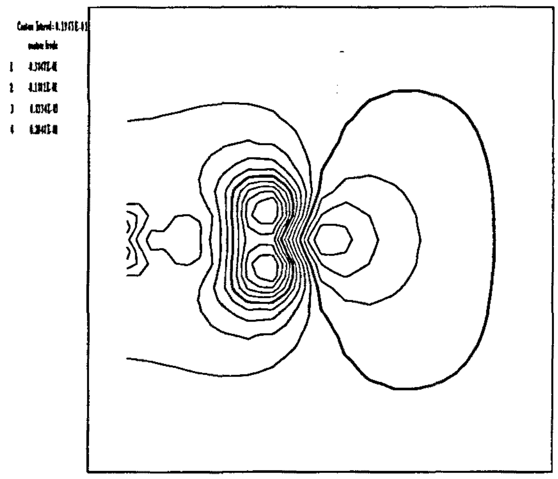

b)

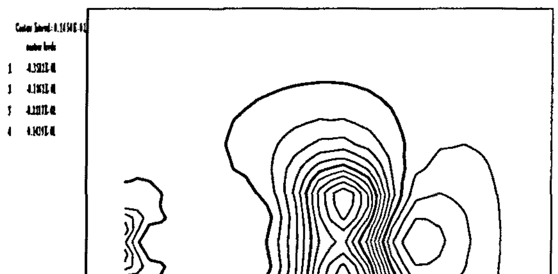

c)

Figure 5.21: Jet flow, Q_2P_1 element, nodal pressure contours: a) $t = 1.2$; b) $t = 2.5$; c) $t = 4.0$.

Conclusions and future work

In this work we have studied fractional step, finite element methods for the numerical solution of incompressible Navier–Stokes equations in primitive variables. Two main objectives have been achieved: on the one hand, the reason why some projection methods (the most popular among fractional step methods) are not restricted by the standard *inf–sup* condition, which is present in most incompressible flow formulations, has been unveiled; space discretizations of such methods are only restricted by a weaker condition, which has been proved to be satisfied by most equal order finite element interpolations of velocities and pressures. On the other hand, a fractional step method has been developed which bypasses the problem of enforcing unphysical boundary conditions encountered in projection methods; this is achieved by introducing a viscous term in the incompressibility phase of the method.

It can be concluded from the present work that projection methods which employ a continuous Pressure Poisson Equation in their formulation are not restricted by the discrete LBB condition; pressure segregation, however, has to be effected before space discretization takes place. Otherwise, a mixed type discrete problem results, and a compatibility condition between the approximating spaces of velocity and pressure still applies. The reason why the LBB restriction is so *circumvented* in standard projection methods has been traced back to the appearance of a matrix $A = L - G^t M^{-1} G$ in the discrete continuity equation; this matrix, which can be understood as the difference between two discrete Laplacian operators, has been proved to be positive semidefinite. This has led to the conclusion that space discretizations of projection methods are only restricted by a certain *inf–sup* condition which is weaker than the standard one; we have then applied the macroelement technique to showing that it is satisfied by equal order simplicial finite elements of arbitrary order in 2 and 3 dimensions, and equal order quadrilateral ($d = 2$) and hexahedral ($d = 3$) finite elements of first order.

During the course of this study, we have also developed a numerical method for the solution of the Stokes problem which allows the use of equal order finite element interpolations. The Stokes problem is employed here as a linear, steady model to study projection methods. Optimal order convergence in the mesh size has been proved for our method, both in the natural norm of the problem and in the L^2–norm, for 'sufficiently smooth' domains and meshes and under the weak compatibility condition just found. We have also studied different iterative schemes for the numerical solution of the resulting system of discrete linear equations. A comparison between the most efficient scheme obtained and the well-known GLS method for the Stokes problem has been given; our scheme seems to be a little more costly, but, in some aspects, it is more accurate.

An extension of the previous method to the steady, incompressible Navier–Stokes equation has also been provided. Optimal order convergence both in natural and in L^2–norm has been proved, in the case of a unique solution of the original problem, under the same weak compatibility condition as in the linear problem and again for 'sufficiently smooth' domains and meshes. A study of different iterative schemes for the numerical solution of the resulting system of discrete nonlinear equations has also been given, as well as a comparison between the most efficient scheme found and the GLS method applied to the incompressible Navier–Stokes equations; once again, our scheme is a little more costly, but it proved to be more accurate in all the cases we solved.

In the second part of this work, we developed an implicit fractional step method which, unlike standard projection methods, allows the imposition of the original boundary conditions of the problem in all phases of the method. Space discretizations of this method, however, are restricted by the standard LBB condition. We first proved convergence of this method in the time step to a continuous solution, following the classical ideas of R. Temam for the standard projection method; the convergence results for the end–of–step velocities are improved with our method, due to the fact that they satisfy the correct boundary conditions. We then obtained some error estimates for both the intermediate and end–of–step velocities and the pressure as a function of the time step, under stronger regularity assumptions on the solution and mesh, and following the recent ideas of J. Shen for the standard projection method, among others. Furthermore, we developed a similar method to the previous one, but this time with pressure correction; we also obtained some error estimates for this alternative method. We then proved independence of the steady solution reached with implicit fractional step methods in steady flow problems, provided pressure correction is used. Finally, we developed an iterative scheme for the numerical solution of the resulting system of linear equations in each time step for our pressure correction method; this scheme is explicit in each iteration. We validated this scheme on some benchmark problems, such as the flows over a backward facing step and around a circular cylinder, with two different finite element space discretizations; good results were obtained in all cases.

Finally, we redeveloped a well–known predictor multicorrector algorithm, in a semidiscrete setting within the context of fractional step methods, with the help of the methods just introduced; this is an iterative algorithm in each time step, in which each iteration is decomposed into two phases, in a similar way to our pressure correction, fractional step method. This allowed us to justify several properties of the algorithm, such as the possibility of imposing the correct boundary conditions in all phases of the algorithm; the need for space interpolations of the algorithm to satisfy the discrete LBB condition; the independence of the steady state reached with respect to the time step in steady flow problems or the fact that a single iteration of the algorithm is enough to achieve first order accuracy in the time step. We obtained several numerical results with two different finite element discretizations of the algorithm, the classical Q_1P_0 element and the Q_2P_1 element.

As for future developments, we would first like to finish some aspects of the present work which have been left open, such as the proof of the satisfaction of our weak inf–sup condition in the case of quadrilateral and hexahedral finite elements of higher order (Q_k for $k \geq 2$), which we tried but not quite succeeded; also, the analysis of our local discrete, reformulated Stokes and Navier–Stokes problems, with parameters α_K defined elementwise, proving optimal order convergence in a suitable mesh–dependent norm. But our main next objectives will be the following: on the one hand, the theoretical analysis and implementation of a second order, viscosity splitting fractional step method; we would like to obtain second order error estimates in the time step size and numerical results which confirm them. This can be achieved by fixing the parameters θ and ϕ to $1/2$ in our pressure correction method. An iterative scheme would then be considered for the solution of the resulting system of linear (or, maybe, nonlinear) equations, which would again be explicit in each iteration. On the other hand, the theoretical analysis of fully discrete fractional step methods: we would like to give error estimates both in the time step size and the mesh size for the fully discrete solution of the standard projection method without assuming that the approximating spaces satisfy the standard inf–sup condition, but only the weak compatibility condition of Chapters 2 and 3. Moreover, we would also like to give error estimates in space and time for the fully discrete solution of our viscosity splitting method, this time assuming the standard inf–sup condition.

Appendix A

Improved error estimates

We give here some improved error estimates which we can prove for our viscosity splitting method, both with and without pressure correction, assuming that the semidiscrete velocities are uniformly bounded in $\mathbf{H}^2(\Omega)$. We also prove some error estimates for the pressure which depend on the improved error estimates for the velocity; these show that the pressure is at least weakly order 1/2 accurate for the method with and without pressure correction.

A.1 Viscosity splitting method

We give here an improved error estimate for the end–of–step velocity of our viscosity splitting method 4.8–4.10. We show that $\mathbf{u}^{n+1}$ is actually a strongly order 1 approximation of the solution in $\mathbf{L}^2(\Omega)$ and weakly order 1 in $\mathbf{H}_0^1(\Omega)$, assuming a uniform bound for $\mathbf{u}^{n+1/2}$ in $\mathbf{H}^2(\Omega)$.

Theorem A.1: *assume that* **A1** *and* **A2** *hold, and that the Stokes problem is regular; assume also that the intermediate velocities satisfy:*

$$||\mathbf{u}^{n+1/2}||_2 < C, \qquad \forall n \geq 0 \tag{A.1}$$

with $C > 0$ independent of k; then, for $N = 0, \ldots, [T/k] - 1$, and small enough k:

$$|\mathbf{e}^{N+1}|^2 \;+\; k\,\nu \sum_{n=0}^{N} ||\mathbf{e}^{n+1}||^2 \;\leq\; C\,k^2 \tag{A.2}$$

PROOF: we recall equation 4.36 here:

$$\begin{aligned} \frac{1}{k}(\mathbf{e}^{n+1} - \mathbf{e}^n) \;&-\; \nu\Delta(\mathbf{e}^{n+1}) \;+\; \nabla q^{n+1} \\ &= \;(\mathbf{u}^n \cdot \nabla)\mathbf{u}^{n+1/2} \;-\; (\mathbf{u}(t_{n+1}) \cdot \nabla)\mathbf{u}(t_{n+1}) \;+\; \mathbf{R}^n \end{aligned} \tag{A.3}$$

Taking the inner product of A.3 with $2k\mathbf{e}^{n+1}$, which is in Y, we get:

$$
\begin{aligned}
|\mathbf{e}^{n+1}|^2 &- |\mathbf{e}^n|^2 + |\mathbf{e}^{n+1}-\mathbf{e}^n|^2 + 2k\nu\,||\mathbf{e}^{n+1}||^2 \\
&= 2k\,c(\mathbf{u}^n,\mathbf{u}^{n+1/2},\mathbf{e}^{n+1}) - 2k\,c(\mathbf{u}(t_{n+1}),\mathbf{u}(t_{n+1}),\mathbf{e}^{n+1}) \\
&+ 2k < \mathbf{R}^n, \mathbf{e}^{n+1} > \qquad \text{(A.4)}
\end{aligned}
$$

The right–hand–side terms are bounded as follows. For the Taylor residual term we have:

$$
\begin{aligned}
2k < \mathbf{R}^n,\mathbf{e}^{n+1} > &\le 2k\,||\mathbf{R}^n||_{Y'}\,||\mathbf{e}^{n+1}|| \\
&\le \frac{k\nu}{4}||\mathbf{e}^{n+1}||^2 + C\,k\,||\mathbf{R}^n||^2_{Y'} \\
&= \frac{k\nu}{4}||\mathbf{e}^{n+1}||^2 + C\,k^{-1}\,||\int_{t_n}^{t_{n+1}}(t-t_n)\,\mathbf{u}_{tt}\,dt||^2_{Y'} \\
&\le \frac{k\nu}{4}||\mathbf{e}^{n+1}||^2 + C\,k^{-1}\int_{t_n}^{t_{n+1}}(t-t_n)^2\,dt\int_{t_n}^{t_{n+1}}||\mathbf{u}_{tt}||^2_{Y'}\,dt \\
&\le \frac{k\nu}{4}||\mathbf{e}^{n+1}||^2 + C\,k^2\int_{t_n}^{t_{n+1}}||\mathbf{u}_{tt}||^2_{Y'}\,dt
\end{aligned}
$$

For the nonlinear terms, we again use the splitting 4.27 to express them as:

$$
\begin{aligned}
&2k\;\left(c(\mathbf{u}^n,\mathbf{u}^{n+1/2},\mathbf{e}^{n+1}) - c(\mathbf{u}(t_{n+1}),\mathbf{u}(t_{n+1}),\mathbf{e}^{n+1})\right) \\
&= 2k\left(-c(\mathbf{u}(t_{n+1}),\mathbf{e}^{n+1/2},\mathbf{e}^{n+1}) + c(\mathbf{u}(t_n)-\mathbf{u}(t_{n+1}),\mathbf{u}^{n+1/2},\mathbf{e}^{n+1})\right. \\
&- \left.c(\mathbf{e}^n,\mathbf{u}^{n+1/2},\mathbf{e}^{n+1})\right)
\end{aligned}
$$

which we call I, II and III, respectively. Then:

$$
\begin{aligned}
\mathrm{I} &= -2k\,c(\mathbf{u}(t_{n+1}),\mathbf{e}^{n+1/2},\mathbf{e}^{n+1}) \\
&= 2k\,c(\mathbf{u}(t_{n+1}),\mathbf{e}^{n+1},\mathbf{e}^{n+1/2}) \\
&\le C\,k\,||\mathbf{u}(t_{n+1})||_2\,||\mathbf{e}^{n+1}||\,|\mathbf{e}^{n+1/2}| \\
&\le C\,k\,||\mathbf{e}^{n+1}||\,|\mathbf{e}^{n+1/2}| \\
&\le \frac{k\nu}{4}||\mathbf{e}^{n+1}||^2 + C\,k\,|\mathbf{e}^{n+1/2}|^2
\end{aligned}
$$

$$
\begin{aligned}
\mathrm{II} &= 2k\,c(\mathbf{u}(t_n)-\mathbf{u}(t_{n+1}),\mathbf{u}^{n+1/2},\mathbf{e}^{n+1}) \\
&\le C\,k\,||\mathbf{u}(t_n)-\mathbf{u}(t_{n+1})||\,||\mathbf{u}^{n+1/2}||\,||\mathbf{e}^{n+1}|| \\
&\le C\,k\,||\mathbf{u}(t_n)-\mathbf{u}(t_{n+1})||\,||\mathbf{e}^{n+1}|| \\
&= C\,k\,||\int_{t_n}^{t_{n+1}}\mathbf{u}_t\,dt||\,||\mathbf{e}^{n+1}||
\end{aligned}
$$

$$
\begin{aligned}
&\leq \; C\,k\,\|\int_{t_n}^{t_{n+1}} \mathbf{u}_t\,dt\|^2 \;+\; \frac{k\nu}{4}\|\mathbf{e}^{n+1}\|^2 \\
&\leq \; C\,k^2 \int_{t_n}^{t_{n+1}} \|\mathbf{u}_t\|^2\,dt \;+\; \frac{k\nu}{4}\|\mathbf{e}^{n+1}\|^2
\end{aligned}
$$

$$
\begin{aligned}
\mathrm{III} \;&=\; -2\,k\,c(\mathbf{e}^n, \mathbf{u}^{n+1/2}, \mathbf{e}^{n+1}) \\
&\leq\; C\,k\,|\mathbf{e}^n|\;\|\mathbf{u}^{n+1/2}\|_2\;\|\mathbf{e}^{n+1}\| \\
&\leq\; C\,k\,|\mathbf{e}^n|\;\|\mathbf{e}^{n+1}\| \\
&\leq\; C\,k\,|\mathbf{e}^n|^2 \;+\; \frac{k\nu}{4}\|\mathbf{e}^{n+1}\|^2
\end{aligned}
$$

where we have used 4.34 and A.1. Adding up A.4 for $n = 0, \ldots, N$, taking into account 4.31 for the term I, and the previous inequalities, we get:

$$
\begin{aligned}
|\mathbf{e}^{N+1}|^2 \;&+\; \sum_{n=0}^{N} |\mathbf{e}^{n+1} - \mathbf{e}^n|^2 \\
&+\; k\,\nu \sum_{n=0}^{N} \|\mathbf{e}^{n+1}\|^2 \;+\; C\,k^2\,\nu \sum_{n=0}^{N} \|\mathbf{e}^{n+1/2}\|^2 \\
&\leq\; C\,k^2 \int_0^T \|\mathbf{u}_{tt}\|_{Y'}^2\,dt \;+\; C\,k^2 \int_0^T \|\mathbf{u}_t\|^2\,dt \\
&+\; C\,k \sum_{n=0}^{N+1} |\mathbf{e}^n|^2 \;+\; C\,k \sum_{n=0}^{N} |\mathbf{e}^{n+1} - \mathbf{e}^{n+1/2}|^2 \\
&+\; C\,k^2 \sum_{n=0}^{N} \left(\|\mathbf{e}^{n+1}\|^2 \;+\; \|\mathbf{e}^{n+1} - \mathbf{e}^{n+1/2}\|^2 \right)
\end{aligned}
$$

For sufficiently small k, we can apply the discrete Gronwall lemma to the last inequality; using the regularity properties of the solution (**R2** and **R4**) and the estimates of Lemma 4.7, we get:

$$
\begin{aligned}
|\mathbf{e}^{N+1}|^2 \;&+\; \sum_{n=0}^{N} |\mathbf{e}^{n+1} - \mathbf{e}^n|^2 \;+\; k\,\nu \sum_{n=0}^{N} \|\mathbf{e}^{n+1}\|^2 \\
&\leq\; C\,k^2
\end{aligned}
$$

and 4.35 is proved. □

We now show that the pressure approximation of our viscosity splitting fractional step method is order 1/2 accurate in the time step, as it is for the classical projection method, according to [90]. We first recall a technical result, similar to that of Lemma A1 in [92]. In Theorem A.1 we have proved that, in particular:

$$\sum_{n=0}^{N} |\mathbf{e}^{n+1} - \mathbf{e}^n|^2 \leq C\, k^2$$

This implies that:

$$\sum_{n=0}^{N} ||\mathbf{e}^{n+1} - \mathbf{e}^n||_{-1}^2 \leq C\, k^2 \tag{A.5}$$

since for all $\mathbf{v} \in \mathbf{L}^2(\Omega)$, $||\mathbf{v}||_{-1} \leq C\,|\mathbf{v}|$. This is what we actually use to prove the following error estimate for the pressure:

<u>Theorem A.2:</u> *assume that* **A1** *and* **A2** *hold, that the Stokes problem is regular and that A.1 also holds; then, for* $N = 0, \ldots, [T/k] - 1$ *and small enough* k*:*

$$k \sum_{n=0}^{N} |p^{n+1} - p(t_{n+1})|_{L_0^2(\Omega)}^2 \leq C\, k \tag{A.6}$$

PROOF: we rewrite A.3 as:

$$\begin{aligned} -\nabla q^{n+1} &= \frac{1}{k}(\mathbf{e}^{n+1} - \mathbf{e}^n) - \nu\Delta(\mathbf{e}^{n+1}) - \mathbf{R}^n \\ &- (\mathbf{u}^n \cdot \nabla)\mathbf{u}^{n+1/2} + (\mathbf{u}(t_{n+1}) \cdot \nabla)\mathbf{u}(t_{n+1}) \end{aligned} \tag{A.7}$$

Using the continuous LBB condition 1.25:

$$|p|_{L_0^2(\Omega)} \leq C \sup_{\mathbf{v}\in\mathbf{H}_0^1(\Omega)} \frac{(\nabla p, \mathbf{v})}{||\mathbf{v}||}, \qquad \forall p \in L_0^2(\Omega) \tag{A.8}$$

for the pressure error $p = q^{n+1}$, we need to bound the products of the RHS of A.7 with $\mathbf{v} \in \mathbf{H}_0^1(\Omega)$. We have:

$$\begin{aligned} \frac{1}{k}(\mathbf{e}^{n+1} - \mathbf{e}^n, \mathbf{v}) &\leq \frac{1}{k}||\mathbf{e}^{n+1} - \mathbf{e}^n||_{-1}\, ||\mathbf{v}|| \\ < -\nu\Delta(\mathbf{e}^{n+1}), \mathbf{v} > &= ((\nu \mathbf{e}^{n+1}, \mathbf{v})) \leq \nu||\mathbf{e}^{n+1}||\, ||\mathbf{v}|| \\ < -\mathbf{R}^n, \mathbf{v} > &\leq ||\mathbf{R}^n||_{-1}\, ||\mathbf{v}|| \leq C\Big(\int_{t_n}^{t_{n+1}} t\, ||\mathbf{u}_{tt}||_{-1}^2\, dt\Big)^{1/2} ||\mathbf{v}|| \end{aligned}$$

For the nonlinear terms, we use the following splitting, taken from [90]:

$$\begin{aligned} -(\mathbf{u}^n \cdot \nabla)\mathbf{u}^{n+1/2} &+ (\mathbf{u}(t_{n+1}) \cdot \nabla)\mathbf{u}(t_{n+1}) \\ &= \Big((\mathbf{u}(t_{n+1}) - \mathbf{u}(t_n)) \cdot \nabla\Big)\mathbf{u}(t_{n+1}) + (\mathbf{e}^n \cdot \nabla)\mathbf{u}(t_{n+1}) \\ &+ (\mathbf{u}^n \cdot \nabla)\mathbf{e}^{n+1/2} \end{aligned} \tag{A.9}$$

so that:

$$\begin{aligned}
T_1 &= c(\mathbf{u}(t_{n+1}) - \mathbf{u}(t_n), \mathbf{u}(t_{n+1}), \mathbf{v}) \\
&\leq C\,|\mathbf{u}(t_{n+1}) - \mathbf{u}(t_n)|\;||\mathbf{u}(t_{n+1})||_2\;||\mathbf{v}|| \\
&\leq C\,|\mathbf{u}(t_{n+1}) - \mathbf{u}(t_n)|\;||\mathbf{v}|| \\
&= C\,|\int_{t_n}^{t_{n+1}} \mathbf{u}_t\,dt|\;||\mathbf{v}|| \\
&\leq C\,(k\int_{t_n}^{t_{n+1}} |\mathbf{u}_t|^2\,dt)^{1/2}\;||\mathbf{v}||
\end{aligned}$$

$$\begin{aligned}
T_2 &= c(\mathbf{e}^n, \mathbf{u}(t_{n+1}), \mathbf{v}) \\
&\leq C\,||\mathbf{e}^n||\;||\mathbf{u}(t_{n+1})||\;||\mathbf{v}|| \\
&\leq C\,||\mathbf{e}^n||\;||\mathbf{v}||
\end{aligned}$$

$$\begin{aligned}
T_3 &= c(\mathbf{u}^n, \mathbf{e}^{n+1/2}, \mathbf{v}) \\
&\leq C\,||\mathbf{u}^n||\;||\mathbf{e}^{n+1/2}||\;||\mathbf{v}|| \\
&\leq C\,||\mathbf{e}^{n+1/2}||\;||\mathbf{v}||
\end{aligned}$$

where we have used 4.33. Thus, taking the product of A.7 with $\mathbf{v}$ and taking into account A.8 and all these inequalities, we obtain:

$$\begin{aligned}
|q^{n+1}|_{L_0^2(\Omega)} &\leq \frac{C}{k}\,||\mathbf{e}^{n+1} - \mathbf{e}^n||_{-1} \\
&+ C\Big\{||\mathbf{e}^{n+1}|| + ||\mathbf{e}^n|| + ||\mathbf{e}^{n+1/2}|| \\
&+ (\int_{t_n}^{t_{n+1}} t\,||\mathbf{u}_{tt}||_{-1}^2\,dt)^{1/2} + (k\int_{t_n}^{t_{n+1}} |\mathbf{u}_t|^2\,dt)^{1/2}\Big\}
\end{aligned}$$

which yields:

$$\begin{aligned}
|q^{n+1}|^2_{L_0^2(\Omega)} &\leq \frac{C}{k^2}\,||\mathbf{e}^{n+1} - \mathbf{e}^n||_{-1}^2 \\
&+ C\Big\{||\mathbf{e}^{n+1}||^2 + ||\mathbf{e}^n||^2 + ||\mathbf{e}^{n+1/2}||^2 \\
&+ \int_{t_n}^{t_{n+1}} t\,||\mathbf{u}_{tt}||_{-1}^2\,dt + k\int_{t_n}^{t_{n+1}} |\mathbf{u}_t|^2\,dt\Big\}
\end{aligned}$$

and A.6 results from A.5, the regularity of $\mathbf{u}$, and Lemma 4.7. □

We have proved, in summary, that the pressure solution is weakly order 1/2 accurate in $L_0^2(\Omega)$.

A.2 Viscosity splitting, pressure correction method

We now give improved error estimates for the end–of–step velocities of our pressure correction method, assuming again uniform bounds for the intermediate velocities in $\mathbf{H}^2(\Omega)$ and uniform bounds for the pressure gradient in $\mathbf{L}^2(\Omega)$.

<u>Theorem A.3:</u> *assume that* **A1** *and* **A2** *hold, and that the Stokes problem is regular; assume also that the intermediate velocities satisfy:*

$$||\tilde{\mathbf{u}}^{n+1/2}||_2 < C, \qquad \forall n \geq 0 \tag{A.10}$$

with $C > 0$ *independent of* k *and that* 4.46 *also holds; then, for* $N = 0, \ldots, [T/k] - 1$, *and small enough* k:

$$|\tilde{\mathbf{e}}^{N+1}|^2 \; + \; k\,\nu \sum_{n=0}^{N} ||\tilde{\mathbf{e}}^{n+1}||^2 \;\leq\; C\,k^2 \tag{A.11}$$

PROOF: the proof is similar to that of Theorem A.1. We recall equation 4.55 here:

$$\begin{aligned}\frac{1}{k}(\tilde{\mathbf{e}}^{n+1} - \tilde{\mathbf{e}}^n) \;&-\; \nu\Delta(\tilde{\mathbf{e}}^{n+1}) \;-\; \nabla(\tilde{p}^{n+\phi} - p(t_{n+1})) \\ &= \; (\tilde{\mathbf{u}}^n \cdot \nabla)\tilde{\mathbf{u}}^{n+1/2} \;-\; (\mathbf{u}(t_{n+1}) \cdot \nabla)\mathbf{u}(t_{n+1}) \;+\; \mathbf{R}^n\end{aligned} \tag{A.12}$$

where $\tilde{p}^{n+\phi} = \phi\tilde{p}^{n+1} + (1-\phi)\tilde{p}^n$. Taking the inner product of A.12 with $2k\tilde{\mathbf{e}}^{n+1}$, which is in Y, we get:

$$\begin{aligned}|\tilde{\mathbf{e}}^{n+1}|^2 \;&-\; |\tilde{\mathbf{e}}^n|^2 \;+\; |\tilde{\mathbf{e}}^{n+1} - \tilde{\mathbf{e}}^n|^2 \;+\; 2\,k\,\nu\,||\tilde{\mathbf{e}}^{n+1}||^2 \\ &= \; 2\,k\,c(\tilde{\mathbf{u}}^n, \tilde{\mathbf{u}}^{n+1/2}, \tilde{\mathbf{e}}^{n+1}) \;-\; 2\,k\,c(\mathbf{u}(t_{n+1}), \mathbf{u}(t_{n+1}), \tilde{\mathbf{e}}^{n+1}) \\ &+ \; 2\,k\, < \mathbf{R}^n, \tilde{\mathbf{e}}^{n+1} >\end{aligned} \tag{A.13}$$

The right–hand–side terms are bounded as in Theorem A.1, using again the splitting 4.27 for the nonlinear terms, yielding:

$$\begin{aligned}2\,k\, < \mathbf{R}^n, \tilde{\mathbf{e}}^{n+1} > \;&\leq\; \frac{k\nu}{4}||\tilde{\mathbf{e}}^{n+1}||^2 \;+\; C\,k^2 \int_{t_n}^{t_{n+1}} ||\mathbf{u}_{tt}||^2_{Y'}\,dt \\ -2\,k\,c(\mathbf{u}(t_{n+1}), \tilde{\mathbf{e}}^{n+1/2}, \tilde{\mathbf{e}}^{n+1}) \;&\leq\; \frac{k\nu}{4}||\tilde{\mathbf{e}}^{n+1}||^2 \;+\; C\,k\,|\tilde{\mathbf{e}}^{n+1/2}|^2 \\ 2\,k\,c(\mathbf{u}(t_n) - \mathbf{u}(t_{n+1}), \tilde{\mathbf{u}}^{n+1/2}, \tilde{\mathbf{e}}^{n+1}) \;&\leq\; C\,k^2 \int_{t_n}^{t_{n+1}} ||\mathbf{u}_t||^2\,dt \;+\; \frac{k\nu}{4}||\tilde{\mathbf{e}}^{n+1}||^2 \\ -2\,k\,c(\tilde{\mathbf{e}}^n, \tilde{\mathbf{u}}^{n+1/2}, \tilde{\mathbf{e}}^{n+1}) \;&\leq\; C\,k\,|\tilde{\mathbf{e}}^n|^2 \;+\; \frac{k\nu}{4}||\tilde{\mathbf{e}}^{n+1}||^2\end{aligned}$$

where A.10 has been used. Adding up A.13 for $n = 0, \ldots, N$, taking into account 4.31 for the nonlinear terms and the previous inequalities, we get:

$$\begin{aligned} |\tilde{\mathbf{e}}^{N+1}|^2 &+ \sum_{n=0}^{N} |\tilde{\mathbf{e}}^{n+1} - \tilde{\mathbf{e}}^n|^2 \\ &+ k\,\nu \sum_{n=0}^{N} ||\tilde{\mathbf{e}}^{n+1}||^2 + C\,k^2\,\nu \sum_{n=0}^{N} ||\tilde{\mathbf{e}}^{n+1/2}||^2 \\ &\leq C\,k^2 \int_0^T ||\mathbf{u}_{tt}||^2_{Y'}\,dt + C\,k^2 \int_0^T ||\mathbf{u}_t||^2\,dt \\ &+ C\,k \sum_{n=0}^{N+1} |\tilde{\mathbf{e}}^n|^2 + C\,k \sum_{n=0}^{N} |\tilde{\mathbf{e}}^{n+1} - \tilde{\mathbf{e}}^{n+1/2}|^2 \\ &+ C\,k^2 \sum_{n=0}^{N} \Big(||\tilde{\mathbf{e}}^{n+1}||^2 + ||\tilde{\mathbf{e}}^{n+1} - \tilde{\mathbf{e}}^{n+1/2}||^2 \Big) \end{aligned}$$

For sufficiently small k, we can apply the discrete Gronwall lemma to the last inequality; using the regularity properties of the solution and the estimates of Lemma 4.8, we get:

$$\begin{aligned} |\tilde{\mathbf{e}}^{N+1}|^2 &+ \sum_{n=0}^{N} |\tilde{\mathbf{e}}^{n+1} - \tilde{\mathbf{e}}^n|^2 + k\,\nu \sum_{n=0}^{N} ||\tilde{\mathbf{e}}^{n+1}||^2 \\ &\leq C\,k^2 \end{aligned}$$

and A.11 is proved. □

We finally show that the pressure approximation of our viscosity splitting fractional step method with pressure correction is also weakly order 1/2 accurate in the time step in the space $L^2_0(\Omega)$. We also need a technical result, which is a consequence of the the proof of Theorem A.3. We have, in particular, that:

$$\sum_{n=0}^{N} |\tilde{\mathbf{e}}^{n+1} - \tilde{\mathbf{e}}^n|^2 \leq C\,k^2$$

which implies that:

$$\sum_{n=0}^{N} ||\tilde{\mathbf{e}}^{n+1} - \tilde{\mathbf{e}}^n||^2_{-1} \leq C\,k^2 \qquad \text{(A.14)}$$

We then have:

<u>Theorem A.4:</u> *assume that* **A1** *and* **A2** *hold, that the Stokes problem is regular, and that* 4.46 *and* A.10 *also hold; then, for* $N = 0, \ldots, [T/k] - 1$, *and small enough* k*:*

$$k \sum_{n=0}^{N} |\tilde{p}^{n+\phi} - p(t_{n+1})|^2_{L^2_0(\Omega)} \leq C\,k \tag{A.15}$$

PROOF: the proof is similar to that of Theorem A.2. We call $g^{n+1} = p(t_{n+1}) - \tilde{p}^{n+\phi}$. We rewrite 4.55 as:

$$\begin{aligned} -\nabla g^{n+1} &= \frac{1}{k}(\tilde{\mathbf{e}}^{n+1} - \tilde{\mathbf{e}}^{n}) - \nu\Delta(\tilde{\mathbf{e}}^{n+1}) - \mathbf{R}^n \\ &- (\tilde{\mathbf{u}}^n \cdot \nabla)\tilde{\mathbf{u}}^{n+1/2} + (\mathbf{u}(t_{n+1}) \cdot \nabla)\mathbf{u}(t_{n+1}) \end{aligned} \tag{A.16}$$

that is, an equality similar to A.7. Using again the LBB condition A.8, we bound the products of the RHS of A.16 with $\mathbf{v} \in \mathbf{H}^1_0(\Omega)$, to get:

$$\begin{aligned} \frac{1}{k}(\tilde{\mathbf{e}}^{n+1} - \tilde{\mathbf{e}}^{n}, \mathbf{v}) &\leq \frac{1}{k}||\tilde{\mathbf{e}}^{n+1} - \tilde{\mathbf{e}}^{n}||_{-1}\,||\mathbf{v}|| \\ < -\nu\Delta(\tilde{\mathbf{e}}^{n+1}), \mathbf{v} > &= ((\nu\tilde{\mathbf{e}}^{n+1}, \mathbf{v})) \leq \nu||\tilde{\mathbf{e}}^{n+1}||\,||\mathbf{v}|| \\ < -\mathbf{R}^n, \mathbf{v} > &\leq ||\mathbf{R}^n||_{-1}\,||\mathbf{v}|| \\ &\leq C\Big(\int_{t_n}^{t_{n+1}} t\,||\mathbf{u}_{tt}||^2_{-1}\,dt\Big)^{1/2}\,||\mathbf{v}|| \end{aligned}$$

As for the nonlinear terms, we use again the splitting 4.27, to get:

$$\begin{aligned} T_1 &= c(\tilde{\mathbf{e}}^n, \tilde{\mathbf{u}}^{n+1/2}, \mathbf{v}) \\ &\leq C\,||\tilde{\mathbf{e}}^n||\,||\tilde{\mathbf{u}}^{n+1/2}||\,||\mathbf{v}|| \\ &\leq ||\tilde{\mathbf{e}}^n||\,||\mathbf{v}|| \end{aligned}$$

$$\begin{aligned} T_2 &= -c(\mathbf{u}(t_n) - \mathbf{u}(t_{n+1}), \tilde{\mathbf{u}}^{n+1/2}, \mathbf{v}) \\ &\leq C\,||\mathbf{u}(t_n) - \mathbf{u}(t_{n+1})||\,||\tilde{\mathbf{u}}^{n+1/2}||\,||\mathbf{v}|| \\ &\leq C\,||\mathbf{u}(t_n) - \mathbf{u}(t_{n+1})||\,||\mathbf{v}|| \\ &= C\,||\int_{t_n}^{t_{n+1}} \mathbf{u}_t\,dt||\,||\mathbf{v}|| \\ &\leq (k\int_{t_n}^{t_{n+1}} ||\mathbf{u}_t||^2\,dt)^{1/2}\,||\mathbf{v}|| \end{aligned}$$

$$\begin{aligned} T_3 &= c(\mathbf{u}(t_{n+1}), \tilde{\mathbf{e}}^{n+1/2}, \mathbf{v}) \\ &= -c(\mathbf{u}(t_{n+1}), \mathbf{v}, \tilde{\mathbf{e}}^{n+1/2}) \\ &\leq C\,||\mathbf{u}(t_{n+1})||_2\,||\mathbf{v}||\,|\tilde{\mathbf{e}}^{n+1/2}| \\ &\leq C\,||\mathbf{v}||\,|\tilde{\mathbf{e}}^{n+1/2}| \end{aligned}$$

This way, we find:

$$
\begin{aligned}
|g^{n+1}|_{L^2_0(\Omega)} &\le \frac{C}{k}\,||\tilde{\mathbf{e}}^{n+1} - \tilde{\mathbf{e}}^{n}||_{-1} \\
&+ C\Big\{||\tilde{\mathbf{e}}^{n+1}|| + ||\tilde{\mathbf{e}}^{n}|| + |\tilde{\mathbf{e}}^{n+1/2}| \\
&+ \Big(\int_{t_n}^{t_{n+1}} t\,||\mathbf{u}_{tt}||^2_{-1}\,dt\Big)^{1/2} + \Big(k\int_{t_n}^{t_{n+1}} ||\mathbf{u}_t||^2\,dt\Big)^{1/2}\Big\}
\end{aligned}
$$

that is:

$$
\begin{aligned}
|g^{n+1}|^2_{L^2_0(\Omega)} &\le \frac{C}{k^2}\,||\tilde{\mathbf{e}}^{n+1} - \tilde{\mathbf{e}}^{n}||^2_{-1} \\
&+ C\Big\{||\tilde{\mathbf{e}}^{n+1}||^2 + ||\tilde{\mathbf{e}}^{n}||^2 + |\tilde{\mathbf{e}}^{n+1/2}|^2 \\
&+ \int_{t_n}^{t_{n+1}} t\,||\mathbf{u}_{tt}||^2_{-1}\,dt + k\int_{t_n}^{t_{n+1}} ||\mathbf{u}_t||^2\,dt\Big\}
\end{aligned}
$$

and A.15 follows from A.14, Theorems A.3 and 4.3 and the regularity **R2** and **R3** of **u**. □

In summary, we have obtained first order error estimates for the end-of-step velocities of our viscosity splitting method with $\theta = 1$, both with and without pressure correction, and order 1/2 estimates for the intermediate velocities, both of them strong in $\mathbf{L}^2(\Omega)$ and weak in $\mathbf{H}^1_0(\Omega)$, under the usual regularity assumptions **A1** and **A2** and the uniform bounds for the intermediate velocities in $\mathbf{H}^2(\Omega)$; we have also obtained order 1/2 weak error estimates for the pressure in $L^2_0(\Omega)$.

List of Tables

2.1 Convergence of the uncoupled block–Gauss–Seidel method. . 65
2.2 Convergence of the coupled block–Gauss–Seidel method. . . . 67
2.3 Convergence of the relaxed coupled block–Gauss–Seidel method. . . . 71
2.4 Comparison of global and local parameters. . . . 72
2.5 Theoretical orders of error in the mesh size h. . . . 80
2.6 Oden's flow: linear regression coefficients for different errors. 83

3.1 Convergence of the nonlinear solvers, Re=400. . . . 109
3.2 Convergence of the nonlinear solvers, Re=1000. . . . 109
3.3 Kovasznay flow: linear regression coefficients for different errors. . . . 117
3.4 Flow in a junction of pipes: comparison of performance of the two methods. . . . 120
3.5 Flow in a junction of pipes: flux through outflow regions. . . 121

4.1 Van Kan's flow, Q_1P_0 element. . . . 157
4.2 Van Kan's flow, Q_2P_1 element. . . . 157

5.1 Q_1P_0 element, $\gamma = 1$, 1 iteration per step. . . . 177
5.2 Q_1P_0 element, $\gamma = 1$, 2 iterations per step. . . . 178
5.3 Q_1P_0 element, $\gamma = 1$, iterating to convergence. . . . 178
5.4 Q_1P_0 element, $\gamma = 1/2$, 2 iterations per step. . . . 178
5.5 Q_1P_0 element, $\gamma = 1/2$, iterating to convergence. . . . 179
5.6 Q_2P_1 element, $\gamma = 1$, 1 iteration per step. . . . 179
5.7 Q_2P_1 element, $\gamma = 1$, 2 iterations per step. . . . 179
5.8 Q_2P_1 element, $\gamma = 1$, iterating to convergence. . . . 180
5.9 Q_2P_1 element, $\gamma = 1/2$, 2 iterations per step. . . . 180
5.10 Q_2P_1 element, $\gamma = 1/2$, iterating to convergence. . . . 180

List of Figures

2.1 Cavity flow, uniform 21×21 mesh. 65
2.2 Convergence history, consistent mass matrix: $+$ P_1 Element; $\bullet$ Q_1 Element; $\circ$ P_2 Element; $\times$ Q_2 Element. 68
2.3 Convergence history, lumped mass matrix: $+$ P_1 Element; $\bullet$ Q_1 Element; $\circ$ P_2 Element; $\times$ Q_2 Element. 69
2.4 Cavity flow, nonuniform 39×39 mesh. 72
2.5 Cavity flow, uniform 21×21 mesh, triangular elements, pressure contours: a) $P_1 - C$; b) $P_1 - L$; c) $P_2 - C$; d) $P_2 - L$. . 75
2.6 Cavity flow, uniform 21×21 mesh, quadrilateral element, pressure contours: a) $Q_1 - C$; b) $Q_1 - L$; c) $Q_2 - C$; d) $Q_2 - L$. . 76
2.7 Cavity flow, nonuniform 39×39 mesh, pressure contours: a) global α, consistent mass matrix; b) global α, lumped mass matrix; c) local α, consistent mass matrix; d) local α, lumped mass matrix. 77
2.8 Error variation with α_0: $\circ = |\mathbf{u} - \mathbf{u}_h|$; $+ = ||\mathbf{u} - \mathbf{u}_h||$; $\bullet = |p - p_h|$; $\times = |\nabla p - \nabla p_h|$; $\diamond = |\nabla p - \mathbf{w}_h|$. 79
2.9 Iteration for convergence with α_0: $+$ P_1 Element; $\bullet$ Q_1 Element; $\circ$ P_2 Element; $\times$ Q_2 Element. 80
2.10 Velocity error in L^2: $+$ P_1 Element; $\bullet$ Q_1 Element; $\circ$ P_2 Element; $\times$ Q_2 Element; $\diamond$ Mixed P_2P_1 Element. 81
2.11 Pressure error in L^2: $+$ P_1 Element; $\bullet$ Q_1 Element; $\circ$ P_2 Element; $\times$ Q_2 Element; $\diamond$ Mixed P_2P_1 Element. 81
2.12 Velocity error in H^1: $+$ P_1 Element; $\bullet$ Q_1 Element; $\circ$ P_2 Element; $\times$ Q_2 Element; $\diamond$ Mixed P_2P_1 Element. 82
2.13 Pressure error in H^1: $+$ P_1 Element; $\bullet$ Q_1 Element; $\circ$ P_2 Element; $\times$ Q_2 Element; $\diamond$ Mixed P_2P_1 Element. 82
2.14 Pressure gradient error in L^2: $+$ P_1 Element; $\bullet$ Q_1 Element; $\circ$ P_2 Element; $\times$ Q_2 Element. 83
2.15 Velocity error in L^2: $\bullet$ Q_1 Element; $\times$ Q_2 Element; $\square =$ GLS method, Q_1 Element; $\diamond$ GLS method, Q_2 Element. . . . 84
2.16 Pressure error in L^2: $\bullet$ Q_1 Element; $\times$ Q_2 Element; $\square =$ GLS method, Q_1 Element; $\diamond$ GLS method, Q_2 Element. . . . 85
2.17 Velocity error in H^1: $\bullet$ Q_1 Element; $\times$ Q_2 Element; $\square =$ GLS method, Q_1 Element; $\diamond$ GLS method, Q_2 Element. . . . 85
2.18 Pressure error in H^1: $\bullet$ Q_1 Element; $\times$ Q_2 Element; $\square =$ GLS method, Q_1 Element; $\diamond$ GLS method, Q_2 Element. . . . 86

2.19 Trapezoidal domain, coarse mesh. 87
2.20 Trapezoidal domain, pressure contours: a) GLS method, coarse mesh; b) GLS method, fine mesh; c) Present method, coarse mesh; d) Present method, fine mesh. 88

3.1 Cavity flow, Re=400, streamlines. 111
3.2 Cavity flow, Re=400, pressure contours. 112
3.3 Cavity flow, Re=1000, streamlines. 112
3.4 Cavity flow, Re=1000, pressure contours. 113
3.5 Kovasznay flow, velocity error in L^2: $+$ P_1 Element; $\bullet$ Q_1 Element; $\circ$ P_2 Element; $\times$ Q_2 Element; $\square =$ GLS method, Q_1Q_1 element. 114
3.6 Kovasznay flow, pressure error in L^2: $+$ P_1 Element; $\bullet$ Q_1 Element; $\circ$ P_2 Element; $\times$ Q_2 Element; $\square =$ GLS method, Q_1Q_1 element. 114
3.7 Kovasznay flow, velocity error in H^1: $+$ P_1 Element; $\bullet$ Q_1 Element; $\circ$ P_2 Element; $\times$ Q_2 Element; $\square =$ GLS method, Q_1Q_1 element. 115
3.8 Kovasznay flow, pressure error in H^1: $+$ P_1 Element; $\bullet$ Q_1 Element; $\circ$ P_2 Element; $\times$ Q_2 Element; $\square =$ GLS method, Q_1Q_1 element. 115
3.9 Kovasznay flow, pressure gradient error in L^2: $+$ P_1 Element; $\bullet$ Q_1 Element; $\circ$ P_2 Element; $\times$ Q_2 Element. 116
3.10 Kovasznay flow, streamlines. 118
3.11 Kovasznay flow, pressure contours. 118
3.12 Flow through a junction, mesh. 119
3.13 Flow through a junction: a) GLS method, streamlines; b) GLS method, pressure contours; c) Present method, streamlines; d) Present method, pressure contours. 122

4.1 Backward facing step, mesh. 158
4.2 Backward facing step, Q_1P_0 element, streamlines: a) $Re = 60$; b) $Re = 200$; c) $Re = 400$. 160
4.3 Backward facing step, Q_2P_1 element, streamlines: a) $Re = 60$; b) $Re = 200$; c) $Re = 400$. 161
4.4 Flow past a cylinder, mesh. 162
4.5 Flow past a cylinder, $Re = 40$, streamlines. 162
4.6 Flow past a cylinder, $Re = 40$, stationary streamlines. 163
4.7 Flow past a cylinder, $Re = 40$, nodal pressure contours. . . . 163
4.8 Flow past a cylinder, $Re = 100$, nodal velocity history. 164
4.9 Flow past a cylinder, $Re = 100$, streamlines. 165
4.10 Flow past a cylinder, $Re = 100$, stationary streamlines. . . . 165
4.11 Flow past a cylinder, $Re = 100$, nodal pressure contours. . . . 166
4.12 Flow past a cylinder, $Re = 100$, Fourier spectrum of the nodal velocity solution. 167

5.1 Kovasznay flow, Q_1P_0 element, streamlines. 182
5.2 Kovasznay flow, Q_2P_1 element, streamlines. 182
5.3 Kovasznay flow, Q_1P_0 element, element pressure values. . . . 183
5.4 Kovasznay flow, Q_2P_1 element, nodal pressure contours. . . . 183
5.5 Kovasznay flow, Q_1P_0 element with checkboard mode filtered, element pressure values. 184
5.6 Kovasznay flow, Q_1P_0 element with checkboard mode filtered, nodal pressure contours. 185
5.7 Kovasznay flow, maximum nodal error: • Q_1P_0 element, ○ Q_2P_1 element. 185
5.8 Cavity flow, streamlines: a) Q_1P_0 element; b) Q_2P_1 element. . 187
5.9 Cavity flow, Q_1P_0 element, element pressure values. 188
5.10 Cavity flow, Q_2P_1 element, nodal pressure contours. 188
5.11 Cavity flow, horizontal velocity profile through cavity centerline $x = 0.5$: — $Q1P0$ element; - - - $Q2P1$ element; ◇ Reference [43]. 189
5.12 Cavity flow, vertical velocity profile through cavity centerline $y = 0.5$: — $Q1P0$ element; - - - $Q2P1$ element; ◇ Reference [43]. 189
5.13 Noflow problem, mesh. 190
5.14 Noflow problem, Q_1P_0 element, velocity vectors. 191
5.15 Noflow problem, Q_2P_1 element, velocity vectors. 191
5.16 Noflow problem, Q_1P_0 element, pressure contours. 192
5.17 Noflow problem, Q_2P_1 element, pressure contours. 192
5.18 Jet flow, Q_1P_0 element, streamlines: a) $t = 1.2$; b) $t = 2.5$; c) $t = 4.0$. 193
5.19 Jet flow, Q_2P_1 element, streamlines: a) $t = 1.2$; b) $t = 2.5$; c) $t = 4.0$. 194
5.20 Jet flow, Q_1P_0 element, nodal pressure contours: a) $t = 1.2$; b) $t = 2.5$; c) $t = 4.0$. 195
5.21 Jet flow, Q_2P_1 element, nodal pressure contours: a) $t = 1.2$; b) $t = 2.5$; c) $t = 4.0$. 196

References

[1] R.A. Adams: *Sobolev spaces.* Academic Press, New York, 1975.

[2] B.F. Armaly, F. Durst, J.C.F. Pereira, B. Shönung: "Experimental and theoretical investigation of backward–facing step flow." *Journal of Fluid Mechanics,* Vol. **127**, p. 473–496, 1983.

[3] D.N. Arnold, F. Brezzi, M. Fortin: "A stable finite element for the Stokes equations." *Calcolo,* Vol. **21**, p. 337–344, 1984.

[4] I. Babuŝka: "Error bounds for the finite element method." *Numerische Mathematik,* Vol. **16**, p. 322–333, 1971.

[5] C. Baiocci, F. Brezzi, L.P. Franca: "Virtual bubbles and Galerkin–least–squares type methods (Ga.L.S.)." *Computer Methods in Applied Mechanics and Engineering,* Vol. **105**, p. 125–141, 1993.

[6] M.A. Behr, L.P. Franca, T.E. Tezduyar: "Stabilized finite element methods for the velocity–pressure–stress formulation of incompressible flows." *Computer Methods in Applied Mechanics and Engineering,* Vol. **104**, p. 31–48, 1993.

[7] M.A. Behr, D. Hastreiter, S. Mittal, T.E. Tezduyar: "Incompressible flow past a circular cylinder: dependence of the computed flow field on the location of the lateral boundaries." *Computer Methods in Applied Mechanics and Engineering,* Vol. **123**, p. 309–316, 1995.

[8] J.B. Bell, P. Colella, H.M. Glaz: "A Second-Order Projection Method for the incompressible Navier–Stokes equations." *Journal of Computational Physics,* Vol. **85**, p. 257–283, 1989.

[9] M Bercovier, O.A. Pironneau: "Error estimates for finite element solution of the Stokes problem in the primitive variables." *Numerische Mathematik,* Vol. **33**, p. 211–224, 1979.

[10] J. Blair Perot: "An Analysis of the fractional–step projection method." *Journal of Computational Physics,* Vol. **108**, p. 51–58, 1993.

[11] J. Blasco, R. Codina, A. Huerta: "A fractional step method for the incompressible Navier–Stokes equations related to a predictor–multicorrector algorithm." *International Journal for Numerical Methods in Fluids,* submitted.

[12] J.M. Boland, R.A. Nicolaides: "Stability of finite elements under divergence constraints." *SIAM Journal of Numerical Analysis,* Vol. **20**, p. 722–731, 1983.

[13] S.C. Brenner, L.R. Scott: *The mathematical theory of finite element methods.* Springer–Verlag, 1994.

[14] F. Brezzi: "On the existence, uniqueness and approximation of saddle–point problems arising from Lagrange multipliers." *RAIRO ,* Vol. **B-R2**, p. 129–151, 1974.

[15] F. Brezzi, K-J. Bathe: "A discourse on the stability conditions for mixed finite element formulations." *Computer Methods in Applied Mechanics and Engineering,* Vol. **82**, p. 27–57, 1990.

[16] F. Brezzi, M.O. Bristeau, L.P. Franca, M. Mallet, G. Rogé: "A relationship between stabilized finite element methods and the Galerkin method with bubble functions." *Computer Methods in Applied Mechanics and Engineering,* Vol. **96**, p. 117–129, 1992.

[17] F. Brezzi, J. Douglas: "Stabilized mixed methods for the Stokes problem." *Numerische Mathematik,* Vol. **53**, p. 225–235, 1988.

[18] F. Brezzi, R.S. Falk: "Stability of higher–order Hood–Taylor methods." *SIAM Journal of Numerical Analysis,* Vol. **28**, p. 581–590, 1991.

[19] F. Brezzi, M. Fortin: *Mixed and Hybrid finite element methods.* Springer Series in Computational Mathematics, 15. Springer–Verlag, 1991.

[20] A.N. Brooks, T.J.R. Hughes: "Streamline upwind Petrov–Galerkin formulations for convection dominated flows with particular enphasis on the incompressible Navier–Stokes equations." *Computer Methods in Applied Mechanics and Engineering,* Vol. **32**, p. 199–259, 1982.

[21] G.F. Carey, R. Krishnan: "Penalty finite element method for the Navier–Stokes equations." *Computer Methods in Applied Mechanics and Engineering,* Vol. **42**, p. 183–224, 1984.

[22] A.J. Chorin: "A numerical method for solving incompressible viscous flow problems." *Journal of Computational Physics,* Vol. **2**, p. 12–26, 1967.

[23] A.J. Chorin: "Numerical solution of the Navier–Stokes equations." *Mathematics of Computation,* Vol. **22**, p. 745–762, 1968.

[24] A.J. Chorin: "On the convergence of discrete approximations to the Navier–Stokes equations." *Mathematics of Computation,* Vol. **23**, p. 341–353, 1969.

[25] P.G. Ciarlet: *The finite element method for elliptic problems.* North–Holland, Amsterdam, 1978.

[26] R. Codina, J. Blasco: "A finite element formulation for the Stokes problem allowing equal order interpolation." *Computer Methods in Applied Mechanics and Engineering,* accepted for publication.

[27] R. Codina, E. Oñate, M. Cervera: "The intrinsic time for the streamline upwind/Petrov–Galerkin formulation using quadratic elements." *Computer Methods in Applied Mechanics and Engineering,* Vol. **94**, p. 239–262, 1992.

[28] R. Codina, M. Vázquez, O.C. Zienkiewicz: "A fractional step method for compressible flows: boundary conditions and incompressible limit." *Proceedings of the IXth. International Conference on Finite Elements in Fluids - New trends and applications, Venezia, Italy,* Vol. **I**, p. 409–418, 1995.

[29] G.K. Despotis, S. Tsangaris: "Fractional step method for solution of incompressible Navier–Stokes equations on unstructured triangular meshes." *International Journal for Numerical Methods in Fluids,* Vol. **20**, p. 1273–1288, 1995.

[30] J. Donea, S. Giuliani, H. Laval, L. Quartapelle: "Finite element solution of the unsteady Navier–Stokes equations by a fractional step method." *Computer Methods in Applied Mechanics and Engineering,* Vol. **30**, p. 53–73, 1982.

[31] J.J. Droux, T.J.R. Hughes: "A boundary integral modification of the Galerkin least squares formulation for the Stokes problem." *Computer Methods in Applied Mechanics and Engineering,* Vol. **113**, p. 173–182, 1994.

[32] J. K. Dukovicz, A. S. Dvinsky: "Approximate Factorization as a High Order Splitting for the Implicit Incompressible Flow Equations." *Journal of Computational Physics,* Vol. **102**, p. 336–347, 1992.

[33] H.A. Dwyer, S. Ibrani: "Time accurate solutions of the incompressible and three–dimensional Navier–Stokes equations." *Computer Methods in Applied Mechanics and Engineering,* Vol. **75**, p. 333–341, 1989.

[34] M.S. Engel, M-A. Jamnia: "Transient flow past a circular cylinder: a benchmark solution." *International Journal for Numerical Methods in Fluids,* Vol. **11**, p. 985–1000, 1990.

[35] L.P. Franca, S.L. Frey, T.J.R. Hughes: "Stabilized finite element methods: I. Application to the advective–diffusive model.." *Computer Methods in Applied Mechanics and Engineering,* Vol. **95**, p. 253–276, 1992.

[36] L.P. Franca, S.L. Frey: "Stabilized finite element methods: II. The incompressible Navier–Stokes equations.." *Computer Methods in Applied Mechanics and Engineering,* Vol. **99**, p. 209–233, 1992.

[37] L.P. Franca, T.J.R. Hughes: "Convergence analyses of Galerkin least–squares methods for symmetric advective–diffusive forms of the Stokes and incompressible Navier–Stokes equations." *Computer Methods in Applied Mechanics and Engineering,* Vol. **105**, p. 285–298, 1993.

[38] E. Fernandez–Cara, M. Marin Beltrán: "The convergence of two numerical schemes for the Navier–Stokes equations." *Numerische Mathematik,* Vol. **55**, p. 33–60, 1989.

[39] M. Fortin, A. Fortin: "Experiments with several elements for viscous incompressible flows." *International Journal for Numerical Methods in Fluids,* Vol. **5**, p. 911–928, 1985.

[40] M. Fortin, A. Fortin: "New and newer elements for incompressible flows." *Finite elements in fluids,* Vol. **6**, p. 171–187, 1985.

[41] M. Fortin, R. Peyret, R. Temam: "Résolution numerique des equations de Navier–Stokes pour un fluide incompressible." *J. Mécanique,* Vol. **10**, p. 357–390, 1971.

[42] U. Ghia, K.N. Ghia, C.T. Shin: "High–Re solutions for incompressible flow using the Navier–Stokes equations and a multigrid method." *Journal of Computational Physics,* Vol. **48**, p. 387–411, 1982.

[43] V. Girault, P. A. Raviart: *Finite Element Approximation of the Navier–Stokes Equation.* Springer–Verlag, New York, 1986.

[44] R. Glowinski, T.W. Pan, J. Periaux: "A fictitious domain method for external incompressible viscous flow modeled by Navier–Stokes equations." *Computer Methods in Applied Mechanics and Engineering,* Vol. **112**, p. 133-148, 1994.

[45] P. M. Gresho: "On the theory of semi–implicit projection methods for viscous incompressible flow and its implementation via a finite element method that also introduces a nearly consistent mass matrix. Part I: theory." *International Journal for Numerical Methods in Fluids,* Vol. **11**, p. 587–620, 1990.

[46] P. M. Gresho, S.T. Chan: "On the theory of semi–implicit projection methods for viscous incompressible flow and its implementation via a finite element method that also introduces a nearly consistent mass matrix. Part 2: implementation." *International Journal for Numerical Methods in Fluids,* Vol. **11**, p. 621–659, 1990.

[47] P.M. Gresho, R.L. Lee, R.L. Sani: "Further studies in equal order interpolation for Navier–Stokes." *Fifth International Symposium on Finite Elements in Flow Problems,* Austin, Texas, 1984.

[48] P. M. Gresho, R. Sani: "On pressure boundary conditions for the incompressible Navier–Stokes equations." *International Journal for Numerical Methods in Fluids,* Vol. **7**, p. 1111–1145, 1987.

[49] P. Grisvard: *Elliptic problems on non–smooth domains.* Pitman, Marschfields, Massachussets, 1985.

[50] J-L. Guermond: "Remarques sur les méthodes de projection pour l'approximation des équations de Navier–Stokes." *Numerische Mathematik,* Vol. **67**, p. 465–473, 1994.

[51] J-L. Guermond, L. Quartapelle: "Unconditionally stable finite–element method for the unsteady Navier–Stokes equations." *Proceedings of the 9–th International Conference on Finite Elements in Fluids - New trends and applications, Venezia, Italy, October 1995,* Vol. **I**, p. 367–376.

[52] S. Hassanzadeh, V. Sonnad, S. Foresti: "Finite element implementation of boundary conditions for the pressure Poisson equation of incompressible flow." *International Journal for Numerical Methods in Fluids,* Vol. **18**, p. 1009–1019, 1994.

[53] D.M. Hawken, H.R. Tamaddon-Jahromi, P. Townsend, M.F. Webster: "A Taylor–Galerkin–based algorithm for viscous incompressible flow." *International Journal for Numerical Methods in Fluids,* Vol. **10**, p. 327–351, 1990.

[54] J.G. Heywood, R Rannacher: "Finite element approximation of the nonstationary Navier–Stokes problem: Part 1: Regularity of solutions and second order error estimates for spatial discretization." *SIAM Journal of Numerical Analysis,* Vol. **19**, p. 275–311, 1982.

[55] J.G. Heywood, R Rannacher: "Finite element approximation of the nonstationary Navier–Stokes problem: Part 4: Error analysis for second–order time discretization." *SIAM Journal of Numerical Analysis,* Vol. **27**, p. 353–384, 1990.

[56] J.G. Heywood, R Rannacher, S. Turek: "Artifitial boundaries and flux and pressure conditions for the incompressible Navier–Stokes equations." *International Journal for Numerical Methods in Fluids,* Vol. **22**, p. 325-352, 1996.

[57] T.J.R. Hughes, M. Mallet, A. Mizukami: "A new finite element formulation for computational fluid dynamics: II. Beyond SUPG." *Computer Methods in Applied Mechanics and Engineering,* Vol. **54**, p. 341–355, 1986.

[58] T.J.R. Hughes, M. Mallet: "A new finite element formulation for computational fluid dynamics: III. The generalized streamline operator for multidimensional advection–diffusion systems." *Computer Methods in Applied Mechanics and Engineering,* Vol. **58**, p. 305–328, 1986.

[59] T.J.R. Hughes, L.P. Franca, M. Balestra: "A new finite element formulation for computational fluid dynamics: V. Circumventing the Babuŝka–Brezzi condition: a stable Petrov–Galerkin formulation of the Stokes problem accomodating equal–order interpolations." *Computer Methods in Applied Mechanics and Engineering,* Vol. **59**, p. 85–99, 1986.

[60] T.J.R. Hughes, L.P. Franca: "A new finite element formulation for computational fluid dynamics: VII. The Stokes problem with various well–posed boundary conditions: symmetric formulations that converge for all velocity/pressure spaces." *Computer Methods in Applied Mechanics and Engineering,* Vol. **65**, p. 85–96, 1987.

[61] T.J.R. Hughes, L.P. Franca, G. M. Hulbert: "A new finite element formulation for computational fluid dynamics: VIII. The Galerkin/least squares method for advective–diffusive equations." *Computer Methods in Applied Mechanics and Engineering,* Vol. **73**, p. 173–189, 1989.

[62] J. van Kan: "A second–order accurate pressure correction scheme for viscous incompressible flow." *SIAM Journal of Sci. Stat. Comp.,* Vol. **7**, N. 3, p. 870–891, 1986.

[63] G.E. Karniadakis, M. Israeli, S.E. Orzag: "High order splittting methods for the incompressible Navier–Stokes equations." *Journal of Computational Physics,* Vol. **59**, p. 414–443, 1991.

[64] M. Kawahara, K. Ohmiya: "Finite element analysis of density flow using the velocity–correction method." *International Journal for Numerical Methods in Fluids,* Vol. **5**, p. 981–993, 1985.

[65] J. Kim, P. Moin: "Application of a Fractional–Step Method to incompressible Navier–Stokes equations." *Journal of Computational Physics,* Vol. **59**, p. 308–323, 1985.

[66] L. Kleiser, U. Shumann: *Treatment of incompressibility and boundary conditions in 3-D numerical spectral simulation of plane channel flows.* Hirschel E. H. ed., Proc. 3rd GAMM Conference on Numerical Methods in Fluid Mechanics, Vieweg–Verlag Braunschweig, 1980.

[67] P. Klouček, F. Rys: "Stability of the fractional step θ–scheme for the nonstationary Navier–Stokes equations." *SIAM Journal of Numerical Analysis,* Vol. **31**, p. 1312–1335, 1990.

[68] A. Kovacs, M. Kawahara: "A finite element scheme based on the velocity–correction method for the solution of the time–dependent incompressible Navier–Stokes equations." *International Journal for Numerical Methods in Fluids,* Vol. **13**, p. 403–423, 1991.

[69] L.I.G. Kovasznay: "Laminar flow behind a two–dimensional grid." *Proc. Cambridge Philos. Soc.,* Vol. **44**, 1948.

[70] Y. Kwok, K. Tam: "Linearized stability analysis of staggered–grid difference schemes for multidimensional viscous incompressible flows." *Numerical Methods for Partial Differential Equations* , Vol. **9**, p. 313–322, 1993.

[71] O. A. Ladyzhenskaya: *The mathematical theory of viscous incompressible flow.* Gordon and Breach, New York, 1969.

[72] L.D. Landau, E.M. Lifshitz: *Course of theoretical Physics, Vol. 6: Fluid Mechanics.* Pergamin Press, Oxford, 1959.

[73] H. Laval, L. Quartapelle: "A fractional–step Taylor–Galerkin method for unsteady incompressible flows." *International Journal for Numerical Methods in Fluids,* Vol. **11**, p. 501–513, 1990.

[74] H. Le, P. Moin: "An improvement of Fractional–Step Methods for the incompressible Navier–Stokes equations." *Journal of Computational Physics,* Vol. **92**, p. 369–379, 1991.

[75] W.K. Liu, J. Gvildys: "Fluid–structure interaction of tanks with an eccentric core barrel." *Computer Methods in Applied Mechanics and Engineering,* Vol. **58**, p. 51–77, 1986.

[76] Y. Lung–an: "Viscosity–splitting scheme for the Navier–Stokes equations." *Numerical Methods for Partial Differential Equations,* Vol. **7**, p. 317–338, 1991.

[77] R. Natarajan: "A Numerical Method for Incompressible Viscous Flow Simulation." *Journal of Computational Physics,* Vol. **100**, p. 384–395, 1992.

[78] J.T. Oden, O-P. Jacquotte: "Stability of some mixed finite element methods for Stokesian flows." *Computer Methods in Applied Mechanics and Engineering,* Vol. **43**, p. 231–247, 1984.

[79] S. A. Orzag, M. Israeli, M. O. Deville: "Boundary conditions for incompressible flows." *Journal of Scientific Computing,* Vol. **1**, N. 1, p. 75–111, 1986.

[80] T.N. Phillips, G.W. Roberts: "The treatment of spurious pressure modes in spectral incompressible flow calculations." *Journal of Computational Physics,* Vol. **105**, p. 150–164, 1993.

[81] A. Pinelli, A. Vacca: "Chebyshev collocation method and multidomain decomposition for the incompressible Navier–Stokes equations." *International Journal for Numerical Methods in Fluids,* Vol. **18**, p. 781–799, 1994.

[82] L. Quartapelle, M. Napolitano: "Integral conditions for the pressure in the computation of incompressible viscous flows." *Journal of Computational Physics,* Vol. **62**, p. 340–348, 1986.

[83] P.A. Raviart, J.M. Thomas: *Introduction à l'analyse numérique des équations aux dérivées partielles.* Masson, Paris, 1983.

[84] G. de Rham: *Varietés Différentiables.* Hermann, 1960.

[85] R.L. Sani, P.M. Gresho, R.L. Lee, D.F. Griffiths: "The cause and cure (?) of the spurious pressures generated by certain FEM solutions of the incompressible Navier–Stokes equations: Part 1." *International Journal for Numerical Methods in Fluids,* Vol. **1**, p. 17–43, 1981.

[86] R.L. Sani, P.M. Gresho, R.L. Lee, D.F. Griffiths, M. Engelman: "The cause and cure (?) of the spurious pressures generated by certain FEM solutions of the incompressible Navier–Stokes equations: Part 2." *International Journal for Numerical Methods in Fluids,* Vol. **1**, p. 171–204, 1981.

[87] G.E. Schneider, G.D. Raithby, M.M. Yovanovich: "Finite element analysis of incompressible fluid flow incorporating equal order pressure and velocity interpolation." *Numerical Methods in Laminar and Turbulent flow,* Pentech Press, Plymouth, 1978.

[88] R. Schreiber, H.B. Keller: "Driven cavity flows by efficient numerical techniques." *Journal of Computational Physics,* Vol. **49**, p. 310–333, 1983.

[89] J. Shen: "Hopf bifurcation of the unsteady regularized driven cavity flow." *Journal of Computational Physics,* Vol. **95**, p. 228–245, 1991.

[90] J. Shen: "On error estimates of projection methods for Navier–Stokes equations: first–order schemes." *SIAM Journal Numerical Analysis,* Vol. **29**, p. 57–77, 1992.

[91] J. Shen: "On error estimates of some higher order projection and penalty–projection methods for Navier–Stokes equations." *Numerische Mathematik,* Vol. **62**, p. 49–73, 1992.

[92] J. Shen: "Remarks on the pressure error estimates for the projection method." *Numerische Mathematik,* Vol. **67**, p. 513–520, 1994.

[93] S.J. Sherwin, G.E. Karniadakis: "A triangular spectral element method; application to the incompressible Navier–Stokes equations." *Computer Methods in Applied Mechanics and Engineering,* Vol. **123**, p. 189–229, 1995.

[94] D. Silvester: "Optimal low order finite element methods for incompressible flow." *Computer Methods in Applied Mechanics and Engineering,* Vol. **111**, p. 357–368, 1994.

[95] D. Silvester, N. Kechkar: "Stabilized bilinear–constant velocity–pressure finite elements for the conjugate gradient solution of the Stokes problem." *Computer Methods in Applied Mechanics and Engineering,* Vol. **79**, p. 71–86, 1990.

[96] J.C. Simó, F. Armero: "Unconditional stability and long–term behaviour of transient algorithms for the incompressible Navier–Stokes and Euler equations." *Computer Methods in Applied Mechanics and Engineering,* Vol. **111**, p. 111–154, 1994.

[97] R. Stenberg: "A technique for analysing finite element methods for viscous incompressible flow." *International Journal for Numerical Methods in Fluids,* Vol. **11**, p. 935–948, 1990.

[98] G. Strang, J. Fix: *An Analisys of the finite element method.* Englewood Cliffs, New Jork, Prentice-Hall 1973.

[99] T. Tanahashi, H. Okanaga, T. Saito: "GSMAC finite element method for unsteady incompressible Navier-Stokes equations at high Reynolds numbers." *International Journal for Numerical Methods in Fluids,* Vol. **11**, p. 479–499, 1990.

[100] R. Temam: "Une méthode d'approximations de la solution des equations de Navier–Stokes." *Bull. Soc. Math. France,* Vol. **98**, p. 115–152, 1968.

[101] R. Temam: "Sur la stabilité et la convergence de la méthode des pas fractionaires." *Ann. Mat. Pura Appl.,* Vol. **LXXIV**, p. 191–380, 1968.

[102] R. Temam: "Sur l'approximation de la solution des équations de Navier–Stokes par la méthode des pas fractionaires (I)." *Arch. Rac. Mech. Anal.,* Vol. **32**, N. 2, p. 135–153, 1969.

[103] R. Temam: "Sur l'approximation de la solution des équations de Navier–Stokes par la méthode des pas fractionaires (II)." *Arch. Rac. Mech. Anal.,* Vol. **33**, p. 377–385, 1969.

[104] R. Temam: *Navier–Stokes equations and Nonlinear Functional Analysis.* CBMS-NSF Regional Conference Series in Applied Mathematics, SIAM, Philadelphia, PA, 1983.

[105] R. Temam: *Navier–Stokes equations. Theory and Numerical Analysis.* North–Holland, Amsterdam, 3rd. Edition, 1984.

[106] R. Temam: "Remark on the Pressure Boundary Condition for the Projection Method." *Theoretical and Computational Fluid Dynamics,* Vol. **3**, p. 181–184, 1991.

[107] T.E. Tezduyar, S. Mittal, S.E. Ray, R. Shih: "Incompressible flow computations using stabilized bilinear and linear equal–order–interpolation velocity–pressure elements." *Computer Methods in Applied Mechanics and Engineering,* Vol. **95**, p. 221–242, 1992.

[108] T.E. Tezduyar, S. Mittal, R. Shih: "Time–accurate incompressible flow computations with quadrilateral elements." *Computer Methods in Applied Mechanics and Engineering,* Vol. **87**, p. 363–384, 1991..

[109] R. Verfürth: "Error estimates for a mixed finite element approximation of the Stokes equation." *RAIRO Anal. Numér.,* Vol. **18**, p. 175–182, 1984.

[110] N. N. Yanenko: *The Method of Fractional Steps.* Springer–Verlag, Berlin, 1971.

[111] K. Yosida: *Functional analysis.* 5th. Ed., Springer–Verlag, Berlin, 1978.

[112] O.C. Zienkiewicz, R. Codina: "A general algorithm for compressible and incompressible flow– Part I. The split, characteristic based scheme." *International Journal for Numerical Methods in Fluids,* Vol. **20**, p. 869–885, 1995.

[113] O.C. Zienkiewicz, J. Wu: "Incompressibility without tears – how to avoid restrictions of mixed formulation." *International Journal for Numerical Methods in Engineering,* Vol. **32**, p. 1189–1203, 1991.

UNIVERSITAT POLITÈCNICA DE CATALUNYA
E.T.S. D'ENGINYERS DE CAMINS, CANALS I PORTS
DEPARTAMENT DE MATEMÀTICA APLICADA III

ANALYSIS OF FRACTIONAL STEP, FINITE ELEMENT METHODS FOR THE INCOMPRESSIBLE NAVIER–STOKES EQUATIONS

by

Jorge Blasco Lorente

Advisors: Antonio Huerta Cerezuela,
Ramon Codina Rovira.

Program: Applied Mathematics.

Barcelona, December 1996.

Chapter 5

A predictor–multicorrector algorithm

In this Chapter we study a form of a predictor–multicorrector algorithm customized to the unsteady, incompressible Navier–Stokes equations. This algorithm, developed originally for general evolution equations in a discrete setting, was applied succesfully to several unsteady incompressible flow problems in the eighties, such as fluid–structure interaction problems. Here, and in the light of the viscositty splitting methods developed in the previous Chapter, we redevelop the algorithm in a semidiscrete formulation, thus providing an interpretation of it within the context of fractional step methods. This gives a theoretical explanation for some properties of the algorithm such the need for the spatial interpolation used to satisfy the discrete LBB condition, the order of accuracy of the discrete solutions with respect to the time step or the reason behind the imposition of boundary conditions in each phase of the algorithm. We will see, in particular, that our viscosity splitting method can in some cases be understood as a predictor–corrector form of this algorithm. Most of these ideas can be found in [26].

The predictor–multicorrector algorithm is usually implemented together with a bilinear velocity, constant pressure (Q_1P_0) finite element interpolation; we implemented also the biquadratic velocity, linear pressure (Q_2P_1) element, which satisfies the LBB condition, to compare the properties of the two discretizations.

The outline of the Chapter is the following: in Section 5.1 we present our semidiscrete formulation of the scheme, proving that it corresponds to the predictor–multicorrector algorithm and showing in what sense it can be understood as a fractional step method. In 5.2 we introduce the two finite element interpolations considered, the resulting fully discrete equations and some considerations relative to the actual implementation of the scheme. Finally, in 5.3 we present some numerical results obtained with the algorithm on several test problems.

5.1 Semidiscrete form of the algorithm

Let us consider the predictor–multicorrector algorithm developed by T.J.R. Hughes and coworkers, which was applied to the incompressible Navier–Stokes equations in [20]; it can also be found in [75] in a similar context. We give here an alternative derivation of the algorithm, within the context of fractional step methods.

Given a time step $\delta t > 0$ and a parameter γ such that $0 < \gamma \leq 1$, and assuming that the velocity $\mathbf{u}^n$ and pressure p^n are known at time $t_n = n\,\delta t$, an implicit method of the form:

$$\begin{aligned} \frac{\mathbf{u}^{n+1} - \mathbf{u}^n}{\delta t} - \gamma\,\mathbf{a}^{n+1} - (1-\gamma)\mathbf{a}^n &= 0 \\ \nabla \cdot (\mathbf{u}^{n+1}) &= 0 \\ \mathbf{u}^{n+1}|_\Gamma &= 0 \end{aligned} \tag{5.1}$$

is considered for the solution of 1.7–1.5 with homogeneous Dirichlet boundary conditions 1.10, where we define:

$$\mathbf{a}^m \;=\; \mathbf{f}(t_m) \;-\; \nabla p^m \;-\; (\mathbf{u}^m \cdot \nabla)\mathbf{u}^m \;+\; \nu\Delta\mathbf{u}^m \tag{5.2}$$

An iterative scheme is introduced for the solution of the nonlinear, coupled problem 5.1. It starts with some predictions $\mathbf{u}_0^{n+1}$ and p_0^{n+1} for $\mathbf{u}^{n+1}$ and p^{n+1}, respectively, which will be specified next. Then, each iteration is split into two steps. The first one accounts for viscous and convective effects, but not for the incompressibility condition; this is dealt with in the second step, in a similar way to the fractional step methods of Chapter 4. Pressure correction is used, and the convective term is approximated explicitly for simplicity. Given the i–th iteration approximations $\mathbf{u}_i^{n+1}$ and p_i^{n+1} to $\mathbf{u}^{n+1}$ and p^{n+1}, the first step of the $(i+1)$–th iteration then consists of finding an *intermediate iteration* velocity $\mathbf{u}_{i+1/2}^{n+1}$ such that:

$$\begin{aligned} \frac{\mathbf{u}_{i+1/2}^{n+1} - \mathbf{u}^n}{\delta t} \;-\; \gamma\nu\Delta\mathbf{u}_{i+1/2}^{n+1} &= \gamma\mathbf{f}(t_{n+1}) \;+\; (1-\gamma)\mathbf{a}^n \\ &- \;\gamma(\mathbf{u}_i^{n+1} \cdot \nabla)\mathbf{u}_i^{n+1} \;-\; \gamma\nabla p_i^{n+1} \\ \mathbf{u}_{i+1/2}^{n+1}|_\Gamma &= 0 \end{aligned} \tag{5.3}$$

The notation $\mathbf{u}_{i+1/2}^{n+1}$ has been chosen deliverately to emphasise that the solution of 5.3 is an intermediate iteration aproximation of the velocity at time t_{n+1}. In the second step of each iteration, a pressure increment is used to enforce incompressibility, in a similar way to the method of Section 4.5. Thus, one looks for an *end–of–iteration* velocity $\mathbf{u}_{i+1}^{n+1}$ and pressure p_{i+1}^{n+1} such that:

$$\begin{aligned} \frac{\mathbf{u}_{i+1}^{n+1}-\mathbf{u}_{i+1/2}^{n+1}}{\delta t} - \gamma\nu\Delta(\mathbf{u}_{i+1}^{n+1}-\mathbf{u}_{i+1/2}^{n+1}) + \gamma\nabla(p_{i+1}^{n+1}-p_i^{n+1}) &= 0 \\ \nabla\cdot\mathbf{u}_{i+1}^{n+1} &= 0 \\ \mathbf{u}_{i+1}^{n+1}|_\Gamma &= 0 \end{aligned} \tag{5.4}$$

The multicorrector scheme 5.3–5.4 is performed, in principle, to convergence in i, that is, until $\mathbf{u}_{i+1}^{n+1}=\mathbf{u}_i^{n+1}$ and $p_{i+1}^{n+1}=p_i^{n+1}$, at which time one sets $\mathbf{u}^{n+1}=\mathbf{u}_{i+1}^{n+1}$ and $p^{n+1}=p_{i+1}^{n+1}$ and goes back to the predictor phase.

We can show that this method is another version, independent of any particular spatial discretization, of the predictor–multicorrector algorithm of [20], which was given in a discrete setting after a Q_1P_0 finite element interpolation of the Navier–Stokes equations, which results in the following constrained system of ODEs:

$$\begin{aligned} M\dot{U} + KU + A(U)U + G_0P &= F \\ G_0^tU &= 0 \end{aligned}$$

In terms of accelerations ($\mathcal{A}$) and time derivatives of elemental pressures ($\dot{P}$), the algorithm then reads:

Predictor phase:

$$\begin{aligned} U_0^{n+1} &= U^n + (1-\gamma)\,\delta t\,\mathcal{A}^n \\ \mathcal{A}_0^{n+1} &= 0 \\ P_0^{n+1} &= P^n + (1-\gamma)\,\delta t\,\dot{P}^n \\ \dot{P}_0^{n+1} &= 0 \end{aligned}$$

Solution phase:

$$B\ \delta\mathcal{A}_1 = R_1 \tag{5.5}$$

$$\gamma^2\ (\delta t)^2\ (G_0^tB^{-1}G_0)\ (\delta\dot{P}) = G_0^t\ (U_i^{n+1}+\gamma\delta t(\delta\mathcal{A}_1)) \tag{5.6}$$

$$B\ \delta\mathcal{A}_2 = -\gamma\,\delta t\,G_0\,(\delta\dot{P}) \tag{5.7}$$

where all the matrices have been defined before and the residual vector R_1 is given by:

$$R_1 = F^{n+1} - M\mathcal{A}_i^{n+1} - KU_i^{n+1} - A(U_i^{n+1})U_i^{n+1} - G_0P_i^{n+1}$$

Corrector phase:

$$\begin{aligned}
\mathcal{A}_{i+1}^{n+1} &= \mathcal{A}_i^{n+1} + \delta\mathcal{A}_1 + \delta\mathcal{A}_2 \\
U_{i+1}^{n+1} &= U^n + (1-\gamma)\,\delta t\,\mathcal{A}^n + \gamma\,\delta t\,\mathcal{A}_{i+1}^{n+1} \\
\dot{P}_{i+1}^{n+1} &= \dot{P}_i^{n+1} + \delta\dot{P} \\
P_{i+1}^{n+1} &= P^n + (1-\gamma)\,\delta t\,\dot{P}^n + \gamma\,\delta t\,\dot{P}_{i+1}^{n+1}
\end{aligned}$$

The value of i is then incremented in 1 and the scheme goes back to the solution phase again. We now have:

Lemma 5.1: *the scheme* 5.3–5.4 *is equivalent to the predictor–multicorrector algorithm of* [20].

PROOF: assume the velocity $\mathbf{u}^n$, acceleration $\mathbf{a}^n$, pressure p^n and pressure temporal variation $\dot{p}^n$ are known at time $t_n = n\delta t$, satisfying 5.2 and the incompressibility condition 1.5. The iterative predictor–multicorrector procedure starts with the following predictions:

$$\begin{aligned}
\mathbf{u}_0^{n+1} &= \mathbf{u}^n + (1-\gamma)\,\delta t\,\mathbf{a}^n && (5.8) \\
\mathbf{a}_0^{n+1} &= 0 && (5.9) \\
p_0^{n+1} &= p^n + (1-\gamma)\,\delta t\,\dot{p}^n && (5.10) \\
\dot{p}_0^{n+1} &= 0 && (5.11)
\end{aligned}$$

Assume, further that after each correction phase the approximation of velocity and pressure may be written as:

$$\begin{aligned}
\mathbf{u}_i^{n+1} &= \mathbf{u}^n + (1-\gamma)\,\delta t\,\mathbf{a}^n + \gamma\,\delta t\,\mathbf{a}_i^{n+1} && (5.12) \\
p_i^{n+1} &= p^n + (1-\gamma)\,\delta t\,\dot{p}^n + \gamma\,\delta t\dot{p}_i^{n+1} && (5.13)
\end{aligned}$$

where $\mathbf{a}_i^{n+1}$ and $\dot{p}_i^{n+1}$ are the corrected values at the end of the i–th iteration. Note that equations 5.12–5.13 are also valid for the initial prediction ($i = 0$).

The objective of each iteration is to compute new approximations $\mathbf{u}_{i+1}^{n+1}$ and p_{i+1}^{n+1} by computing corrected values of $\mathbf{a}_{i+1}^{n+1}$ and $\dot{p}_{i+1}^{n+1}$. Since each iteration is split into two steps, an intermediate velocity $\mathbf{u}_{i+1/2}^{n+1}$ and acceleration $\mathbf{a}_{i+1/2}^{n+1}$ are first calculated. If the intermediate velocity is expressed as:

$$\mathbf{u}_{i+1/2}^{n+1} = \mathbf{u}^n + (1-\gamma)\,\delta t\,\mathbf{a}^n + \gamma\,\delta t\,\mathbf{a}_{i+1/2}^{n+1} \qquad (5.14)$$

and the intermediate acceleration is defined as:

$$\mathbf{a}_{i+1/2}^{n+1} = \mathbf{a}_i^{n+1} + \delta\mathbf{a}_1$$

then the following relation is deduced from 5.12:

$$\mathbf{u}_{i+1/2}^{n+1} = \mathbf{u}_i^{n+1} + \gamma\,\delta t\,\delta\mathbf{a}_1$$

The intermediate velocity and acceleration are computed from the first split step, namely equations 5.3, which can thus be rewritten as:

$$\begin{aligned} \delta\mathbf{a}_1 - \gamma\nu\delta t(\Delta\delta\mathbf{a}_1) &= \mathbf{f}^{n+1} - \mathbf{a}_i^{n+1} - \nabla p_i^{n+1} + \nu\Delta\mathbf{u}_i^{n+1} - (\mathbf{u}_i^{n+1}\cdot\nabla)\mathbf{u}_i^{n+1} \\ \delta\mathbf{a}_1|_\Gamma &= 0 \end{aligned} \qquad (5.15)$$

The end–of–step velocity $\mathbf{u}_{i+1}^{n+1}$ is expressed, using 5.12, as:

$$\mathbf{u}_{i+1}^{n+1} = \mathbf{u}^n + (1-\gamma)\,\delta t\,\mathbf{a}^n + \gamma\,\delta t\,\mathbf{a}_{i+1}^{n+1} \qquad (5.16)$$

and can be further simplified in terms of the intermediate velocity, using equation 5.14, and the end–of–step acceleration, which is defined as:

$$\mathbf{a}_{i+1}^{n+1} = \mathbf{a}_{i+1/2}^{n+1} + \delta\mathbf{a}_2$$

Thus:

$$\mathbf{u}_{i+1}^{n+1} = \mathbf{u}_{i+1/2}^{n+1} + \gamma\,\delta t\,\delta\mathbf{a}_2 \qquad (5.17)$$

Likewise, from 5.13, the end–of–step pressure p_{i+1}^{n+1} is expressed as:

$$p_{i+1}^{n+1} = p^n + (1-\gamma)\,\delta t\,\dot{p}^n + \gamma\,\delta t\,\dot{p}_{i+1}^{n+1} \qquad (5.18)$$

where the new pressure variation is determined by:

$$\dot{p}_{i+1}^{n+1} = \dot{p}_i^{n+1} + \delta\dot{p}$$

and consequently one gets:

$$p_{i+1}^{n+1} = p_i^{n+1} + \gamma\,\delta t\,\delta\dot{p} \qquad (5.19)$$

With the previous expressions of the end–of–step velocity and pressure, equations 5.17 and 5.19 respectively, the second split step defined by the equation system 5.4 can be written as:

$$\begin{aligned} \delta\mathbf{a}_2 - \gamma\nu\delta t(\Delta\delta\mathbf{a}_2) + \gamma\delta t\nabla(\delta\dot{p}) &= 0 \\ \nabla\cdot(\delta\mathbf{a}_2) &= \frac{-1}{\gamma\delta t}\nabla\cdot(\mathbf{u}_i^{n+1} + \gamma\delta t\,\delta\mathbf{a}_1) \\ \delta\mathbf{a}_2|_\Gamma &= 0 \end{aligned} \qquad (5.20)$$

Given the time–discretization scheme defined by 5.12–5.13, equations 5.15 and 5.20 are another version of the two split–step equations 5.3 and 5.4 defined previously. After they have been solved, the corresponding corrections are performed, namely equations 5.16 and 5.18. The weak for of the split equations 5.3–5.4 is the following:

First step: find $\mathbf{u}_{i+1/2}^{n+1} \in \mathbf{H}_0^1(\Omega)$ such that:

$$\frac{1}{\delta t}(\mathbf{u}_{i+1/2}^{n+1} - \mathbf{u}^n, \mathbf{v}) + \gamma\nu((\mathbf{u}_{i+1/2}^{n+1}, \mathbf{v})) = \gamma(\mathbf{f}(t_{n+1}), \mathbf{v}) + (1-\gamma)(\mathbf{a}^n, \mathbf{v}) - \gamma c(\mathbf{u}_i^{n+1}, \mathbf{u}_i^{n+1}, \mathbf{v}) - \gamma b(\mathbf{v}, p_i^{n+1}), \forall \mathbf{v} \in \mathbf{H}_0^1(\Omega) \quad (5.21)$$

Second step: find $\mathbf{u}_{i+1}^{n+1} \in \mathbf{H}_0^1(\Omega)$ and $s_{i+1}^{n+1} = \gamma\,\delta t\, p_{i+1}^{n+1} \in L_0^2(\Omega)$ such that:

$$\begin{aligned} a_\gamma(\mathbf{u}_{i+1}^{n+1}, \mathbf{v}) + b(\mathbf{v}, s^{n+1}) &= a_\gamma(\mathbf{u}_{i+1/2}^{n+1}, \mathbf{v}), \quad && \forall \mathbf{v} \in \mathbf{H}_0^1(\Omega) \\ b(\mathbf{u}_{i+1}^{n+1}, q) &= 0, && \forall q \in L_0^2(\Omega) \quad (5.22) \end{aligned}$$

where the bilinear form a_γ was defined in 4.14. Existence and uniqueness of solutions to these problems are established the same way as for the fractional step methods of Chapter 4. In terms of accelerations and pressure time derivatives, the corresponding weak forms of equations 5.15 and 5.20 are:

First step: find $\delta\mathbf{a}_1 \in \mathbf{H}_0^1(\Omega)$ such that:

$$\begin{aligned} a_\gamma(\delta\mathbf{a}_1, \mathbf{v}) &= (\mathbf{f}^{n+1}, \mathbf{v}) - (\mathbf{a}_i^{n+1}, \mathbf{v}) - b(\mathbf{v}, p_i^{n+1}) \\ &- \nu((\mathbf{u}_i^{n+1}, \mathbf{v})) - c(\mathbf{u}_i^{n+1}, \mathbf{u}_i^{n+1}, \mathbf{v}), \quad \forall \mathbf{v} \in \mathbf{H}_0^1(\Omega) \quad (5.23) \end{aligned}$$

Second step: find $\delta\mathbf{a}_2 \in \mathbf{H}_0^1(\Omega)$ and $\delta\dot{p} \in L_0^2(\Omega)$ such that:

$$\begin{aligned} a_\gamma(\delta\mathbf{a}_2, \mathbf{v}) + \gamma\,\delta t\, b(\mathbf{v}, \delta\dot{p}) &= 0, && \forall \mathbf{v} \in \mathbf{H}_0^1(\Omega) \\ b(\delta\mathbf{a}_2, q) &= \frac{1}{\gamma\,\delta t} b(\mathbf{u}_i^{n+1} + \gamma\delta t\,\delta\mathbf{a}_1, q), && \forall q \in L_0^2(\Omega) (5.24) \end{aligned}$$

A finite element discretization of this scheme is the same algorithm as the one considered in [20]. □

There is a clear formal relationship between the structure of the split equations 5.3–5.4 and the viscosity–splitting pressure–correction method of Section 4.3. In fact, the latter method with parameters $\theta = \phi = 1$ is equivalent to a single correction of the former with $\gamma = 1$, since in that case $\mathbf{u}_0^{n+1} = \mathbf{u}^n$ and $p_0^{n+1} = p^n$ (see 5.8 and 5.10); the only difference, though, is the treatment of the nonlinear term, which is then explicit in the predictor–multicorrector algorithm. One then has that $\mathbf{u}_{1/2}^{n+1} = \mathbf{u}^{n+1/2}$, $\mathbf{u}_1^{n+1} = \mathbf{u}^{n+1}$ and $p_1^{n+1} = p^{n+1}$. The paralelism between these two methods implies that discrete interpolations of the predictor–multicorrector algorithm are subject to the satisfaction of the LBB condition, so that in confined flow problems the Q_1P_0 element will develop checkboard pressure modes; that, at least for $\gamma = 1$, one correction is enough to achieve first order accuracy in the time step, and that when a steady state is reached with this algorithm, it will be independent of the time step.

5.2 Finite element discretization

We now introduce a finite element space discretization into the multicorrector scheme 5.23–5.24. If $V_h \subset \mathbf{H}_0^1(\Omega)$ and $Q_h \subset L_0^2(\Omega)$ denote finite dimensional subspaces defined through a finite element discretization of Ω, the discrete version of 5.23 consists of finding $\delta \mathbf{a}_{1,h} \in V_h$ such that:

$$\begin{aligned} a_\gamma(\delta \mathbf{a}_{1,h}, \mathbf{v}_h) &= (\mathbf{f}^{n+1}, \mathbf{v}_h) - (\mathbf{a}_{i,h}^{n+1}, \mathbf{v}_h) - b(\mathbf{v}_h, p_{i,h}^{n+1}) \\ &- \nu((\mathbf{u}_{i,h}^{n+1}, \mathbf{v}_h)) - c(\mathbf{u}_{i,h}^{n+1}, \mathbf{u}_{i,h}^{n+1}, \mathbf{v}_h), \quad \forall \mathbf{v}_h \in V_h \qquad (5.25) \end{aligned}$$

whereas in the discrete version of 5.24 we look for $\delta \mathbf{a}_{2,h} \in V_h$ and $\delta \dot{p}_h \in Q_h$ such that:

$$\begin{aligned} a_\gamma(\delta \mathbf{a}_{2,h}, \mathbf{v}_h) + \gamma\, \delta t\, b(\mathbf{v}_h, \delta \dot{p}_h) &= 0, \qquad \forall \mathbf{v}_h \in V_h \qquad (5.26) \\ b(\delta \mathbf{a}_{2,h}, q_h) &= \frac{1}{\gamma\, \delta t} b(\mathbf{u}_{i,h}^{n+1} + \gamma \delta t\, \delta \mathbf{a}_{1,h}, q_h), \forall q_h \in Q_h \end{aligned}$$

Calling again $\mathcal{A}$ and $\dot{P}$ the vectors of nodal accelerations and pressure time derivatives representing the functions $\mathbf{a}_h$ and $\dot{p}_h$, respectively, the weak form of equations 5.25–5.26 can be written in matrix form, with the notation introduced up to now, as:

$$B\, \delta \mathcal{A}_1 = R_1 \qquad (5.27)$$

$$B\, \delta \mathcal{A}_2 + \gamma\, \delta t\, G_0\, (\delta \dot{P}) = 0 \qquad (5.28)$$

$$G_0^t\, \mathcal{A}_2 = -\frac{1}{\gamma\, \delta t} G_0^t\, (U_i^{n+1} + \gamma\, \delta t\, \delta \mathcal{A}_1) \qquad (5.29)$$

By isolating $\delta \mathcal{A}_2$ from 5.28 and substituting it into 5.29, one gets equation 5.6, that is, the pressure update equation of the solution phase of the predictor multicorrector algorithm. This equation, however, is not affordable in practice, since it involves the inversion of a full matrix B to form the system matrix $G_0^t B^{-1} G_0$, which is prohibitive in general. Some approximations are introduced in [20] in this scheme, which make it computationally feasible. The matrix B is approximated by M in all its appearances (the difference between the two, $\delta t\, \nu\, L$, is dropped). This approximation is first order accurate in the time step, so that the errors it introduces are of the same order of magnitude as those of the method itself. Moreover, the matrix M is then lumped, which allows the pressure system 5.6 to be a possible way to compute the pressure variation in each iteration. Thus, the final scheme reads:

$$\begin{aligned} M^L\, \delta A_1 &= R_1 \\ \gamma^2\, (\delta t)^2\, (G_0^t (M^L)^{-1} G_0)\, (\delta \dot{P}) &= G_0^t\, (U_i^{n+1} + \gamma \delta t (\delta A_1)) \\ M^L\, \delta A_2 &= -\gamma\, \delta t\, G_0\, (\delta \dot{P}) \end{aligned}$$

Inversion of the diagonal matrix M^L is now trivial. This is the algorithm actually implemented in practice. It has to be said that the introduction of these simplifications (which are due to T.J.R. Hughes and coworkers) has a double theoretical implication: on the one hand, the approximation of B by M in 5.5 leads to an explicit treatment of diffusion in each iteration (although not in each time step, if the algorithm is iterated at least twice per step); on the other hand, the approximation of B by M in 5.6 and 5.7 implies that the algorithm actually used admits an interpretation within the context of fractional step methods relative to the standard projection method, that is, without a viscous term in the incompressibility phase. A single iteration of this simplified predictor–multicorrector algorithm is actually equivalent to the standard projection method. If it is understood this way, a question arises about which boundary conditions are to be imposed in the incompressibility phase, whether the full Dirichlet condition or only the normal component of it.

If two or more iterations of this scheme are performed, all terms in the Navier–Stokes equations are treated implicitly. Thus, no δt limitations are expected for the stability of the algorithm over a wide range of Reynolds numbers. However, the iterative nature of the scheme and the simplifications introduced in it (such as the explicit treatment of the convective term) impose restrictions on δt for the stability of the iterative process, specially for quadratic elements, as will be seen in the next Section.

5.3 Numerical results

We now present some results obtained with the predictor–multicorrector algorithm just considered, both with a Q_1P_0 and a Q_2P_1 finite element interpolation, on five test problems. First, van Kan's problem is used again to study numerically the order of accuracy in the time step of this algorithm with different values of the parameter γ and different numbers of iterations per time step; then, we consider again the Kovasznay flow problem, this time to prove numerically the independence of the steady state reached with a pressure correction algorithm from the time step used, and to study the dependence of the error with respect to the analytical solution on the mesh size for each of the two elements; we then solve the standard cavity flow problem with both interpolations, and the so called 'no flow test', and finally, we consider a plane jet simulation as another example of a purely unsteady problem.

5.3.1 Numerical accuracy study

We considered again the test problem introduced by van Kan in [62], this time to study numerically the order of accuracy with respect to the time step of the predictor–multicorrector algorithm with different values of the parameter γ and different number of iterations in each time step. The same mesh, boundary conditions and Reynolds number as in Subsection 4.5.1 were

δt	$\kappa_1(\delta t)$	$\kappa_2(\delta t)$	$\kappa_p(\delta t)$
1/16	2.04	2.02	2.03
1/32	2.02	2.01	2.02
1/64	2.01	2.01	2.01
1/128	1.99	1.99	2.00

Table 5.1: Q_1P_0 element, $\gamma = 1$, 1 iteration per step.

considered, and also the same definitions of the quotients $\kappa_i(\delta t)$ $(i = 1, 2)$ and $\kappa_p(\delta t)$.

In Tables 5.1 to 5.10, we present the results obtained with $\gamma = 1$ both for 1 and 2 iterations of the multicorrector scheme per time step and iterating it to convergence in each time step, and for $\gamma = 1/2$ with 2 iterations and iterating to convergence, both for the Q_1P_0 and the Q_2P_1 elements (the latter was unstable for large values of the time step).

The backward Euler scheme $\gamma = 1$ is clearly first order accurate, both for the Q_1P_0 and the Q_2P_1 elements and both for 1 and 2 iterations per step and iterating to convergence in each time step. In this last case, it took an average of 10 iterations per time–step to reduce the initial residuals by 7 orders of magnitude. For this value of γ, anyway, it is unnecessary to converge in each time step in order to obtain first order accuracy, since either 1 or 2 iterations are sufficient for that purpose. In all these cases, the pressure solution was also first order accurate.

For the Crank–Nicholson case $\gamma = 1/2$, however, iterating to convergence is compulsory to achieve second order accuracy in the velocity solution. If a fixed number of 2 iterations per time step is chosen, second order accuracy is lost, but the quotients obtained are still larger than 2 (indicating a higher order than 1).

5.3.2 Kovasznay flow

We then solved the Kovasznay flow problem considered in Section 3.5, this time with the predictor–multicorrector algorithm of the previous Section, with $\gamma = 1$ and 1 iteration per step, until a steady state was reached. Our main interest here was proving numerically that the steady state obtained with this pressure–correction method is independent of the time step used, in agreement with the theoretical results of Section 4.6, as well as performing a numerical study of the order of accuracy of the solution with respect to the mesh size, for each of the two finite elements employed.

δt	$\kappa_1(\delta t)$	$\kappa_2(\delta t)$	$\kappa_p(\delta t)$
1/16	2.55	3.73	2.11
1/32	1.99	2.23	2.03
1/64	1.98	2.06	2.01
1/128	1.98	1.99	2.00

Table 5.2: Q_1P_0 element, $\gamma = 1$, 2 iterations per step.

δt	$\kappa_1(\delta t)$	$\kappa_2(\delta t)$	$\kappa_p(\delta t)$
1/16	2.00	1.99	2.02
1/32	1.97	2.02	2.00
1/64	1.97	1.95	2.00
1/128	2.01	1.83	2.01

Table 5.3: Q_1P_0 element, $\gamma = 1$, iterating to convergence.

δt	$\kappa_1(\delta t)$	$\kappa_2(\delta t)$
1/7	4.41	5.90
1/8	2.47	4.08
1/10	1.69	2.91
1/12	1.66	2.51
1/14	1.70	2.33

Table 5.4: Q_1P_0 element, $\gamma = 1/2$, 2 iterations per step.

δt	$\kappa_1(\delta t)$	$\kappa_2(\delta t)$
1/7	4.06	4.08
1/8	4.04	4.04
1/10	4.03	4.01
1/12	3.75	3.99
1/14	4.00	3.79

Table 5.5: Q_1P_0 element, $\gamma = 1/2$, iterating to convergence.

δt	$\kappa_1(\delta t)$	$\kappa_2(\delta t)$	$\kappa_p(\delta t)$
1/16	2.24	2.27	2.04
1/32	2.01	1.99	2.02
1/64	2.00	1.99	2.01
1/128	1.97	1.99	2.01

Table 5.6: Q_2P_1 element, $\gamma = 1$, 1 iteration per step.

δt	$\kappa_1(\delta t)$	$\kappa_2(\delta t)$	$\kappa_p(\delta t)$
1/32	3.87	5.62	2.57
1/64	2.20	2.60	2.09
1/128	2.05	2.15	2.03
1/256	2.01	2.05	2.02

Table 5.7: Q_2P_1 element, $\gamma = 1$, 2 iterations per step.

δt	$\kappa_1(\delta t)$	$\kappa_2(\delta t)$	$\kappa_p(\delta t)$
1/32	1.98	1.98	2.01
1/64	1.99	2.00	2.01
1/128	2.00	1.95	1.99

Table 5.8: Q_2P_1 element, $\gamma = 1$, iterating to convergence.

δt	$\kappa_1(\delta t)$	$\kappa_2(\delta t)$
1/16	5.80	6.07
1/20	3.38	4.05
1/24	2.57	3.30

Table 5.9: Q_2P_1 element, $\gamma = 1/2$, 2 iterations per step.

δt	$\kappa_1(\delta t)$	$\kappa_2(\delta t)$
1/16	3.83	4.15
1/20	3.96	4.04
1/24	3.86	3.92

Table 5.10: Q_2P_1 element, $\gamma = 1/2$, iterating to convergence.

We took again $\Omega = [-\frac{1}{2}, 1] \times [-\frac{1}{2}, \frac{1}{2}]$ and a uniform mesh consisting of 31×21 nodes, which is used to define the elements for both the Q_1P_0 and Q_2P_1 cases. The Reynold's number was 10 this time. Since the flow is confined, i.e., the velocity is prescribed on all the boundary (and equal to the analytical solution 3.32), a linear restriction should be imposed on the pressure to remove the hydrostatic (constant) pressure mode. In our code we set the value of the pressure in the last element in the element numbering strategy equal to zero (this corresponds to the degree of freedom number $(3 \times n_e - 2)$ for the Q_2P_1 element, where n_e is the number of elements).

In order to compare the steady state obtained with two different time steps δt_i and δt_j, starting from the fluid at rest in the interior of Ω and the analytical solution on the boundary, we define the difference between these two solutions as the Euclidean norm of the difference of the nodal velocity vectors, namely:

$$\text{Diff}(\delta t_i, \delta t_j) \doteq |U(\delta t_i) - U(\delta t_j)|_2$$

where $|.|_2$ is again the Euclidean norm of a vector and $U(\delta t)$ is the nodal velocity vector obtained at steady state with time step δt. In this problem we can also compare the numerical solutions with the analytical solution 3.32; for that purpose we considered the relative maximum difference between the exact and computed nodal velocity vector:

$$\text{Err}(\delta t) \doteq \frac{\max_{i=1,\dots n_p}\left\{|U_{x,i}(\delta t) - U^{\text{ex}}_{x,i}|, |U_{y,i}(\delta t) - U^{\text{ex}}_{y,i}|\right\}}{\max_{i=1,\dots n_p}\left\{|U^{\text{ex}}_{x,i}|, |U^{\text{ex}}_{y,i}|\right\}} \qquad (5.30)$$

where the subindex i refers to node a_i ($i = 1, \dots, n_p$, n_p being the number of nodal points), the subindeces x and y refer to the two components of velocity and U^{ex} is the vector of exact nodal velocities.

For the Q_1P_0 element and the present mesh, we tried with time steps $\delta t_1 = 0.01$, $\delta t_2 = 0.005$ and $\delta t_3 = 0.001$. In each case, a steady state was reached when $|U^n(\delta t) - U^{n+1}(\delta t)|_2$ was less than 10^{-12}. The three differences $\text{Diff}(\delta t_i, \delta t_j)$ computed were smaller than 10^{-10}, thus confirming independence of the steady state with respect to the time step.

For the Q_2P_1 element we took $\delta t_1 = 0.0025$, $\delta t_2 = 0.001$ and $\delta t_3 = 0.0005$, and a steady state was reached again at a tolerance of 10^{-12}. The differences were also smaller than 10^{-10} this time.

The velocity solutions obtained can be seen in Figures 5.1 and 5.2, where we show the streamlines for the two elements. As for the pressures, the Q_1P_0 developed an obvious *checkboard* mode, as could be anticipated by the structure of the second step of the method 5.22. The elemental pressures for this element can be seen in Figure 5.3; we also show, in Figure 5.4, the nodal pressure contours obtained with the Q_2P_1 element after a least–squares nodal interpolation process.

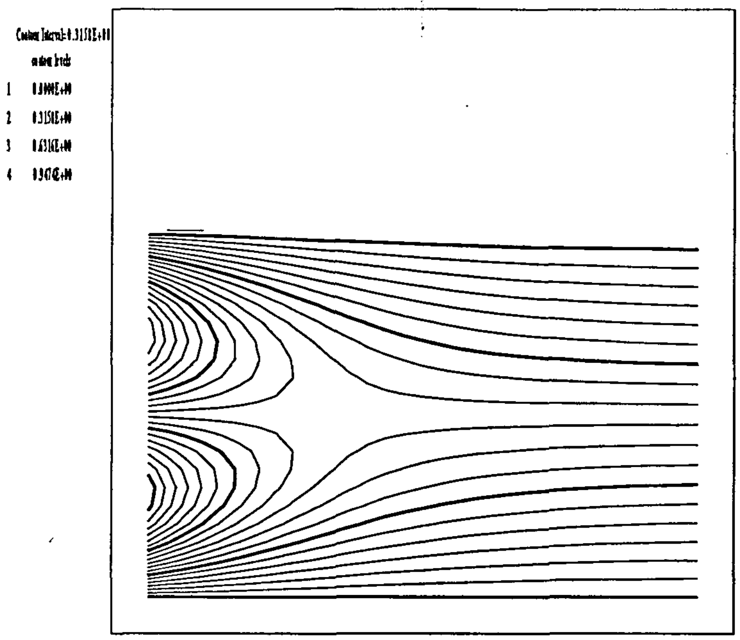

Figure 5.1: Kovasznay flow, Q_1P_0 element, streamlines.

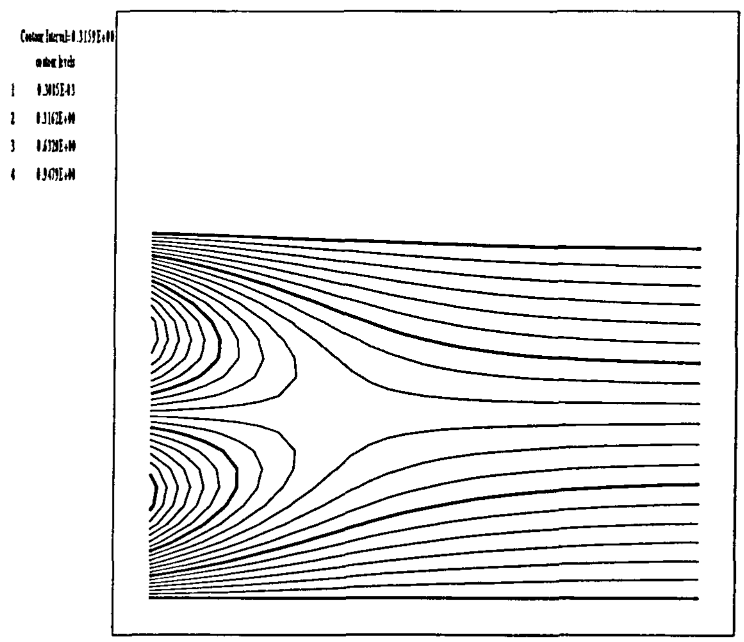

Figure 5.2: Kovasznay flow, Q_2P_1 element, streamlines.

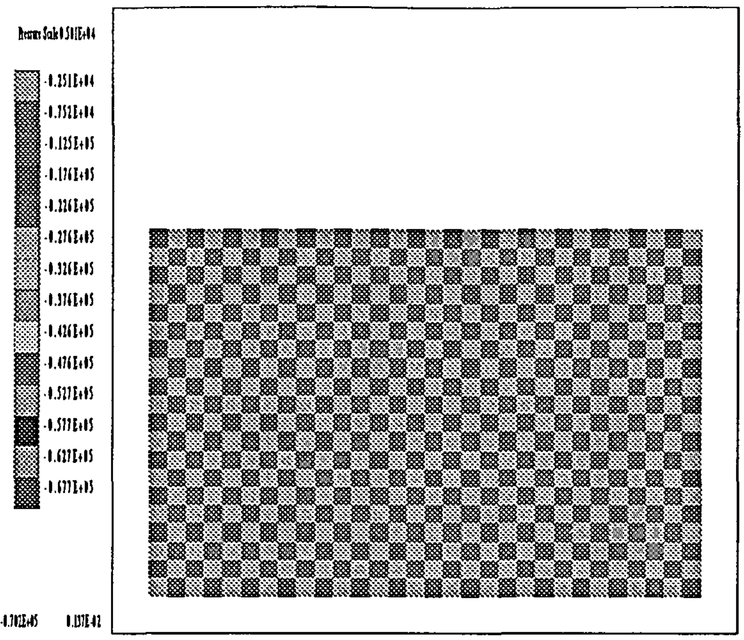

Figure 5.3: Kovasznay flow, Q_1P_0 element, element pressure values.

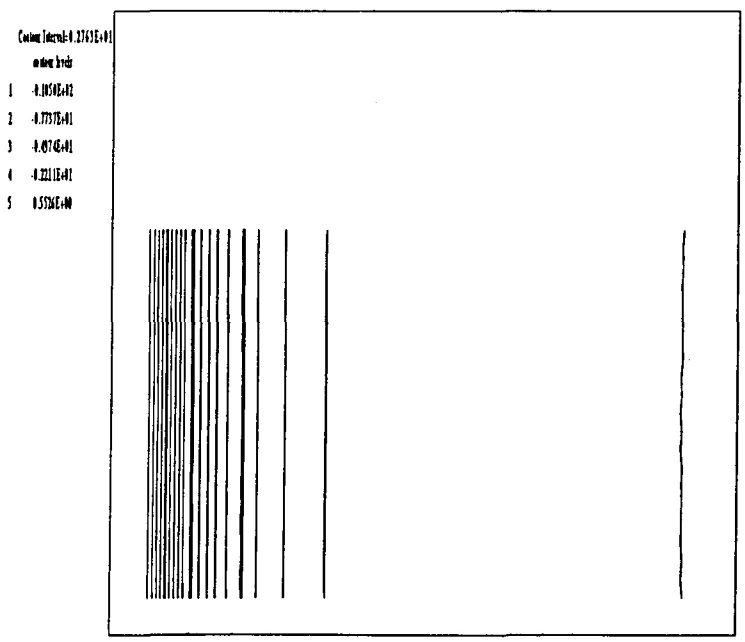

Figure 5.4: Kovasznay flow, Q_2P_1 element, nodal pressure contours.

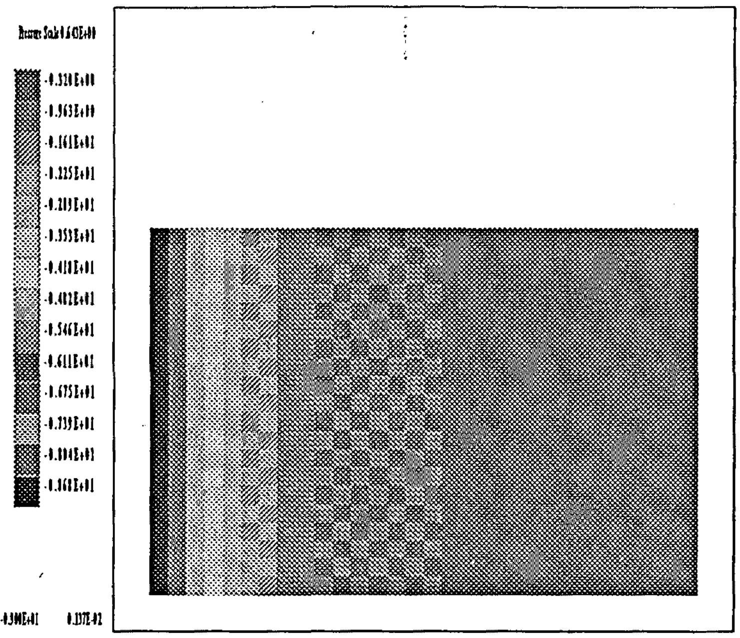

Figure 5.5: Kovasznay flow, Q_1P_0 element with checkboard mode filtered, element pressure values.

Since in this problem we know the exact pressure solution, we can determine the actual value of the spurious pressure mode present in the Q_1P_0 element solution. We can then filter this mode by subtracting it from the elements that it affects, given that on a uniform mesh the value of the *checkboard* mode is the same on all the 'red' cells of the mesh, assuming that the last element is 'black' (the value of the spurious mode on 'black' cells is thus 0). We did so, and recovered the exact analytical solution, which we show in Figures 5.5, in the form of elemental pressures, and 5.6, as nodal pressure contours.

Finally, we solved this problem on three different uniform meshes with each of the two elements, and computed the errors Errr (as defined in 5.30) with respect to the exact solution; we plot them in Figure 5.7 as a function of the mesh size. It can be seen that the steady states reached with this method provide optimal order accuracy in the mesh size for the velocity solution in the norm of $\mathbf{L}^2(\Omega)$ for these two elements, that is, quadratic for the Q_1P_0 and cubic for the Q_2P_1. These steady states are the solutions of a standard Galerkin mixed approximation of the steady, incompressible Navier–Stokes equations.

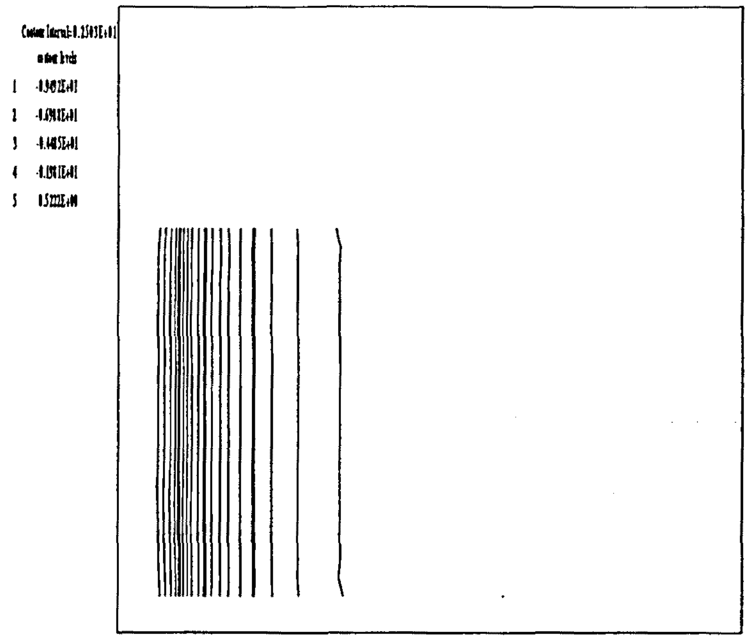

Figure 5.6: Kovasznay flow, Q_1P_0 element with checkboard mode filtered, nodal pressure contours.

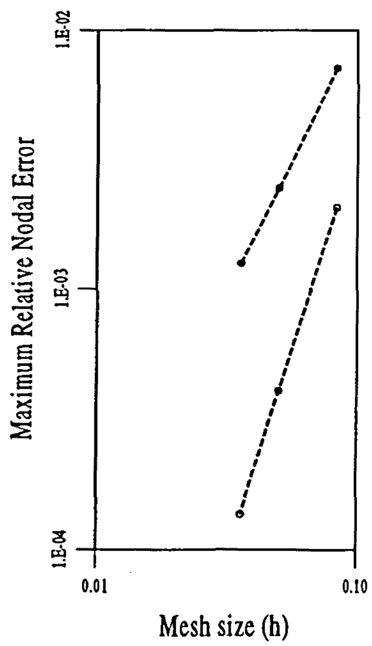

Figure 5.7: Kovasznay flow, maximum nodal error: • Q_1P_0 element, ∘ Q_2P_1 element.

5.3.3 Cavity flow problem

The third case we considered was again the lid-driven cavity flow problem, this time solved with the predictor-multicorrector algorithm starting from the fluid at rest (but for the velocity boundary condition) until a steady state was reached. We took the leaky lid case (that is, with unit horizontal velocity on the two top corners of the cavity) and a Reynolds number of 1000. A regular, nonuniform mesh, which is finer near the boundaries, was used; it is made up with 31×31 nodes. Two iterations of the multicorrector scheme were performed per time step, and the value of γ was set equal to 1 so as to get a converged solution fastest.

Figure 5.8 shows the steady streamlines obtained with both the Q_1P_0 and the Q_2P_1 elements. Secondary bottom left and right vortices can be observed, but no top left vortex was found. Again, this is in good agreement with benchmark solutions for this problem, ([42] or [88]) and other published numerical solutions ([30], [65], [96] or [99])

The element pressures computed with the Q_1P_0 element are shown in Figure 5.9. A checkerboarding phenomenon becomes apparent, which invalidates the pressure approximation without affecting the velocities. On the other hand, the Q_2P_1 element gave satisfactory pressure results; the pressure contours obtained can be seen in Figure 5.10, and compare well with those of the above mentioned references.

Finally, Figures 5.11 and 5.12 show the velocity profiles through the cavity centerlines $x = 0.5$ (horizontal velocity) and $y = 0.5$ (vertical velocity), respectively. As can be seen, these results compare well with the reference data of U. Ghia *et al.* ([42]), specially for biquadratic elements.

5.3.4 Noflow problem

The fourth example we present is the noflow test, introduced by P. Gresho *et al.* in [47] and studied in [39] and [40]. The geometry and mesh for this problem can be seen in Figure 5.13. Homogeneous Dirichlet boundary conditions are imposed on all the boundary, and an external gravitational force $\mathbf{f} = (0, -1)$ is applied. The exact analytical solution of this problem is $\mathbf{u} = \mathbf{0}$ and $p = -y + p_0$.

This simple case highlights another misbehaviour of the Q_1P_0 element (and some other related constant pressure elements). Although it is a confined flow problem, this time it is not the presence of checkboard pressure modes, since the distorted character of the mesh filters them out, or the lack of satisfaction of the LBB condition. The pressure space does not contain the analytical solution, and a wrong pressure field induces the appearance of a vortex of $O(h)$.

In this problem, we started from the fluid at rest and zero pressure until a steady state was reached, with a time step of 0.01, two iterations per step and a value of γ equal to 1. The same results as in [39] and [40] were obtained for the Q_1P_0 element after 300 steps, which can be seen in Figures 5.14 and

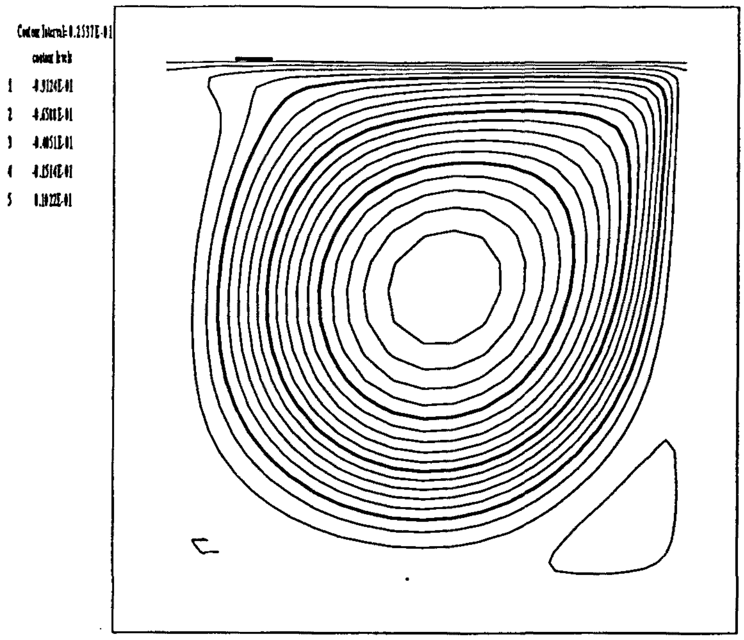

a)

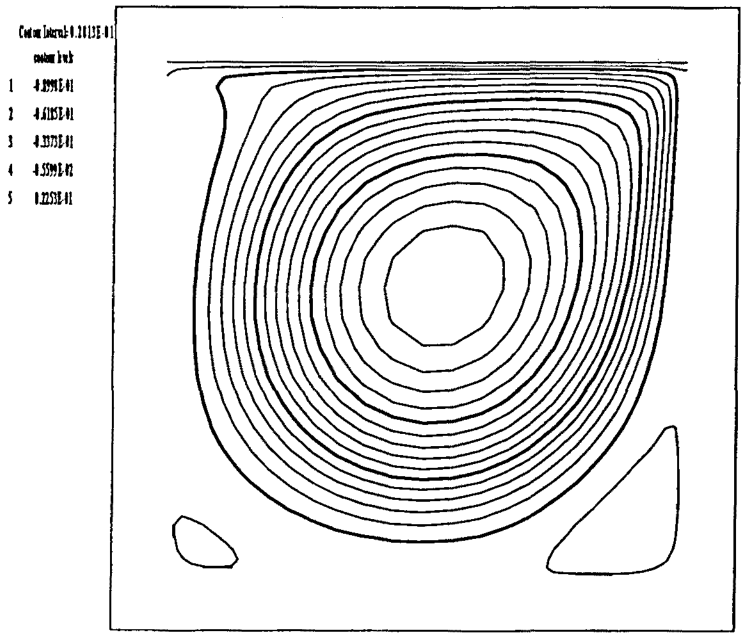

b)

Figure 5.8: Cavity flow, streamlines: a) Q_1P_0 element; b) Q_2P_1 element.

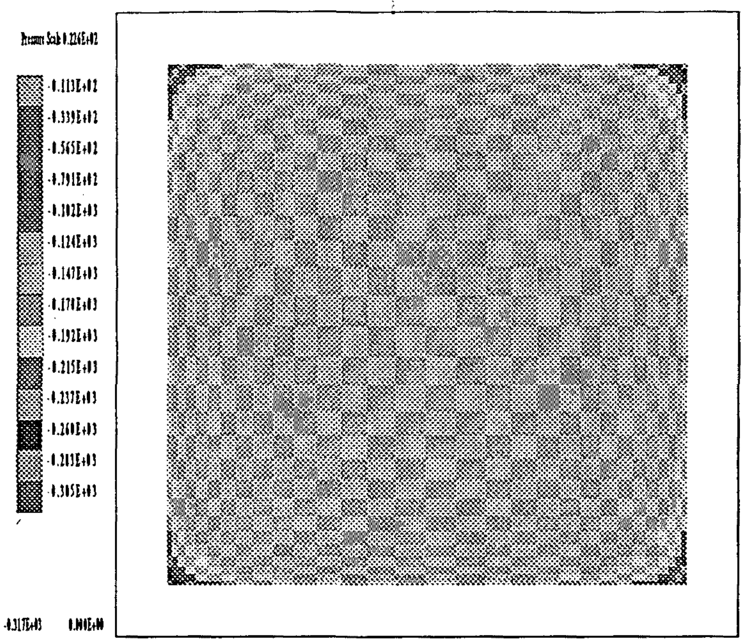

Figure 5.9: Cavity flow, Q_1P_0 element, element pressure values.

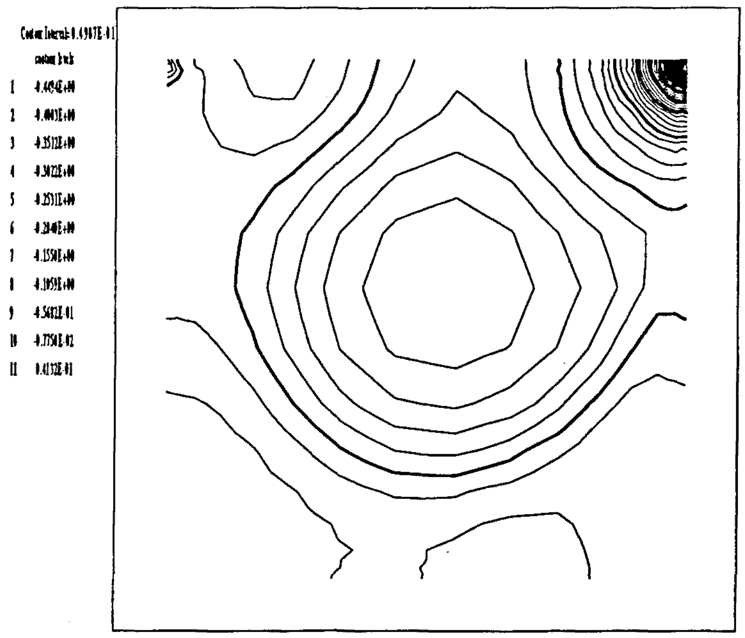

Figure 5.10: Cavity flow, Q_2P_1 element, nodal pressure contours.

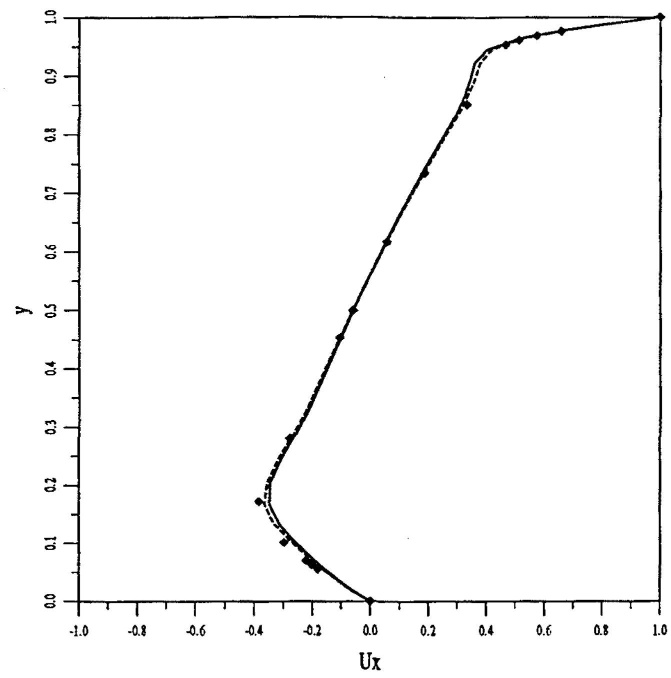

Figure 5.11: Cavity flow, horizontal velocity profile through cavity centerline $x = 0.5$: — $Q1P0$ element; - - - $Q2P1$ element; ◇ Reference [43].

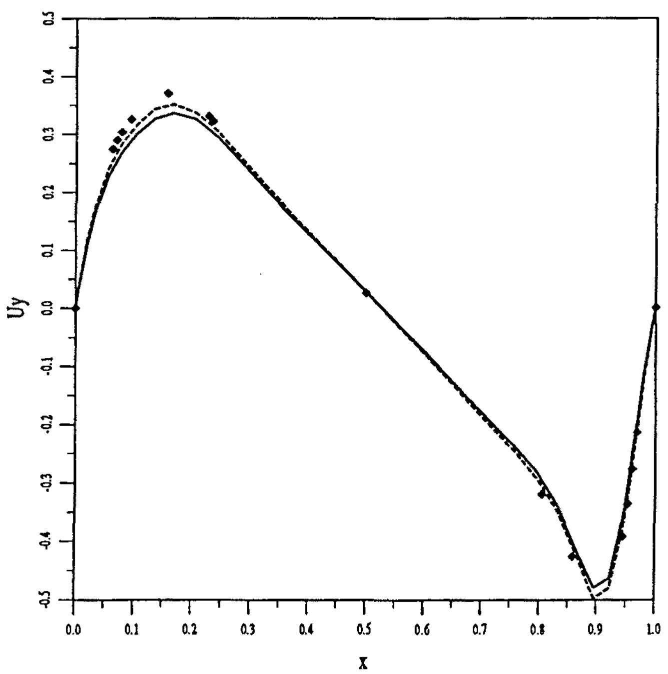

Figure 5.12: Cavity flow, vertical velocity profile through cavity centerline $y = 0.5$: — $Q1P0$ element; - - - $Q2P1$ element; ◇ Reference [43].

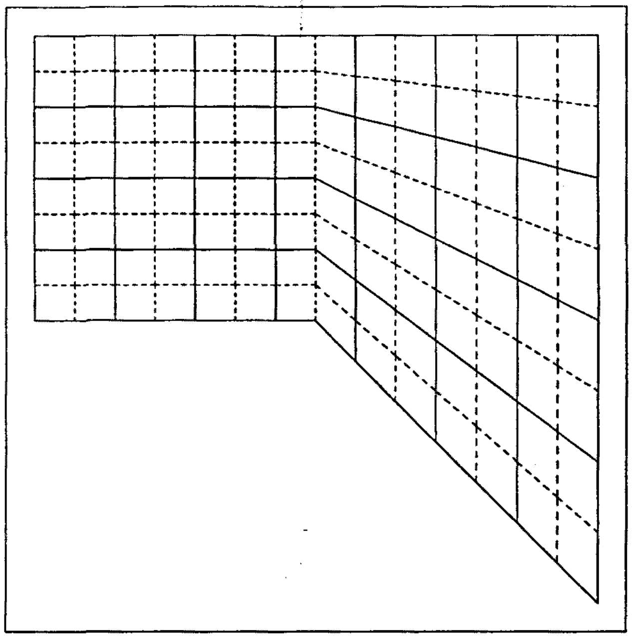

Figure 5.13: Noflow problem, mesh.

5.16 in the form of nodal velocity vectors and pressure contours, respectively. The Q_2P_1 element, on the contrary, yielded the exact analytical solution in 2 steps (see Figures 5.15 and 5.17).

5.3.5 Plane jet simulation

The fifth example considered is a purely unsteady case, consisting of a plane jet simulation. The same conditions and mesh as in [73] were taken, which are: a uniform 32×32 mesh of the 4 noded elements in the square $[0,1] \times [-0.5, 0.5]$; a viscosity of $\nu = 5 \times 10^{-4}$; unit horizontal velocity at the central node of the left wall, with natural boundary conditions on the other walls and the fluid at rest at $t = 0$. A time step of $\delta t = 0.01$ was taken. Once again, 2 iterations per time step of the algorithm were performed, and γ was set equal to 1. The streamlines at different times are shown in Figures 5.18 and 5.19 for the Q_1P_0 and Q_2P_1 elements, respectively; the pressure contours for the same times can be found in Figures 5.20 and 5.21. They are all in good agreement with the results of [73]. The presence of outlet boundary conditions on part of the boundary prevents the appearance of spurious checkboard modes for the Q_1P_0 element. This example shows the capability of the algorithm to reproduce purely unsteady situations.

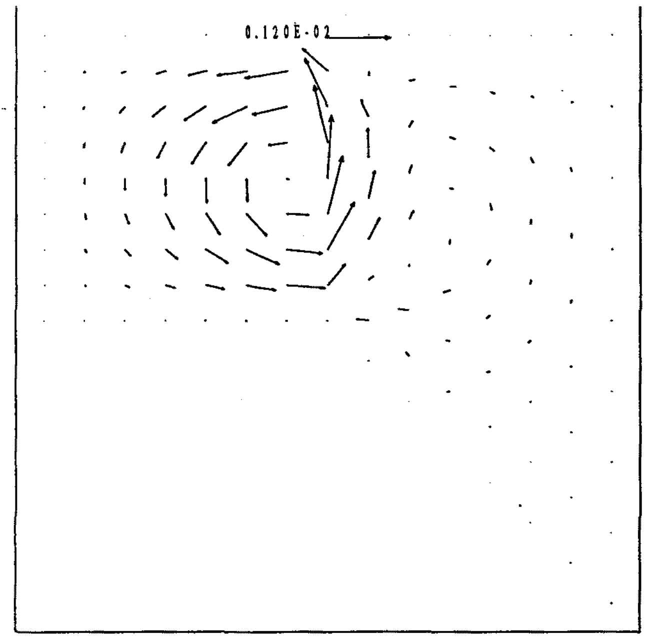

Figure 5.14: Noflow problem, Q_1P_0 element, velocity vectors.

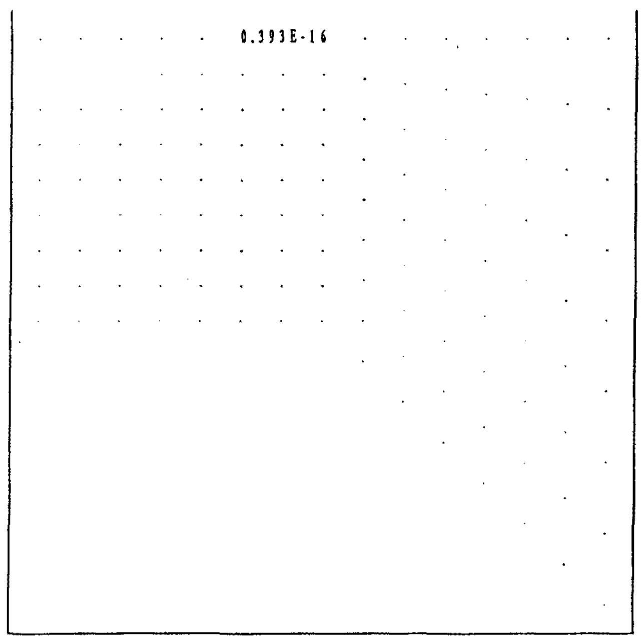

Figure 5.15: Noflow problem, Q_2P_1 element, velocity vectors.

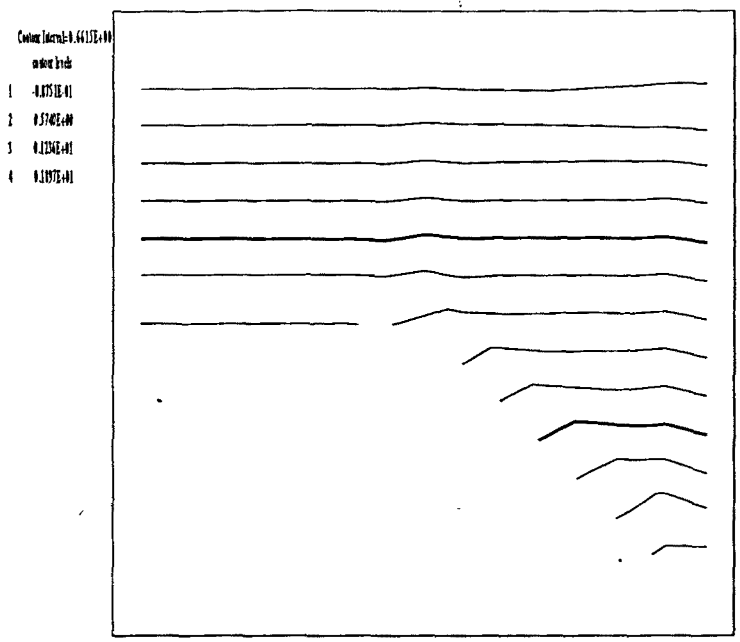

Figure 5.16: Noflow problem, Q_1P_0 element, pressure contours.

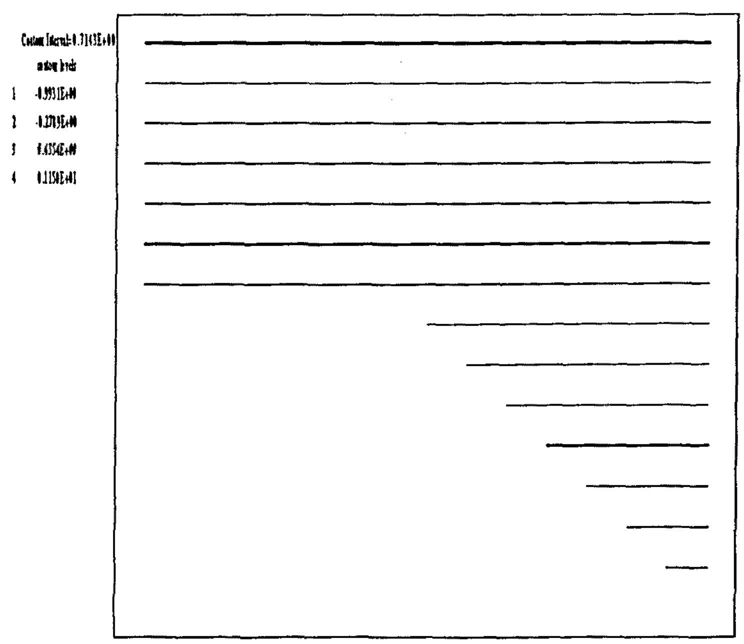

Figure 5.17: Noflow problem, Q_2P_1 element, pressure contours.

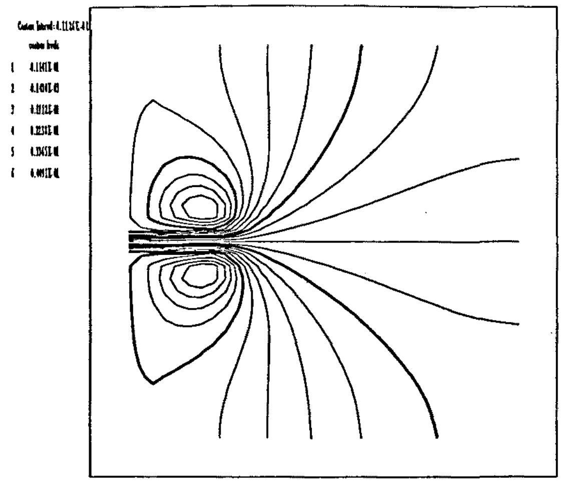

a)

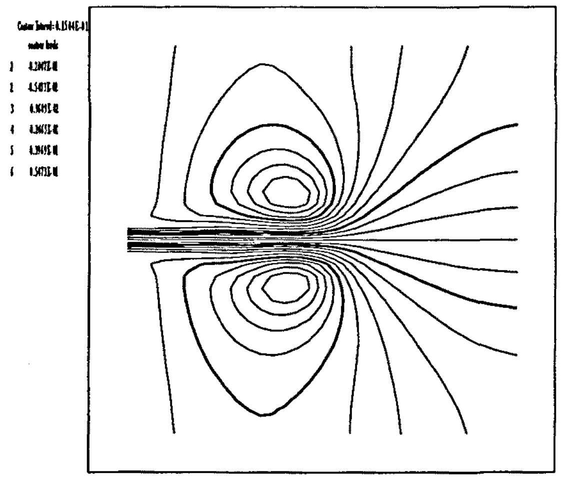

b)

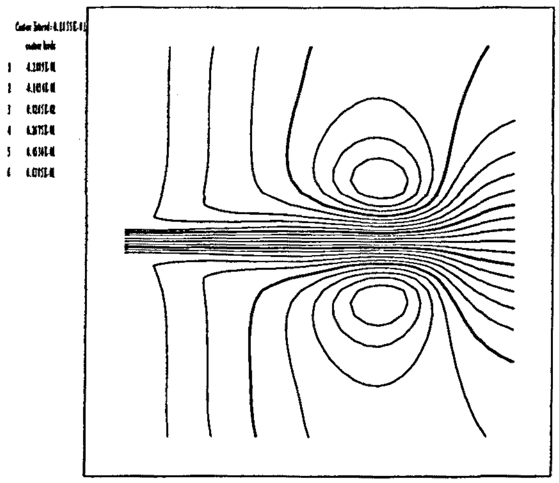

c)

Figure 5.18: Jet flow, Q_1P_0 element, streamlines: a) $t = 1.2$; b) $t = 2.5$; c) $t = 4.0$.

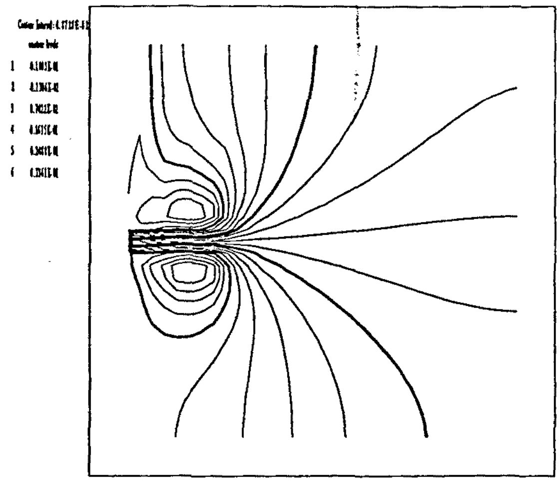

a)

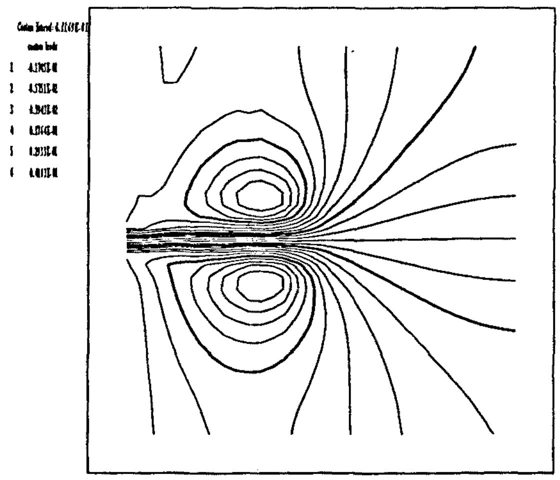

b)

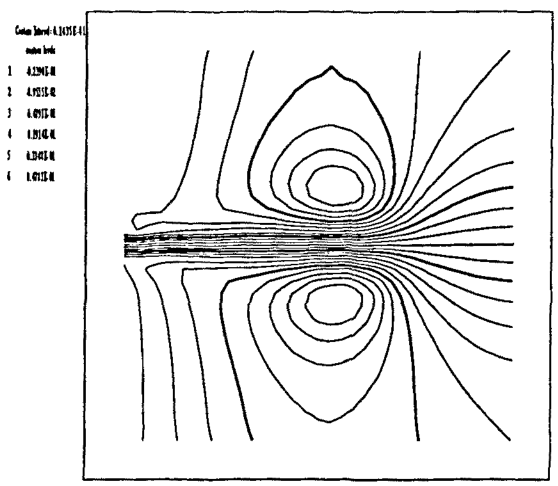

c)

Figure 5.19: Jet flow, Q_2P_1 element, streamlines: a) $t = 1.2$; b) $t = 2.5$; c) $t = 4.0$.

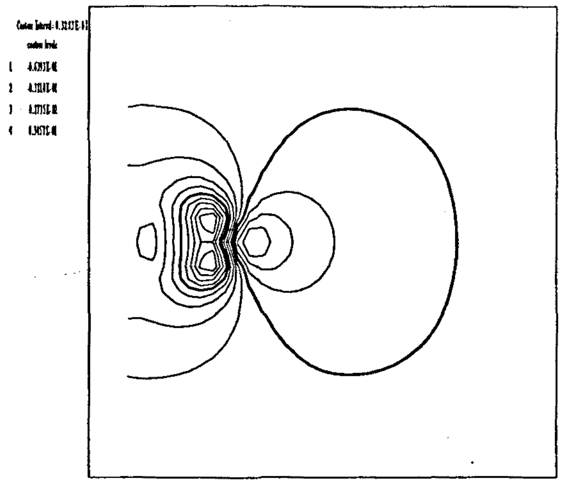

a)

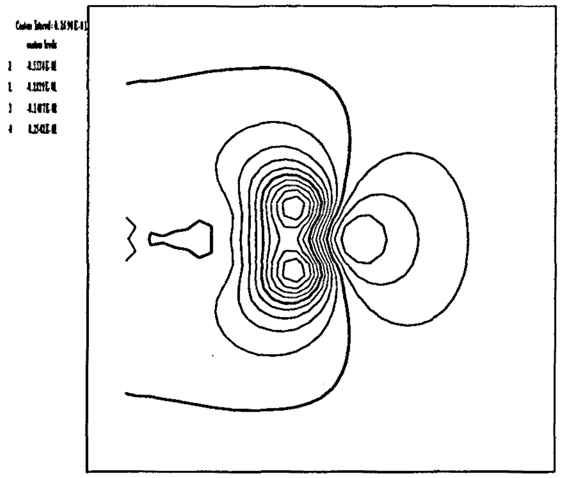

b)

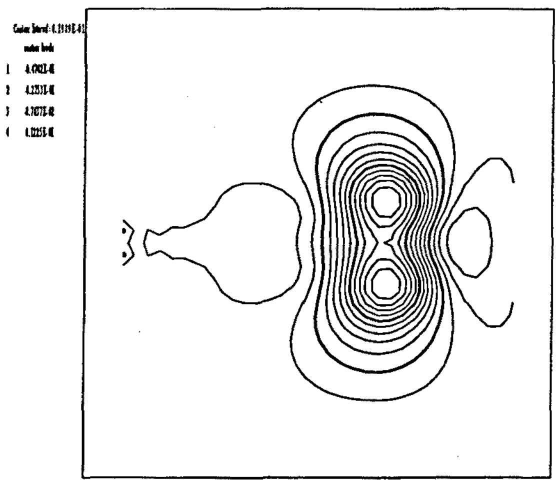

c)

Figure 5.20: Jet flow, Q_1P_0 element, nodal pressure contours: a) $t = 1.2$; b) $t = 2.5$; c) $t = 4.0$.

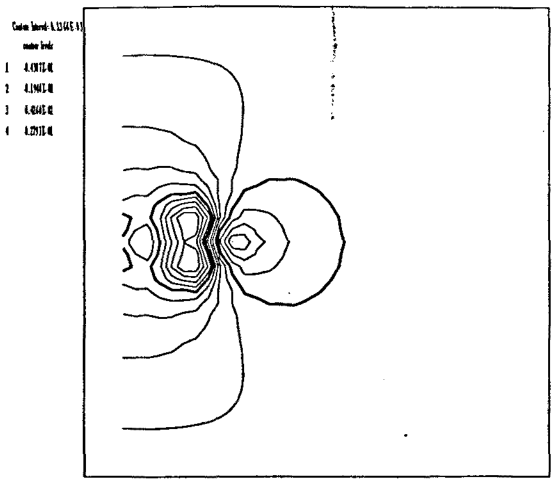

a)

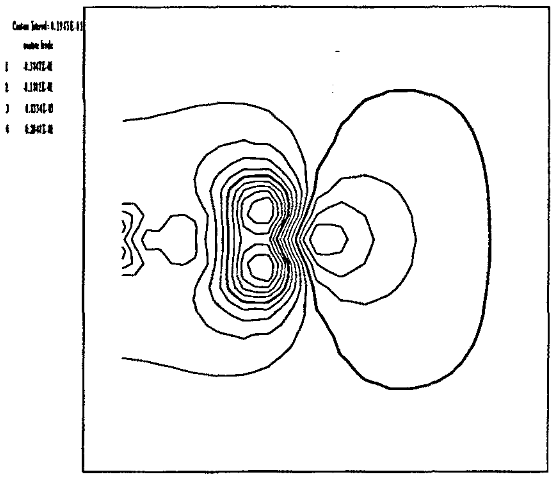

b)

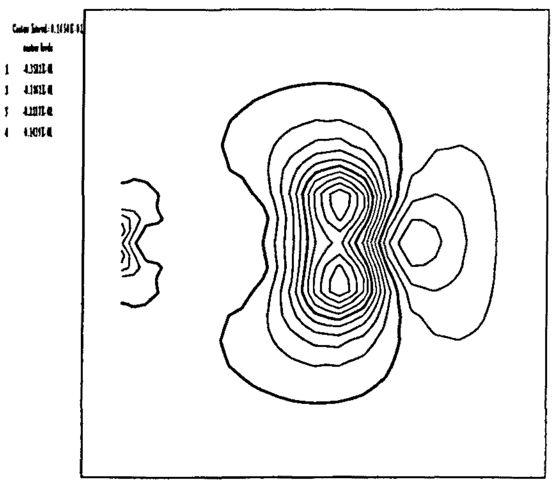

c)

Figure 5.21: Jet flow, Q_2P_1 element, nodal pressure contours: a) $t = 1.2$; b) $t = 2.5$; c) $t = 4.0$.

Conclusions and future work

In this work we have studied fractional step, finite element methods for the numerical solution of incompressible Navier–Stokes equations in primitive variables. Two main objectives have been achieved: on the one hand, the reason why some projection methods (the most popular among fractional step methods) are not restricted by the standard *inf–sup* condition, which is present in most incompressible flow formulations, has been unveiled; space discretizations of such methods are only restricted by a weaker condition, which has been proved to be satisfied by most equal order finite element interpolations of velocities and pressures. On the other hand, a fractional step method has been developed which bypasses the problem of enforcing unphysical boundary conditions encountered in projection methods; this is achieved by introducing a viscous term in the incompressibility phase of the method.

It can be concluded from the present work that projection methods which employ a continuous Pressure Poisson Equation in their formulation are not restricted by the discrete LBB condition; pressure segregation, however, has to be effected before space discretization takes place. Otherwise, a mixed type discrete problem results, and a compatibility condition between the approximating spaces of velocity and pressure still applies. The reason why the LBB restriction is so *circumvented* in standard projection methods has been traced back to the appearance of a matrix $A = L - G^t M^{-1} G$ in the discrete continuity equation; this matrix, which can be understood as the difference between two discrete Laplacian operators, has been proved to be positive semidefinite. This has led to the conclusion that space discretizations of projection methods are only restricted by a certain *inf–sup* condition which is weaker than the standard one; we have then applied the macroelement technique to showing that it is satisfied by equal order simplicial finite elements of arbitrary order in 2 and 3 dimensions, and equal order quadrilateral ($d = 2$) and hexahedral ($d = 3$) finite elements of first order.

During the course of this study, we have also developed a numerical method for the solution of the Stokes problem which allows the use of equal order finite element interpolations. The Stokes problem is employed here as a linear, steady model to study projection methods. Optimal order convergence in the mesh size has been proved for our method, both in the natural norm of the problem and in the L^2–norm, for 'sufficiently smooth' domains and meshes and under the weak compatibility condition just found. We have also studied different iterative schemes for the numerical solution of the resulting system of discrete linear equations. A comparison between the most efficient scheme obtained and the well-known GLS method for the Stokes problem has been given; our scheme seems to be a little more costly, but, in some aspects, it is more accurate.

An extension of the previous method to the steady, incompressible Navier–Stokes equation has also been provided. Optimal order convergence both in natural and in L^2–norm has been proved, in the case of a unique solution of the original problem, under the same weak compatibility condition as in the linear problem and again for 'sufficiently smooth' domains and meshes. A study of different iterative schemes for the numerical solution of the resulting system of discrete nonlinear equations has also been given, as well as a comparison between the most efficient scheme found and the GLS method applied to the incompressible Navier–Stokes equations; once again, our scheme is a little more costly, but it proved to be more accurate in all the cases we solved.

In the second part of this work, we developed an implicit fractional step method which, unlike standard projection methods, allows the imposition of the original boundary conditions of the problem in all phases of the method. Space discretizations of this method, however, are restricted by the standard LBB condition. We first proved convergence of this method in the time step to a continuous solution, following the classical ideas of R. Temam for the standard projection method; the convergence results for the end–of–step velocities are improved with our method, due to the fact that they satisfy the correct boundary conditions. We then obtained some error estimates for both the intermediate and end–of–step velocities and the pressure as a function of the time step, under stronger regularity assumptions on the solution and mesh, and following the recent ideas of J. Shen for the standard projection method, among others. Furthermore, we developed a similar method to the previous one, but this time with pressure correction; we also obtained some error estimates for this alternative method. We then proved independence of the steady solution reached with implicit fractional step methods in steady flow problems, provided pressure correction is used. Finally, we developed an iterative scheme for the numerical solution of the resulting system of linear equations in each time step for our pressure correction method; this scheme is explicit in each iteration. We validated this scheme on some benchmark problems, such as the flows over a backward facing step and around a circular cylinder, with two different finite element space discretizations; good results were obtained in all cases.

Finally, we redeveloped a well–known predictor multicorrector algorithm, in a semidiscrete setting within the context of fractional step methods, with the help of the methods just introduced; this is an iterative algorithm in each time step, in which each iteration is decomposed into two phases, in a similar way to our pressure correction, fractional step method. This allowed us to justify several properties of the algorithm, such as the possibility of imposing the correct boundary conditions in all phases of the algorithm; the need for space interpolations of the algorithm to satisfy the discrete LBB condition; the independence of the steady state reached with respect to the time step in steady flow problems or the fact that a single iteration of the algorithm is enough to achieve first order accuracy in the time step. We obtained several numerical results with two different finite element discretizations of the algorithm, the classical Q_1P_0 element and the Q_2P_1 element.

As for future developments, we would first like to finish some aspects of the present work which have been left open, such as the proof of the satisfaction of our weak inf–sup condition in the case of quadrilateral and hexahedral finite elements of higher order (Q_k for $k \geq 2$), which we tried but not quite succeeded; also, the analysis of our local discrete, reformulated Stokes and Navier–Stokes problems, with parameters α_K defined elementwise, proving optimal order convergence in a suitable mesh–dependent norm. But our main next objectives will be the following: on the one hand, the theoretical analysis and implementation of a second order, viscosity splitting fractional step method; we would like to obtain second order error estimates in the time step size and numerical results which confirm them. This can be achieved by fixing the parameters θ and ϕ to $1/2$ in our pressure correction method. An iterative scheme would then be considered for the solution of the resulting system of linear (or, maybe, nonlinear) equations, which would again be explicit in each iteration. On the other hand, the theoretical analysis of fully discrete fractional step methods: we would like to give error estimates both in the time step size and the mesh size for the fully discrete solution of the standard projection method without assuming that the approximating spaces satisfy the standard inf–sup condition, but only the weak compatibility condition of Chapters 2 and 3. Moreover, we would also like to give error estimates in space and time for the fully discrete solution of our viscosity splitting method, this time assuming the standard inf–sup condition.

Appendix A

Improved error estimates

We give here some improved error estimates which we can prove for our viscosity splitting method, both with and without pressure correction, assuming that the semidiscrete velocities are uniformly bounded in $\mathbf{H}^2(\Omega)$. We also prove some error estimates for the pressure which depend on the improved error estimates for the velocity; these show that the pressure is at least weakly order 1/2 accurate for the method with and without pressure correction.

A.1 Viscosity splitting method

We give here an improved error estimate for the end–of–step velocity of our viscosity splitting method 4.8–4.10. We show that $\mathbf{u}^{n+1}$ is actually a strongly order 1 approximation of the solution in $\mathbf{L}^2(\Omega)$ and weakly order 1 in $\mathbf{H}_0^1(\Omega)$, assuming a uniform bound for $\mathbf{u}^{n+1/2}$ in $\mathbf{H}^2(\Omega)$.

<u>Theorem A.1:</u> *assume that* **A1** *and* **A2** *hold, and that the Stokes problem is regular; assume also that the intermediate velocities satisfy:*

$$||\mathbf{u}^{n+1/2}||_2 < C, \qquad \forall n \geq 0 \tag{A.1}$$

with $C > 0$ independent of k; then, for $N = 0, \ldots, [T/k] - 1$, and small enough k:

$$|\mathbf{e}^{N+1}|^2 \; + \; k\,\nu \sum_{n=0}^{N} ||\mathbf{e}^{n+1}||^2 \;\; \leq \;\; C\,k^2 \tag{A.2}$$

PROOF: we recall equation 4.36 here:

$$\begin{aligned} \frac{1}{k}(\mathbf{e}^{n+1} - \mathbf{e}^n) \; &- \; \nu\Delta(\mathbf{e}^{n+1}) \; + \; \nabla q^{n+1} \\ &= \; (\mathbf{u}^n \cdot \nabla)\mathbf{u}^{n+1/2} \; - \; (\mathbf{u}(t_{n+1}) \cdot \nabla)\mathbf{u}(t_{n+1}) \; + \; \mathbf{R}^n \end{aligned} \tag{A.3}$$

Taking the inner product of A.3 with $2k\mathbf{e}^{n+1}$, which is in Y, we get:

$$\begin{aligned} |\mathbf{e}^{n+1}|^2 \;&-\; |\mathbf{e}^n|^2 + |\mathbf{e}^{n+1}-\mathbf{e}^n|^2 + 2k\nu\,||\mathbf{e}^{n+1}||^2 \\ &= 2k\,c(\mathbf{u}^n,\mathbf{u}^{n+1/2},\mathbf{e}^{n+1}) - 2k\,c(\mathbf{u}(t_{n+1}),\mathbf{u}(t_{n+1}),\mathbf{e}^{n+1}) \\ &+ 2k < \mathbf{R}^n, \mathbf{e}^{n+1} > \qquad \text{(A.4)} \end{aligned}$$

The right–hand–side terms are bounded as follows. For the Taylor residual term we have:

$$\begin{aligned} 2k < \mathbf{R}^n,\mathbf{e}^{n+1} > \;&\le\; 2k\,||\mathbf{R}^n||_{Y'}\,||\mathbf{e}^{n+1}|| \\ &\le \frac{k\nu}{4}||\mathbf{e}^{n+1}||^2 + C\,k\,||\mathbf{R}^n||^2_{Y'} \\ &= \frac{k\nu}{4}||\mathbf{e}^{n+1}||^2 + C\,k^{-1}\,||\int_{t_n}^{t_{n+1}}(t-t_n)\,\mathbf{u}_{tt}\,dt||^2_{Y'} \\ &\le \frac{k\nu}{4}||\mathbf{e}^{n+1}||^2 + C\,k^{-1}\int_{t_n}^{t_{n+1}}(t-t_n)^2\,dt\int_{t_n}^{t_{n+1}}||\mathbf{u}_{tt}||^2_{Y'}\,dt \\ &\le \frac{k\nu}{4}||\mathbf{e}^{n+1}||^2 + C\,k^2\int_{t_n}^{t_{n+1}}||\mathbf{u}_{tt}||^2_{Y'}\,dt \end{aligned}$$

For the nonlinear terms, we again use the splitting 4.27 to express them as:

$$\begin{aligned} 2k\;&\Big(c(\mathbf{u}^n,\mathbf{u}^{n+1/2},\mathbf{e}^{n+1}) - c(\mathbf{u}(t_{n+1}),\mathbf{u}(t_{n+1}),\mathbf{e}^{n+1})\Big) \\ =\;& 2k\Big(-c(\mathbf{u}(t_{n+1}),\mathbf{e}^{n+1/2},\mathbf{e}^{n+1}) + c(\mathbf{u}(t_n)-\mathbf{u}(t_{n+1}),\mathbf{u}^{n+1/2},\mathbf{e}^{n+1}) \\ -\;& c(\mathbf{e}^n,\mathbf{u}^{n+1/2},\mathbf{e}^{n+1})\Big) \end{aligned}$$

which we call I, II and III, respectively. Then:

$$\begin{aligned} \mathrm{I} &= -2k\,c(\mathbf{u}(t_{n+1}),\mathbf{e}^{n+1/2},\mathbf{e}^{n+1}) \\ &= 2k\,c(\mathbf{u}(t_{n+1}),\mathbf{e}^{n+1},\mathbf{e}^{n+1/2}) \\ &\le C\,k\,||\mathbf{u}(t_{n+1})||_2\,||\mathbf{e}^{n+1}||\,|\mathbf{e}^{n+1/2}| \\ &\le C\,k\,||\mathbf{e}^{n+1}||\,|\mathbf{e}^{n+1/2}| \\ &\le \frac{k\nu}{4}||\mathbf{e}^{n+1}||^2 + C\,k\,|\mathbf{e}^{n+1/2}|^2 \end{aligned}$$

$$\begin{aligned} \mathrm{II} &= 2k\,c(\mathbf{u}(t_n)-\mathbf{u}(t_{n+1}),\mathbf{u}^{n+1/2},\mathbf{e}^{n+1}) \\ &\le C\,k\,||\mathbf{u}(t_n)-\mathbf{u}(t_{n+1})||\,||\mathbf{u}^{n+1/2}||\,||\mathbf{e}^{n+1}|| \\ &\le C\,k\,||\mathbf{u}(t_n)-\mathbf{u}(t_{n+1})||\,||\mathbf{e}^{n+1}|| \\ &= C\,k\,||\int_{t_n}^{t_{n+1}}\mathbf{u}_t\,dt||\,||\mathbf{e}^{n+1}|| \end{aligned}$$

$$
\begin{aligned}
&\leq \; C\,k \,\|\int_{t_n}^{t_{n+1}} \mathbf{u}_t\, dt\|^2 \;+\; \frac{k\nu}{4}\|\mathbf{e}^{n+1}\|^2 \\
&\leq \; C\,k^2 \int_{t_n}^{t_{n+1}} \|\mathbf{u}_t\|^2\, dt \;+\; \frac{k\nu}{4}\|\mathbf{e}^{n+1}\|^2
\end{aligned}
$$

$$
\begin{aligned}
\mathrm{III} \;&=\; -2\,k\,c(\mathbf{e}^n, \mathbf{u}^{n+1/2}, \mathbf{e}^{n+1}) \\
&\leq\; C\,k\,|\mathbf{e}^n|\;\|\mathbf{u}^{n+1/2}\|_2\;\|\mathbf{e}^{n+1}\| \\
&\leq\; C\,k\,|\mathbf{e}^n|\;\|\mathbf{e}^{n+1}\| \\
&\leq\; C\,k\,|\mathbf{e}^n|^2 \;+\; \frac{k\nu}{4}\|\mathbf{e}^{n+1}\|^2
\end{aligned}
$$

where we have used 4.34 and A.1. Adding up A.4 for $n = 0, \ldots, N$, taking into account 4.31 for the term I, and the previous inequalities, we get:

$$
\begin{aligned}
|\mathbf{e}^{N+1}|^2 \;&+\; \sum_{n=0}^{N} |\mathbf{e}^{n+1} - \mathbf{e}^n|^2 \\
&+\; k\,\nu \sum_{n=0}^{N} \|\mathbf{e}^{n+1}\|^2 \;+\; C\,k^2\,\nu \sum_{n=0}^{N} \|\mathbf{e}^{n+1/2}\|^2 \\
&\leq\; C\,k^2 \int_0^T \|\mathbf{u}_{tt}\|_{Y'}^2\, dt \;+\; C\,k^2 \int_0^T \|\mathbf{u}_t\|^2\, dt \\
&+\; C\,k \sum_{n=0}^{N+1} |\mathbf{e}^n|^2 \;+\; C\,k \sum_{n=0}^{N} |\mathbf{e}^{n+1} - \mathbf{e}^{n+1/2}|^2 \\
&+\; C\,k^2 \sum_{n=0}^{N} \Big(\|\mathbf{e}^{n+1}\|^2 + \|\mathbf{e}^{n+1} - \mathbf{e}^{n+1/2}\|^2 \Big)
\end{aligned}
$$

For sufficiently small k, we can apply the discrete Gronwall lemma to the last inequality; using the regularity properties of the solution (**R2** and **R4**) and the estimates of Lemma 4.7, we get:

$$
\begin{aligned}
|\mathbf{e}^{N+1}|^2 \;&+\; \sum_{n=0}^{N} |\mathbf{e}^{n+1} - \mathbf{e}^n|^2 \;+\; k\,\nu \sum_{n=0}^{N} \|\mathbf{e}^{n+1}\|^2 \\
&\leq\; C\,k^2
\end{aligned}
$$

and 4.35 is proved. □

We now show that the pressure approximation of our viscosity splitting fractional step method is order 1/2 accurate in the time step, as it is for the classical projection method, according to [90]. We first recall a technical result, similar to that of Lemma A1 in [92]. In Theorem A.1 we have proved that, in particular:

$$\sum_{n=0}^{N} |\mathbf{e}^{n+1} - \mathbf{e}^n|^2 \leq C\,k^2$$

This implies that:

$$\sum_{n=0}^{N} ||\mathbf{e}^{n+1} - \mathbf{e}^n||_{-1}^2 \leq C\,k^2 \tag{A.5}$$

since for all $\mathbf{v} \in \mathbf{L}^2(\Omega)$, $||\mathbf{v}||_{-1} \leq C\,|\mathbf{v}|$. This is what we actually use to prove the following error estimate for the pressure:

Theorem A.2: *assume that* **A1** *and* **A2** *hold, that the Stokes problem is regular and that A.1 also holds; then, for* $N = 0, \ldots, [T/k] - 1$ *and small enough* k*:*

$$k \sum_{n=0}^{N} |p^{n+1} - p(t_{n+1})|_{L_0^2(\Omega)}^2 \leq C\,k \tag{A.6}$$

PROOF: we rewrite A.3 as:

$$\begin{aligned} -\nabla q^{n+1} &= \frac{1}{k}(\mathbf{e}^{n+1} - \mathbf{e}^n) - \nu\Delta(\mathbf{e}^{n+1}) - \mathbf{R}^n \\ &- (\mathbf{u}^n \cdot \nabla)\mathbf{u}^{n+1/2} + (\mathbf{u}(t_{n+1}) \cdot \nabla)\mathbf{u}(t_{n+1}) \end{aligned} \tag{A.7}$$

Using the continuous LBB condition 1.25:

$$|p|_{L_0^2(\Omega)} \leq C \sup_{\mathbf{v}\in\mathbf{H}_0^1(\Omega)} \frac{(\nabla p, \mathbf{v})}{||\mathbf{v}||}, \qquad \forall p \in L_0^2(\Omega) \tag{A.8}$$

for the pressure error $p = q^{n+1}$, we need to bound the products of the RHS of A.7 with $\mathbf{v} \in \mathbf{H}_0^1(\Omega)$. We have:

$$\begin{aligned} \frac{1}{k}(\mathbf{e}^{n+1} - \mathbf{e}^n, \mathbf{v}) &\leq \frac{1}{k}||\mathbf{e}^{n+1} - \mathbf{e}^n||_{-1}\,||\mathbf{v}|| \\ < -\nu\Delta(\mathbf{e}^{n+1}), \mathbf{v} > &= ((\nu\mathbf{e}^{n+1}, \mathbf{v})) \leq \nu||\mathbf{e}^{n+1}||\,||\mathbf{v}|| \\ < -\mathbf{R}^n, \mathbf{v} > &\leq ||\mathbf{R}^n||_{-1}\,||\mathbf{v}|| \leq C\Big(\int_{t_n}^{t_{n+1}} t\,||\mathbf{u}_{tt}||_{-1}^2\,dt\Big)^{1/2}\,||\mathbf{v}|| \end{aligned}$$

For the nonlinear terms, we use the following splitting, taken from [90]:

$$\begin{aligned} -(\mathbf{u}^n \cdot \nabla)\mathbf{u}^{n+1/2} &+ (\mathbf{u}(t_{n+1}) \cdot \nabla)\mathbf{u}(t_{n+1}) \\ &= \Big((\mathbf{u}(t_{n+1}) - \mathbf{u}(t_n)) \cdot \nabla\Big)\mathbf{u}(t_{n+1}) + (\mathbf{e}^n \cdot \nabla)\mathbf{u}(t_{n+1}) \\ &+ (\mathbf{u}^n \cdot \nabla)\mathbf{e}^{n+1/2} \end{aligned} \tag{A.9}$$

so that:

$$\begin{aligned}
T_1 &= c(\mathbf{u}(t_{n+1}) - \mathbf{u}(t_n), \mathbf{u}(t_{n+1}), \mathbf{v}) \\
&\leq C\,|\mathbf{u}(t_{n+1}) - \mathbf{u}(t_n)|\;||\mathbf{u}(t_{n+1})||_2\;||\mathbf{v}|| \\
&\leq C\,|\mathbf{u}(t_{n+1}) - \mathbf{u}(t_n)|\;||\mathbf{v}|| \\
&= C\,|\int_{t_n}^{t_{n+1}} \mathbf{u}_t\,dt|\;||\mathbf{v}|| \\
&\leq C\,(k\int_{t_n}^{t_{n+1}} |\mathbf{u}_t|^2\,dt)^{1/2}\;||\mathbf{v}||
\end{aligned}$$

$$\begin{aligned}
T_2 &= c(\mathbf{e}^n, \mathbf{u}(t_{n+1}), \mathbf{v}) \\
&\leq C\,||\mathbf{e}^n||\;||\mathbf{u}(t_{n+1})||\;||\mathbf{v}|| \\
&\leq C\,||\mathbf{e}^n||\;||\mathbf{v}||
\end{aligned}$$

$$\begin{aligned}
T_3 &= c(\mathbf{u}^n, \mathbf{e}^{n+1/2}, \mathbf{v}) \\
&\leq C\,||\mathbf{u}^n||\;||\mathbf{e}^{n+1/2}||\;||\mathbf{v}|| \\
&\leq C\,||\mathbf{e}^{n+1/2}||\;||\mathbf{v}||
\end{aligned}$$

where we have used 4.33. Thus, taking the product of A.7 with $\mathbf{v}$ and taking into account A.8 and all these inequalities, we obtain:

$$\begin{aligned}
|q^{n+1}|_{L_0^2(\Omega)} &\leq \frac{C}{k}\,||\mathbf{e}^{n+1} - \mathbf{e}^n||_{-1} \\
&+ C\Big\{||\mathbf{e}^{n+1}|| + ||\mathbf{e}^n|| + ||\mathbf{e}^{n+1/2}|| \\
&+ (\int_{t_n}^{t_{n+1}} t\,||\mathbf{u}_{tt}||_{-1}^2\,dt)^{1/2} + (k\int_{t_n}^{t_{n+1}} |\mathbf{u}_t|^2\,dt)^{1/2}\Big\}
\end{aligned}$$

which yields:

$$\begin{aligned}
|q^{n+1}|_{L_0^2(\Omega)}^2 &\leq \frac{C}{k^2}\,||\mathbf{e}^{n+1} - \mathbf{e}^n||_{-1}^2 \\
&+ C\Big\{||\mathbf{e}^{n+1}||^2 + ||\mathbf{e}^n||^2 + ||\mathbf{e}^{n+1/2}||^2 \\
&+ \int_{t_n}^{t_{n+1}} t\,||\mathbf{u}_{tt}||_{-1}^2\,dt + k\int_{t_n}^{t_{n+1}} |\mathbf{u}_t|^2\,dt\Big\}
\end{aligned}$$

and A.6 results from A.5, the regularity of $\mathbf{u}$, and Lemma 4.7. □

We have proved, in summary, that the pressure solution is weakly order 1/2 accurate in $L_0^2(\Omega)$.

A.2 Viscosity splitting, pressure correction method

We now give improved error estimates for the end-of-step velocities of our pressure correction method, assuming again uniform bounds for the intermediate velocities in $\mathbf{H}^2(\Omega)$ and uniform bounds for the pressure gradient in $\mathbf{L}^2(\Omega)$.

Theorem A.3: *assume that* **A1** *and* **A2** *hold, and that the Stokes problem is regular; assume also that the intermediate velocities satisfy:*

$$||\tilde{\mathbf{u}}^{n+1/2}||_2 < C, \qquad \forall n \geq 0 \tag{A.10}$$

with $C > 0$ *independent of* k *and that* 4.46 *also holds; then, for* $N = 0, \ldots, [T/k] - 1$*, and small enough* k*:*

$$|\tilde{\mathbf{e}}^{N+1}|^2 \; + \; k\,\nu \sum_{n=0}^{N} ||\tilde{\mathbf{e}}^{n+1}||^2 \;\leq\; C\,k^2 \tag{A.11}$$

PROOF: the proof is similar to that of Theorem A.1. We recall equation 4.55 here:

$$\begin{aligned}\frac{1}{k}(\tilde{\mathbf{e}}^{n+1} - \tilde{\mathbf{e}}^n) \;&-\; \nu\Delta(\tilde{\mathbf{e}}^{n+1}) \;-\; \nabla(\tilde{p}^{n+\phi} - p(t_{n+1})) \\ &= \; (\tilde{\mathbf{u}}^n \cdot \nabla)\tilde{\mathbf{u}}^{n+1/2} \;-\; (\mathbf{u}(t_{n+1}) \cdot \nabla)\mathbf{u}(t_{n+1}) \;+\; \mathbf{R}^n\end{aligned} \tag{A.12}$$

where $\tilde{p}^{n+\phi} = \phi\tilde{p}^{n+1} + (1-\phi)\tilde{p}^n$. Taking the inner product of A.12 with $2k\tilde{\mathbf{e}}^{n+1}$, which is in Y, we get:

$$\begin{aligned}|\tilde{\mathbf{e}}^{n+1}|^2 \;&-\; |\tilde{\mathbf{e}}^n|^2 + |\tilde{\mathbf{e}}^{n+1} - \tilde{\mathbf{e}}^n|^2 + 2\,k\,\nu\,||\tilde{\mathbf{e}}^{n+1}||^2 \\ &= \; 2\,k\,c(\tilde{\mathbf{u}}^n, \tilde{\mathbf{u}}^{n+1/2}, \tilde{\mathbf{e}}^{n+1}) \;-\; 2\,k\,c(\mathbf{u}(t_{n+1}), \mathbf{u}(t_{n+1}), \tilde{\mathbf{e}}^{n+1}) \\ &+ \; 2\,k\, < \mathbf{R}^n, \tilde{\mathbf{e}}^{n+1} >\end{aligned} \tag{A.13}$$

The right-hand-side terms are bounded as in Theorem A.1, using again the splitting 4.27 for the nonlinear terms, yielding:

$$\begin{aligned}2\,k\, < \mathbf{R}^n, \tilde{\mathbf{e}}^{n+1} > \;&\leq\; \frac{k\nu}{4}||\tilde{\mathbf{e}}^{n+1}||^2 \;+\; C\,k^2 \int_{t_n}^{t_{n+1}} ||\mathbf{u}_{tt}||^2_{Y'}\,dt \\ -2\,k\,c(\mathbf{u}(t_{n+1}), \tilde{\mathbf{e}}^{n+1/2}, \tilde{\mathbf{e}}^{n+1}) \;&\leq\; \frac{k\nu}{4}||\tilde{\mathbf{e}}^{n+1}||^2 \;+\; C\,k\,|\tilde{\mathbf{e}}^{n+1/2}|^2 \\ 2\,k\,c(\mathbf{u}(t_n) - \mathbf{u}(t_{n+1}), \tilde{\mathbf{u}}^{n+1/2}, \tilde{\mathbf{e}}^{n+1}) \;&\leq\; C\,k^2 \int_{t_n}^{t_{n+1}} ||\mathbf{u}_t||^2\,dt \;+\; \frac{k\nu}{4}||\tilde{\mathbf{e}}^{n+1}||^2 \\ -2\,k\,c(\tilde{\mathbf{e}}^n, \tilde{\mathbf{u}}^{n+1/2}, \tilde{\mathbf{e}}^{n+1}) \;&\leq\; C\,k\,|\tilde{\mathbf{e}}^n|^2 \;+\; \frac{k\nu}{4}||\tilde{\mathbf{e}}^{n+1}||^2\end{aligned}$$

where A.10 has been used. Adding up A.13 for $n = 0, \ldots, N$, taking into account 4.31 for the nonlinear terms and the previous inequalities, we get:

$$\begin{aligned} |\tilde{\mathbf{e}}^{N+1}|^2 &+ \sum_{n=0}^{N} |\tilde{\mathbf{e}}^{n+1} - \tilde{\mathbf{e}}^n|^2 \\ &+ k\,\nu \sum_{n=0}^{N} ||\tilde{\mathbf{e}}^{n+1}||^2 + C\,k^2\,\nu \sum_{n=0}^{N} ||\tilde{\mathbf{e}}^{n+1/2}||^2 \\ &\leq C\,k^2 \int_0^T ||\mathbf{u}_{tt}||^2_{Y'}\,dt + C\,k^2 \int_0^T ||\mathbf{u}_t||^2\,dt \\ &+ C\,k \sum_{n=0}^{N+1} |\tilde{\mathbf{e}}^n|^2 + C\,k \sum_{n=0}^{N} |\tilde{\mathbf{e}}^{n+1} - \tilde{\mathbf{e}}^{n+1/2}|^2 \\ &+ C\,k^2 \sum_{n=0}^{N} \left(||\tilde{\mathbf{e}}^{n+1}||^2 + ||\tilde{\mathbf{e}}^{n+1} - \tilde{\mathbf{e}}^{n+1/2}||^2 \right) \end{aligned}$$

For sufficiently small k, we can apply the discrete Gronwall lemma to the last inequality; using the regularity properties of the solution and the estimates of Lemma 4.8, we get:

$$\begin{aligned} |\tilde{\mathbf{e}}^{N+1}|^2 &+ \sum_{n=0}^{N} |\tilde{\mathbf{e}}^{n+1} - \tilde{\mathbf{e}}^n|^2 + k\,\nu \sum_{n=0}^{N} ||\tilde{\mathbf{e}}^{n+1}||^2 \\ &\leq C\,k^2 \end{aligned}$$

and A.11 is proved. □

We finally show that the pressure approximation of our viscosity splitting fractional step method with pressure correction is also weakly order 1/2 accurate in the time step in the space $L^2_0(\Omega)$. We also need a technical result, which is a consequence of the the proof of Theorem A.3. We have, in particular, that:

$$\sum_{n=0}^{N} |\tilde{\mathbf{e}}^{n+1} - \tilde{\mathbf{e}}^n|^2 \leq C\,k^2$$

which implies that:

$$\sum_{n=0}^{N} ||\tilde{\mathbf{e}}^{n+1} - \tilde{\mathbf{e}}^n||^2_{-1} \leq C\,k^2 \tag{A.14}$$

We then have:

Theorem A.4: *assume that* **A1** *and* **A2** *hold, that the Stokes problem is regular, and that* 4.46 *and* A.10 *also hold; then, for* $N = 0, \ldots, [T/k] - 1$, *and small enough* k:

$$k \sum_{n=0}^{N} |\tilde{p}^{n+\phi} - p(t_{n+1})|^2_{L^2_0(\Omega)} \leq C\, k \tag{A.15}$$

PROOF: the proof is similar to that of Theorem A.2. We call $g^{n+1} = p(t_{n+1}) - \tilde{p}^{n+\phi}$. We rewrite 4.55 as:

$$\begin{aligned} -\nabla g^{n+1} &= \frac{1}{k}(\tilde{\mathbf{e}}^{n+1} - \tilde{\mathbf{e}}^{n}) - \nu\Delta(\tilde{\mathbf{e}}^{n+1}) - \mathbf{R}^n \\ &- (\tilde{\mathbf{u}}^n \cdot \nabla)\tilde{\mathbf{u}}^{n+1/2} + (\mathbf{u}(t_{n+1}) \cdot \nabla)\mathbf{u}(t_{n+1}) \end{aligned} \tag{A.16}$$

that is, an equality similar to A.7. Using again the LBB condition A.8, we bound the products of the RHS of A.16 with $\mathbf{v} \in \mathbf{H}^1_0(\Omega)$, to get:

$$\begin{aligned} \frac{1}{k}(\tilde{\mathbf{e}}^{n+1} - \tilde{\mathbf{e}}^{n}, \mathbf{v}) &\leq \frac{1}{k}||\tilde{\mathbf{e}}^{n+1} - \tilde{\mathbf{e}}^{n}||_{-1}\, ||\mathbf{v}|| \\ < -\nu\Delta(\tilde{\mathbf{e}}^{n+1}), \mathbf{v} > &= ((\nu\tilde{\mathbf{e}}^{n+1}, \mathbf{v})) \leq \nu||\tilde{\mathbf{e}}^{n+1}||\, ||\mathbf{v}|| \\ < -\mathbf{R}^n, \mathbf{v} > &\leq ||\mathbf{R}^n||_{-1}\, ||\mathbf{v}|| \\ &\leq C\Big(\int_{t_n}^{t_{n+1}} t\, ||\mathbf{u}_{tt}||^2_{-1}\, dt\Big)^{1/2}\, ||\mathbf{v}|| \end{aligned}$$

As for the nonlinear terms, we use again the splitting 4.27, to get:

$$\begin{aligned} T_1 &= c(\tilde{\mathbf{e}}^n, \tilde{\mathbf{u}}^{n+1/2}, \mathbf{v}) \\ &\leq C\, ||\tilde{\mathbf{e}}^n||\, ||\tilde{\mathbf{u}}^{n+1/2}||\, ||\mathbf{v}|| \\ &\leq ||\tilde{\mathbf{e}}^n||\, ||\mathbf{v}|| \end{aligned}$$

$$\begin{aligned} T_2 &= -c(\mathbf{u}(t_n) - \mathbf{u}(t_{n+1}), \tilde{\mathbf{u}}^{n+1/2}, \mathbf{v}) \\ &\leq C\, ||\mathbf{u}(t_n) - \mathbf{u}(t_{n+1})||\, ||\tilde{\mathbf{u}}^{n+1/2}||\, ||\mathbf{v}|| \\ &\leq C\, ||\mathbf{u}(t_n) - \mathbf{u}(t_{n+1})||\, ||\mathbf{v}|| \\ &= C\, ||\int_{t_n}^{t_{n+1}} \mathbf{u}_t\, dt||\, ||\mathbf{v}|| \\ &\leq (k \int_{t_n}^{t_{n+1}} ||\mathbf{u}_t||^2\, dt)^{1/2}\, ||\mathbf{v}|| \end{aligned}$$

$$\begin{aligned} T_3 &= c(\mathbf{u}(t_{n+1}), \tilde{\mathbf{e}}^{n+1/2}, \mathbf{v}) \\ &= -c(\mathbf{u}(t_{n+1}), \mathbf{v}, \tilde{\mathbf{e}}^{n+1/2}) \\ &\leq C\, ||\mathbf{u}(t_{n+1})||_2\, ||\mathbf{v}||\, |\tilde{\mathbf{e}}^{n+1/2}| \\ &\leq C\, ||\mathbf{v}||\, |\tilde{\mathbf{e}}^{n+1/2}| \end{aligned}$$

This way, we find:

$$
\begin{aligned}
|g^{n+1}|_{L_0^2(\Omega)} \;\leq\; & \frac{C}{k}\,||\tilde{\mathbf{e}}^{n+1} - \tilde{\mathbf{e}}^{n}||_{-1} \\
+ \; & C\Big\{||\tilde{\mathbf{e}}^{n+1}|| + ||\tilde{\mathbf{e}}^{n}|| + |\tilde{\mathbf{e}}^{n+1/2}| \\
+ \; & \Big(\int_{t_n}^{t_{n+1}} t\,||\mathbf{u}_{tt}||_{-1}^2\,dt\Big)^{1/2} + \Big(k\int_{t_n}^{t_{n+1}} ||\mathbf{u}_t||^2\,dt\Big)^{1/2}\Big\}
\end{aligned}
$$

that is:

$$
\begin{aligned}
|g^{n+1}|^2_{L_0^2(\Omega)} \;\leq\; & \frac{C}{k^2}\,||\tilde{\mathbf{e}}^{n+1} - \tilde{\mathbf{e}}^{n}||_{-1}^2 \\
+ \; & C\Big\{||\tilde{\mathbf{e}}^{n+1}||^2 + ||\tilde{\mathbf{e}}^{n}||^2 + |\tilde{\mathbf{e}}^{n+1/2}|^2 \\
+ \; & \int_{t_n}^{t_{n+1}} t\,||\mathbf{u}_{tt}||_{-1}^2\,dt + k\int_{t_n}^{t_{n+1}} ||\mathbf{u}_t||^2\,dt\Big\}
\end{aligned}
$$

and A.15 follows from A.14, Theorems A.3 and 4.3 and the regularity **R2** and **R3** of **u**. □

In summary, we have obtained first order error estimates for the end-of-step velocities of our viscosity splitting method with $\theta = 1$, both with and without pressure correction, and order 1/2 estimates for the intermediate velocities, both of them strong in $\mathbf{L}^2(\Omega)$ and weak in $\mathbf{H}_0^1(\Omega)$, under the usual regularity assumptions **A1** and **A2** and the uniform bounds for the intermediate velocities in $\mathbf{H}^2(\Omega)$; we have also obtained order 1/2 weak error estimates for the pressure in $L_0^2(\Omega)$.

List of Tables

2.1 Convergence of the uncoupled block–Gauss–Seidel method. . 65
2.2 Convergence of the coupled block–Gauss–Seidel method. . . . 67
2.3 Convergence of the relaxed coupled block–Gauss–Seidel method. . . . 71
2.4 Comparison of global and local parameters. 72
2.5 Theoretical orders of error in the mesh size h. 80
2.6 Oden's flow: linear regression coefficients for different errors. 83

3.1 Convergence of the nonlinear solvers, Re=400. 109
3.2 Convergence of the nonlinear solvers, Re=1000. 109
3.3 Kovasznay flow: linear regression coefficients for different errors. 117
3.4 Flow in a junction of pipes: comparison of performance of the two methods. 120
3.5 Flow in a junction of pipes: flux through outflow regions. . . 121

4.1 Van Kan's flow, Q_1P_0 element. 157
4.2 Van Kan's flow, Q_2P_1 element. 157

5.1 Q_1P_0 element, $\gamma = 1$, 1 iteration per step. 177
5.2 Q_1P_0 element, $\gamma = 1$, 2 iterations per step. 178
5.3 Q_1P_0 element, $\gamma = 1$, iterating to convergence. 178
5.4 Q_1P_0 element, $\gamma = 1/2$, 2 iterations per step. 178
5.5 Q_1P_0 element, $\gamma = 1/2$, iterating to convergence. 179
5.6 Q_2P_1 element, $\gamma = 1$, 1 iteration per step. 179
5.7 Q_2P_1 element, $\gamma = 1$, 2 iterations per step. 179
5.8 Q_2P_1 element, $\gamma = 1$, iterating to convergence. 180
5.9 Q_2P_1 element, $\gamma = 1/2$, 2 iterations per step. 180
5.10 Q_2P_1 element, $\gamma = 1/2$, iterating to convergence. 180

List of Figures

2.1 Cavity flow, uniform 21×21 mesh. 65
2.2 Convergence history, consistent mass matrix: $+$ P_1 Element; $\bullet$ Q_1 Element; $\circ$ P_2 Element; $\times$ Q_2 Element. 68
2.3 Convergence history, lumped mass matrix: $+$ P_1 Element; $\bullet$ Q_1 Element; $\circ$ P_2 Element; $\times$ Q_2 Element. 69
2.4 Cavity flow, nonuniform 39×39 mesh. 72
2.5 Cavity flow, uniform 21×21 mesh, triangular elements, pressure contours: a) $P_1 - C$; b) $P_1 - L$; c) $P_2 - C$; d) $P_2 - L$. . 75
2.6 Cavity flow, uniform 21×21 mesh, quadrilateral element, pressure contours: a) $Q_1 - C$; b) $Q_1 - L$; c) $Q_2 - C$; d) $Q_2 - L$. . 76
2.7 Cavity flow, nonuniform 39×39 mesh, pressure contours: a) global α, consistent mass matrix; b) global α, lumped mass matrix; c) local α, consistent mass matrix; d) local α, lumped mass matrix. 77
2.8 Error variation with α_0: $\circ = |\mathbf{u} - \mathbf{u}_h|$; $+ = ||\mathbf{u} - \mathbf{u}_h||$; $\bullet = |p - p_h|$; $\times = |\nabla p - \nabla p_h|$; $\diamond = |\nabla p - \mathbf{w}_h|$. 79
2.9 Iteration for convergence with α_0: $+$ P_1 Element; $\bullet$ Q_1 Element; $\circ$ P_2 Element; $\times$ Q_2 Element. 80
2.10 Velocity error in L^2: $+$ P_1 Element; $\bullet$ Q_1 Element; $\circ$ P_2 Element; $\times$ Q_2 Element; $\diamond$ Mixed P_2P_1 Element. 81
2.11 Pressure error in L^2: $+$ P_1 Element; $\bullet$ Q_1 Element; $\circ$ P_2 Element; $\times$ Q_2 Element; $\diamond$ Mixed P_2P_1 Element. 81
2.12 Velocity error in H^1: $+$ P_1 Element; $\bullet$ Q_1 Element; $\circ$ P_2 Element; $\times$ Q_2 Element; $\diamond$ Mixed P_2P_1 Element. 82
2.13 Pressure error in H^1: $+$ P_1 Element; $\bullet$ Q_1 Element; $\circ$ P_2 Element; $\times$ Q_2 Element; $\diamond$ Mixed P_2P_1 Element. 82
2.14 Pressure gradient error in L^2: $+$ P_1 Element; $\bullet$ Q_1 Element; $\circ$ P_2 Element; $\times$ Q_2 Element. 83
2.15 Velocity error in L^2: $\bullet$ Q_1 Element; $\times$ Q_2 Element; $\square =$ GLS method, Q_1 Element; $\diamond$ GLS method, Q_2 Element. . . . 84
2.16 Pressure error in L^2: $\bullet$ Q_1 Element; $\times$ Q_2 Element; $\square =$ GLS method, Q_1 Element; $\diamond$ GLS method, Q_2 Element. . . . 85
2.17 Velocity error in H^1: $\bullet$ Q_1 Element; $\times$ Q_2 Element; $\square =$ GLS method, Q_1 Element; $\diamond$ GLS method, Q_2 Element. . . . 85
2.18 Pressure error in H^1: $\bullet$ Q_1 Element; $\times$ Q_2 Element; $\square =$ GLS method, Q_1 Element; $\diamond$ GLS method, Q_2 Element. . . . 86

2.19 Trapezoidal domain, coarse mesh. 87
2.20 Trapezoidal domain, pressure contours: a) GLS method, coarse mesh; b) GLS method, fine mesh; c) Present method, coarse mesh; d) Present method, fine mesh. 88

3.1 Cavity flow, Re=400, streamlines. 111
3.2 Cavity flow, Re=400, pressure contours. 112
3.3 Cavity flow, Re=1000, streamlines. 112
3.4 Cavity flow, Re=1000, pressure contours. 113
3.5 Kovasznay flow, velocity error in L^2: $+$ P_1 Element; $\bullet$ Q_1 Element; $\circ$ P_2 Element; $\times$ Q_2 Element; $\Box =$ GLS method, Q_1Q_1 element. 114
3.6 Kovasznay flow, pressure error in L^2: $+$ P_1 Element; $\bullet$ Q_1 Element; $\circ$ P_2 Element; $\times$ Q_2 Element; $\Box =$ GLS method, Q_1Q_1 element. 114
3.7 Kovasznay flow, velocity error in H^1: $+$ P_1 Element; $\bullet$ Q_1 Element; $\circ$ P_2 Element; $\times$ Q_2 Element; $\Box =$ GLS method, Q_1Q_1 element. 115
3.8 Kovasznay flow, pressure error in H^1: $+$ P_1 Element; $\bullet$ Q_1 Element; $\circ$ P_2 Element; $\times$ Q_2 Element; $\Box =$ GLS method, Q_1Q_1 element. 115
3.9 Kovasznay flow, pressure gradient error in L^2: $+$ P_1 Element; $\bullet$ Q_1 Element; $\circ$ P_2 Element; $\times$ Q_2 Element. 116
3.10 Kovasznay flow, streamlines. 118
3.11 Kovasznay flow, pressure contours. 118
3.12 Flow through a junction, mesh. 119
3.13 Flow through a junction: a) GLS method, streamlines; b) GLS method, pressure contours; c) Present method, streamlines; d) Present method, pressure contours. 122

4.1 Backward facing step, mesh. 158
4.2 Backward facing step, Q_1P_0 element, streamlines: a) $Re = 60$; b) $Re = 200$; c) $Re = 400$. 160
4.3 Backward facing step, Q_2P_1 element, streamlines: a) $Re = 60$; b) $Re = 200$; c) $Re = 400$. 161
4.4 Flow past a cylinder, mesh. 162
4.5 Flow past a cylinder, $Re = 40$, streamlines. 162
4.6 Flow past a cylinder, $Re = 40$, stationary streamlines. 163
4.7 Flow past a cylinder, $Re = 40$, nodal pressure contours. . . . 163
4.8 Flow past a cylinder, $Re = 100$, nodal velocity history. 164
4.9 Flow past a cylinder, $Re = 100$, streamlines. 165
4.10 Flow past a cylinder, $Re = 100$, stationary streamlines. . . . 165
4.11 Flow past a cylinder, $Re = 100$, nodal pressure contours. . . . 166
4.12 Flow past a cylinder, $Re = 100$, Fourier spectrum of the nodal velocity solution. 167

5.1 Kovasznay flow, Q_1P_0 element, streamlines. 182
5.2 Kovasznay flow, Q_2P_1 element, streamlines. 182
5.3 Kovasznay flow, Q_1P_0 element, element pressure values. . . . 183
5.4 Kovasznay flow, Q_2P_1 element, nodal pressure contours. . . . 183
5.5 Kovasznay flow, Q_1P_0 element with checkboard mode filtered, element pressure values. 184
5.6 Kovasznay flow, Q_1P_0 element with checkboard mode filtered, nodal pressure contours. 185
5.7 Kovasznay flow, maximum nodal error: • Q_1P_0 element, ∘ Q_2P_1 element. 185
5.8 Cavity flow, streamlines: a) Q_1P_0 element; b) Q_2P_1 element. . 187
5.9 Cavity flow, Q_1P_0 element, element pressure values. 188
5.10 Cavity flow, Q_2P_1 element, nodal pressure contours. 188
5.11 Cavity flow, horizontal velocity profile through cavity centerline $x = 0.5$: — $Q1P0$ element; - - - $Q2P1$ element; ◇ Reference [43]. 189
5.12 Cavity flow, vertical velocity profile through cavity centerline $y = 0.5$: — $Q1P0$ element; - - - $Q2P1$ element; ◇ Reference [43]. 189
5.13 Noflow problem, mesh. 190
5.14 Noflow problem, Q_1P_0 element, velocity vectors. 191
5.15 Noflow problem, Q_2P_1 element, velocity vectors. 191
5.16 Noflow problem, Q_1P_0 element, pressure contours. 192
5.17 Noflow problem, Q_2P_1 element, pressure contours. 192
5.18 Jet flow, Q_1P_0 element, streamlines: a) $t = 1.2$; b) $t = 2.5$; c) $t = 4.0$. 193
5.19 Jet flow, Q_2P_1 element, streamlines: a) $t = 1.2$; b) $t = 2.5$; c) $t = 4.0$. 194
5.20 Jet flow, Q_1P_0 element, nodal pressure contours: a) $t = 1.2$; b) $t = 2.5$; c) $t = 4.0$. 195
5.21 Jet flow, Q_2P_1 element, nodal pressure contours: a) $t = 1.2$; b) $t = 2.5$; c) $t = 4.0$. 196

References

[1] R.A. Adams: *Sobolev spaces.* Academic Press, New York, 1975.

[2] B.F. Armaly, F. Durst, J.C.F. Pereira, B. Shönung: "Experimental and theoretical investigation of backward-facing step flow." *Journal of Fluid Mechanics,* Vol. **127**, p. 473–496, 1983.

[3] D.N. Arnold, F. Brezzi, M. Fortin: "A stable finite element for the Stokes equations." *Calcolo,* Vol. **21**, p. 337–344, 1984.

[4] I. Babuŝka: "Error bounds for the finite element method." *Numerische Mathematik,* Vol. **16**, p. 322–333, 1971.

[5] C. Baiocci, F. Brezzi, L.P. Franca: "Virtual bubbles and Galerkin-least-squares type methods (Ga.L.S.)." *Computer Methods in Applied Mechanics and Engineering,* Vol. **105**, p. 125–141, 1993.

[6] M.A. Behr, L.P. Franca, T.E. Tezduyar: "Stabilized finite element methods for the velocity–pressure–stress formulation of incompressible flows." *Computer Methods in Applied Mechanics and Engineering,* Vol. **104**, p. 31–48, 1993.

[7] M.A. Behr, D. Hastreiter, S. Mittal, T.E. Tezduyar: "Incompressible flow past a circular cylinder: dependence of the computed flow field on the location of the lateral boundaries." *Computer Methods in Applied Mechanics and Engineering,* Vol. **123**, p. 309–316, 1995.

[8] J.B. Bell, P. Colella, H.M. Glaz: "A Second-Order Projection Method for the incompressible Navier–Stokes equations." *Journal of Computational Physics,* Vol. **85**, p. 257–283, 1989.

[9] M Bercovier, O.A. Pironneau: "Error estimates for finite element solution of the Stokes problem in the primitive variables." *Numerische Mathematik,* Vol. **33**, p. 211–224, 1979.

[10] J. Blair Perot: "An Analysis of the fractional–step projection method." *Journal of Computational Physics,* Vol. **108**, p. 51–58, 1993.

[11] J. Blasco, R. Codina, A. Huerta: "A fractional step method for the incompressible Navier–Stokes equations related to a predictor–multicorrector algorithm." *International Journal for Numerical Methods in Fluids,* submitted.

[12] J.M. Boland, R.A. Nicolaides: "Stability of finite elements under divergence constraints." *SIAM Journal of Numerical Analysis,* Vol. **20**, p. 722–731, 1983.

[13] S.C. Brenner, L.R. Scott: *The mathematical theory of finite element methods.* Springer–Verlag, 1994.

[14] F. Brezzi: "On the existence, uniqueness and approximation of saddle–point problems arising from Lagrange multipliers." *RAIRO* , Vol. **B-R2**, p. 129–151, 1974.

[15] F. Brezzi, K-J. Bathe: "A discourse on the stability conditions for mixed finite element formulations." *Computer Methods in Applied Mechanics and Engineering,* Vol. **82**, p. 27–57, 1990.

[16] F. Brezzi, M.O. Bristeau, L.P. Franca, M. Mallet, G. Rogé: "A relationship between stabilized finite element methods and the Galerkin method with bubble functions." *Computer Methods in Applied Mechanics and Engineering,* Vol. **96**, p. 117–129, 1992.

[17] F. Brezzi, J. Douglas: "Stabilized mixed methods for the Stokes problem." *Numerische Mathematik,* Vol. **53**, p. 225–235, 1988.

[18] F. Brezzi, R.S. Falk: "Stability of higher–order Hood–Taylor methods." *SIAM Journal of Numerical Analysis,* Vol. **28**, p. 581–590, 1991.

[19] F. Brezzi, M. Fortin: *Mixed and Hybrid finite element methods.* Springer Series in Computational Mathematics, 15. Springer–Verlag, 1991.

[20] A.N. Brooks, T.J.R. Hughes: "Streamline upwind Petrov–Galerkin formulations for convection dominated flows with particular enphasis on the incompressible Navier–Stokes equations." *Computer Methods in Applied Mechanics and Engineering,* Vol. **32**, p. 199–259, 1982.

[21] G.F. Carey, R. Krishnan: "Penalty finite element method for the Navier–Stokes equations." *Computer Methods in Applied Mechanics and Engineering,* Vol. **42**, p. 183–224, 1984.

[22] A.J. Chorin: "A numerical method for solving incompressible viscous flow problems." *Journal of Computational Physics,* Vol. **2**, p. 12–26, 1967.

[23] A.J. Chorin: "Numerical solution of the Navier–Stokes equations." *Mathematics of Computation,* Vol. **22**, p. 745–762, 1968.

[24] A.J. Chorin: "On the convergence of discrete approximations to the Navier–Stokes equations." *Mathematics of Computation,* Vol. **23**, p. 341–353, 1969.

[25] P.G. Ciarlet: *The finite element method for elliptic problems.* North–Holland, Amsterdam, 1978.

[26] R. Codina, J. Blasco: "A finite element formulation for the Stokes problem allowing equal order interpolation." *Computer Methods in Applied Mechanics and Engineering,* accepted for publication.

[27] R. Codina, E. Oñate, M. Cervera: "The intrinsic time for the streamline upwind/Petrov–Galerkin formulation using quadratic elements." *Computer Methods in Applied Mechanics and Engineering,* Vol. **94**, p. 239–262, 1992.

[28] R. Codina, M. Vázquez, O.C. Zienkiewicz: "A fractional step method for compressible flows: boundary conditions and incompressible limit." *Proceedings of the IXth. International Conference on Finite Elements in Fluids - New trends and applications, Venezia, Italy,* Vol. **I**, p. 409–418, 1995.

[29] G.K. Despotis, S. Tsangaris: "Fractional step method for solution of incompressible Navier–Stokes equations on unstructured triangular meshes." *International Journal for Numerical Methods in Fluids,* Vol. **20**, p. 1273–1288, 1995.

[30] J. Donea, S. Giuliani, H. Laval, L. Quartapelle: "Finite element solution of the unsteady Navier–Stokes equations by a fractional step method." *Computer Methods in Applied Mechanics and Engineering,* Vol. **30**, p. 53–73, 1982.

[31] J.J. Droux, T.J.R. Hughes: "A boundary integral modification of the Galerkin least squares formulation for the Stokes problem." *Computer Methods in Applied Mechanics and Engineering,* Vol. **113**, p. 173–182, 1994.

[32] J. K. Dukovicz, A. S. Dvinsky: "Approximate Factorization as a High Order Splitting for the Implicit Incompressible Flow Equations." *Journal of Computational Physics,* Vol. **102**, p. 336–347, 1992.

[33] H.A. Dwyer, S. Ibrani: "Time accurate solutions of the incompressible and three–dimensional Navier–Stokes equations." *Computer Methods in Applied Mechanics and Engineering,* Vol. **75**, p. 333–341, 1989.

[34] M.S. Engel, M-A. Jamnia: "Transient flow past a circular cylinder: a benchmark solution." *International Journal for Numerical Methods in Fluids,* Vol. **11**, p. 985–1000, 1990.

[35] L.P. Franca, S.L. Frey, T.J.R. Hughes: "Stabilized finite element methods: I. Application to the advective–diffusive model.." *Computer Methods in Applied Mechanics and Engineering,* Vol. **95**, p. 253–276, 1992.

[36] L.P. Franca, S.L. Frey: "Stabilized finite element methods: II. The incompressible Navier–Stokes equations.." *Computer Methods in Applied Mechanics and Engineering,* Vol. **99**, p. 209–233, 1992.

[37] L.P. Franca, T.J.R. Hughes: "Convergence analyses of Galerkin least–squares methods for symmetric advective–diffusive forms of the Stokes and incompressible Navier–Stokes equations." *Computer Methods in Applied Mechanics and Engineering,* Vol. **105**, p. 285–298, 1993.

[38] E. Fernandez–Cara, M. Marin Beltrán: "The convergence of two numerical schemes for the Navier–Stokes equations." *Numerische Mathematik,* Vol. **55**, p. 33–60, 1989.

[39] M. Fortin, A. Fortin: "Experiments with several elements for viscous incompressible flows." *International Journal for Numerical Methods in Fluids,* Vol. **5**, p. 911–928, 1985.

[40] M. Fortin, A. Fortin: "New and newer elements for incompressible flows." *Finite elements in fluids,* Vol. **6**, p. 171–187, 1985.

[41] M. Fortin, R. Peyret, R. Temam: "Résolution numerique des equations de Navier–Stokes pour un fluide incompressible." *J. Mécanique,* Vol. **10**, p. 357–390, 1971.

[42] U. Ghia, K.N. Ghia, C.T. Shin: "High–Re solutions for incompressible flow using the Navier–Stokes equations and a multigrid method." *Journal of Computational Physics,* Vol. **48**, p. 387–411, 1982.

[43] V. Girault, P. A. Raviart: *Finite Element Approximation of the Navier–Stokes Equation.* Springer–Verlag, New York, 1986.

[44] R. Glowinski, T.W. Pan, J. Periaux: "A fictitious domain method for external incompressible viscous flow modeled by Navier–Stokes equations." *Computer Methods in Applied Mechanics and Engineering,* Vol. **112**, p. 133-148, 1994.

[45] P. M. Gresho: "On the theory of semi–implicit projection methods for viscous incompressible flow and its implementation via a finite element method that also introduces a nearly consistent mass matrix. Part I: theory." *International Journal for Numerical Methods in Fluids,* Vol. **11**, p. 587–620, 1990.

[46] P. M. Gresho, S.T. Chan: "On the theory of semi–implicit projection methods for viscous incompressible flow and its implementation via a finite element method that also introduces a nearly consistent mass matrix. Part 2: implementation." *International Journal for Numerical Methods in Fluids,* Vol. **11**, p. 621–659, 1990.

[47] P.M. Gresho, R.L. Lee, R.L. Sani: "Further studies in equal order interpolation for Navier–Stokes." *Fifth International Symposium on Finite Elements in Flow Problems,* Austin, Texas, 1984.

[48] P. M. Gresho, R. Sani: "On pressure boundary conditions for the incompressible Navier–Stokes equations." *International Journal for Numerical Methods in Fluids,* Vol. **7**, p. 1111–1145, 1987.

[49] P. Grisvard: *Elliptic problems on non–smooth domains.* Pitman, Marschfields, Massachussets, 1985.

[50] J-L. Guermond: "Remarques sur les méthodes de projection pour l'approximation des équations de Navier–Stokes." *Numerische Mathematik,* Vol. **67**, p. 465–473, 1994.

[51] J-L. Guermond, L. Quartapelle: "Unconditionally stable finite–element method for the unsteady Navier–Stokes equations." *Proceedings of the 9–th International Conference on Finite Elements in Fluids - New trends and applications, Venezia, Italy, October 1995,* Vol. **I**, p. 367–376.

[52] S. Hassanzadeh, V. Sonnad, S. Foresti: "Finite element implementation of boundary conditions for the pressure Poisson equation of incompressible flow." *International Journal for Numerical Methods in Fluids,* Vol. **18**, p. 1009–1019, 1994.

[53] D.M. Hawken, H.R. Tamaddon-Jahromi, P. Townsend, M.F. Webster: "A Taylor–Galerkin–based algorithm for viscous incompressible flow." *International Journal for Numerical Methods in Fluids,* Vol. **10**, p. 327–351, 1990.

[54] J.G. Heywood, R Rannacher: "Finite element approximation of the nonstationary Navier–Stokes problem: Part 1: Regularity of solutions and second order error estimates for spatial discretization." *SIAM Journal of Numerical Analysis,* Vol. **19**, p. 275–311, 1982.

[55] J.G. Heywood, R Rannacher: "Finite element approximation of the nonstationary Navier–Stokes problem: Part 4: Error analysis for second–order time discretization." *SIAM Journal of Numerical Analysis,* Vol. **27**, p. 353–384, 1990.

[56] J.G. Heywood, R Rannacher, S. Turek: "Artifitial boundaries and flux and pressure conditions for the incompressible Navier–Stokes equations." *International Journal for Numerical Methods in Fluids,* Vol. **22**, p. 325-352, 1996.

[57] T.J.R. Hughes, M. Mallet, A. Mizukami: "A new finite element formulation for computational fluid dynamics: II. Beyond SUPG." *Computer Methods in Applied Mechanics and Engineering,* Vol. **54**, p. 341–355, 1986.

[58] T.J.R. Hughes, M. Mallet: "A new finite element formulation for computational fluid dynamics: III. The generalized streamline operator for multidimensional advection–diffusion systems." *Computer Methods in Applied Mechanics and Engineering,* Vol. **58**, p. 305–328, 1986.

[59] T.J.R. Hughes, L.P. Franca, M. Balestra: "A new finite element formulation for computational fluid dynamics: V. Circumventing the Babuŝka–Brezzi condition: a stable Petrov–Galerkin formulation of the Stokes problem accomodating equal–order interpolations." *Computer Methods in Applied Mechanics and Engineering,* Vol. **59**, p. 85–99, 1986.

[60] T.J.R. Hughes, L.P. Franca: "A new finite element formulation for computational fluid dynamics: VII. The Stokes problem with various well–posed boundary conditions: symmetric formulations that converge for all velocity/pressure spaces." *Computer Methods in Applied Mechanics and Engineering,* Vol. **65**, p. 85–96, 1987.

[61] T.J.R. Hughes, L.P. Franca, G. M. Hulbert: "A new finite element formulation for computational fluid dynamics: VIII. The Galerkin/least squares method for advective–diffusive equations." *Computer Methods in Applied Mechanics and Engineering,* Vol. **73**, p. 173–189, 1989.

[62] J. van Kan: "A second–order accurate pressure correction scheme for viscous incompressible flow." *SIAM Journal of Sci. Stat. Comp.,* Vol. **7**, N. 3, p. 870–891, 1986.

[63] G.E. Karniadakis, M. Israeli, S.E. Orzag: "High order splittting methods for the incompressible Navier–Stokes equations." *Journal of Computational Physics,* Vol. **59**, p. 414–443, 1991.

[64] M. Kawahara, K. Ohmiya: "Finite element analysis of density flow using the velocity–correction method." *International Journal for Numerical Methods in Fluids,* Vol. **5**, p. 981–993, 1985.

[65] J. Kim, P. Moin: "Application of a Fractional–Step Method to incompressible Navier–Stokes equations." *Journal of Computational Physics,* Vol. **59**, p. 308–323, 1985.

[66] L. Kleiser, U. Shumann: *Treatment of incompressibility and boundary conditions in 3-D numerical spectral simulation of plane channel flows.* Hirschel E. H. ed., Proc. 3rd GAMM Conference on Numerical Methods in Fluid Mechanics, Vieweg–Verlag Braunschweig, 1980.

[67] P. Klouček, F. Rys: "Stability of the fractional step θ–scheme for the nonstationary Navier–Stokes equations." *SIAM Journal of Numerical Analysis,* Vol. **31**, p. 1312–1335, 1990.

[68] A. Kovacs, M. Kawahara: "A finite element scheme based on the velocity–correction method for the solution of the time–dependent incompressible Navier–Stokes equations." *International Journal for Numerical Methods in Fluids,* Vol. **13**, p. 403–423, 1991.

[69] L.I.G. Kovasznay: "Laminar flow behind a two–dimensional grid." *Proc. Cambridge Philos. Soc.,* Vol. **44**, 1948.

[70] Y. Kwok, K. Tam: "Linearized stability analysis of staggered–grid difference schemes for multidimensional viscous incompressible flows." *Numerical Methods for Partial Differential Equations* , Vol. **9**, p. 313–322, 1993.

[71] O. A. Ladyzhenskaya: *The mathematical theory of viscous incompressible flow.* Gordon and Breach, New York, 1969.

[72] L.D. Landau, E.M. Lifshitz: *Course of theoretical Physics, Vol. 6: Fluid Mechanics.* Pergamin Press, Oxford, 1959.

[73] H. Laval, L. Quartapelle: "A fractional–step Taylor–Galerkin method for unsteady incompressible flows." *International Journal for Numerical Methods in Fluids,* Vol. **11**, p. 501–513, 1990.

[74] H. Le, P. Moin: "An improvement of Fractional–Step Methods for the incompressible Navier–Stokes equations." *Journal of Computational Physics,* Vol. **92**, p. 369–379, 1991.

[75] W.K. Liu, J. Gvildys: "Fluid–structure interaction of tanks with an eccentric core barrel." *Computer Methods in Applied Mechanics and Engineering,* Vol. **58**, p. 51–77, 1986.

[76] Y. Lung–an: "Viscosity–splitting scheme for the Navier–Stokes equations." *Numerical Methods for Partial Differential Equations,* Vol. **7**, p. 317–338, 1991.

[77] R. Natarajan: "A Numerical Method for Incompressible Viscous Flow Simulation." *Journal of Computational Physics,* Vol. **100**, p. 384–395, 1992.

[78] J.T. Oden, O-P. Jacquotte: "Stability of some mixed finite element methods for Stokesian flows." *Computer Methods in Applied Mechanics and Engineering,* Vol. **43**, p. 231–247, 1984.

[79] S. A. Orzag, M. Israeli, M. O. Deville: "Boundary conditions for incompressible flows." *Journal of Scientific Computing,* Vol. **1**, N. 1, p. 75–111, 1986.

[80] T.N. Phillips, G.W. Roberts: "The treatment of spurious pressure modes in spectral incompressible flow calculations." *Journal of Computational Physics,* Vol. **105**, p. 150–164, 1993.

[81] A. Pinelli, A. Vacca: "Chebyshev collocation method and multidomain decomposition for the incompressible Navier–Stokes equations." *International Journal for Numerical Methods in Fluids,* Vol. **18**, p. 781–799, 1994.

[82] L. Quartapelle, M. Napolitano: "Integral conditions for the pressure in the computation of incompressible viscous flows." *Journal of Computational Physics,* Vol. **62**, p. 340–348, 1986.

[83] P.A. Raviart, J.M. Thomas: *Introduction à l'analyse numérique des équations aux dérivées partielles.* Masson, Paris, 1983.

[84] G. de Rham: *Varietés Différentiables.* Hermann, 1960.

[85] R.L. Sani, P.M. Gresho, R.L. Lee, D.F. Griffiths: "The cause and cure (?) of the spurious pressures generated by certain FEM solutions of the incompressible Navier–Stokes equations: Part 1." *International Journal for Numerical Methods in Fluids,* Vol. **1**, p. 17–43, 1981.

[86] R.L. Sani, P.M. Gresho, R.L. Lee, D.F. Griffiths, M. Engelman: "The cause and cure (?) of the spurious pressures generated by certain FEM solutions of the incompressible Navier–Stokes equations: Part 2." *International Journal for Numerical Methods in Fluids,* Vol. **1**, p. 171–204, 1981.

[87] G.E. Schneider, G.D. Raithby, M.M. Yovanovich: "Finite element analysis of incompressible fluid flow incorporating equal order pressure and velocity interpolation." *Numerical Methods in Laminar and Turbulent flow,* Pentech Press, Plymouth, 1978.

[88] R. Schreiber, H.B. Keller: "Driven cavity flows by efficient numerical techniques." *Journal of Computational Physics,* Vol. **49**, p. 310–333, 1983.

[89] J. Shen: "Hopf bifurcation of the unsteady regularized driven cavity flow." *Journal of Computational Physics,* Vol. **95**, p. 228–245, 1991.

[90] J. Shen: "On error estimates of projection methods for Navier–Stokes equations: first–order schemes." *SIAM Journal Numerical Analysis,* Vol. **29**, p. 57–77, 1992.

[91] J. Shen: "On error estimates of some higher order projection and penalty–projection methods for Navier–Stokes equations." *Numerische Mathematik,* Vol. **62**, p. 49–73, 1992.

[92] J. Shen: "Remarks on the pressure error estimates for the projection method." *Numerische Mathematik,* Vol. **67**, p. 513–520, 1994.

[93] S.J. Sherwin, G.E. Karniadakis: "A triangular spectral element method; application to the incompressible Navier–Stokes equations." *Computer Methods in Applied Mechanics and Engineering,* Vol. **123**, p. 189–229, 1995.

[94] D. Silvester: "Optimal low order finite element methods for incompressible flow." *Computer Methods in Applied Mechanics and Engineering,* Vol. **111**, p. 357–368, 1994.

[95] D. Silvester, N. Kechkar: "Stabilized bilinear–constant velocity–pressure finite elements for the conjugate gradient solution of the Stokes problem." *Computer Methods in Applied Mechanics and Engineering,* Vol. **79**, p. 71–86, 1990.

[96] J.C. Simó, F. Armero: "Unconditional stability and long–term behaviour of transient algorithms for the incompressible Navier–Stokes and Euler equations." *Computer Methods in Applied Mechanics and Engineering,* Vol. **111**, p. 111–154, 1994.

[97] R. Stenberg: "A technique for analysing finite element methods for viscous incompressible flow." *International Journal for Numerical Methods in Fluids,* Vol. **11**, p. 935–948, 1990.

[98] G. Strang, J. Fix: *An Analisys of the finite element method.* Englewood Cliffs, New Jork, Prentice-Hall 1973.

[99] T. Tanahashi, H. Okanaga, T. Saito: "GSMAC finite element method for unsteady incompressible Navier-Stokes equations at high Reynolds numbers." *International Journal for Numerical Methods in Fluids,* Vol. **11**, p. 479–499, 1990.

[100] R. Temam: "Une méthode d'approximations de la solution des équations de Navier–Stokes." *Bull. Soc. Math. France,* Vol. **98**, p. 115–152, 1968.

[101] R. Temam: "Sur la stabilité et la convergence de la méthode des pas fractionaires." *Ann. Mat. Pura Appl.,* Vol. **LXXIV**, p. 191–380, 1968.

[102] R. Temam: "Sur l'approximation de la solution des équations de Navier–Stokes par la méthode des pas fractionaires (I)." *Arch. Rac. Mech. Anal.,* Vol. **32**, N. 2, p. 135–153, 1969.

[103] R. Temam: "Sur l'approximation de la solution des équations de Navier–Stokes par la méthode des pas fractionaires (II)." *Arch. Rac. Mech. Anal.,* Vol. **33**, p. 377–385, 1969.

[104] R. Temam: *Navier–Stokes equations and Nonlinear Functional Analysis.* CBMS-NSF Regional Conference Series in Applied Mathematics, SIAM, Philadelphia, PA, 1983.

[105] R. Temam: *Navier–Stokes equations. Theory and Numerical Analysis.* North–Holland, Amsterdam, 3rd. Edition, 1984.

[106] R. Temam: "Remark on the Pressure Boundary Condition for the Projection Method." *Theoretical and Computational Fluid Dynamics,* Vol. **3**, p. 181–184, 1991.

[107] T.E. Tezduyar, S. Mittal, S.E. Ray, R. Shih: "Incompressible flow computations using stabilized bilinear and linear equal–order–interpolation velocity–pressure elements." *Computer Methods in Applied Mechanics and Engineering,* Vol. **95**, p. 221–242, 1992.

[108] T.E. Tezduyar, S. Mittal, R. Shih: "Time–accurate incompressible flow computations with quadrilateral elements." *Computer Methods in Applied Mechanics and Engineering,* Vol. **87**, p. 363–384, 1991..

[109] R. Verfürth: "Error estimates for a mixed finite element approximation of the Stokes equation." *RAIRO Anal. Numér.,* Vol. **18**, p. 175–182, 1984.

[110] N. N. Yanenko: *The Method of Fractional Steps.* Springer–Verlag, Berlin, 1971.

[111] K. Yosida: *Functional analysis.* 5th. Ed., Springer–Verlag, Berlin, 1978.

[112] O.C. Zienkiewicz, R. Codina: "A general algorithm for compressible and incompressible flow– Part I. The split, characteristic based scheme." *International Journal for Numerical Methods in Fluids,* Vol. **20**, p. 869–885, 1995.

[113] O.C. Zienkiewicz, J. Wu: "Incompressibility without tears – how to avoid restrictions of mixed formulation." *International Journal for Numerical Methods in Engineering,* Vol. **32**, p. 1189–1203, 1991.